International Journal of Chemical Engineering

Bioprocess Development for Biofuels and Bioproducts

Guest Editors: Michael K. Danquah, Ravichandra Potumarthi, and Pogaku Ravindra

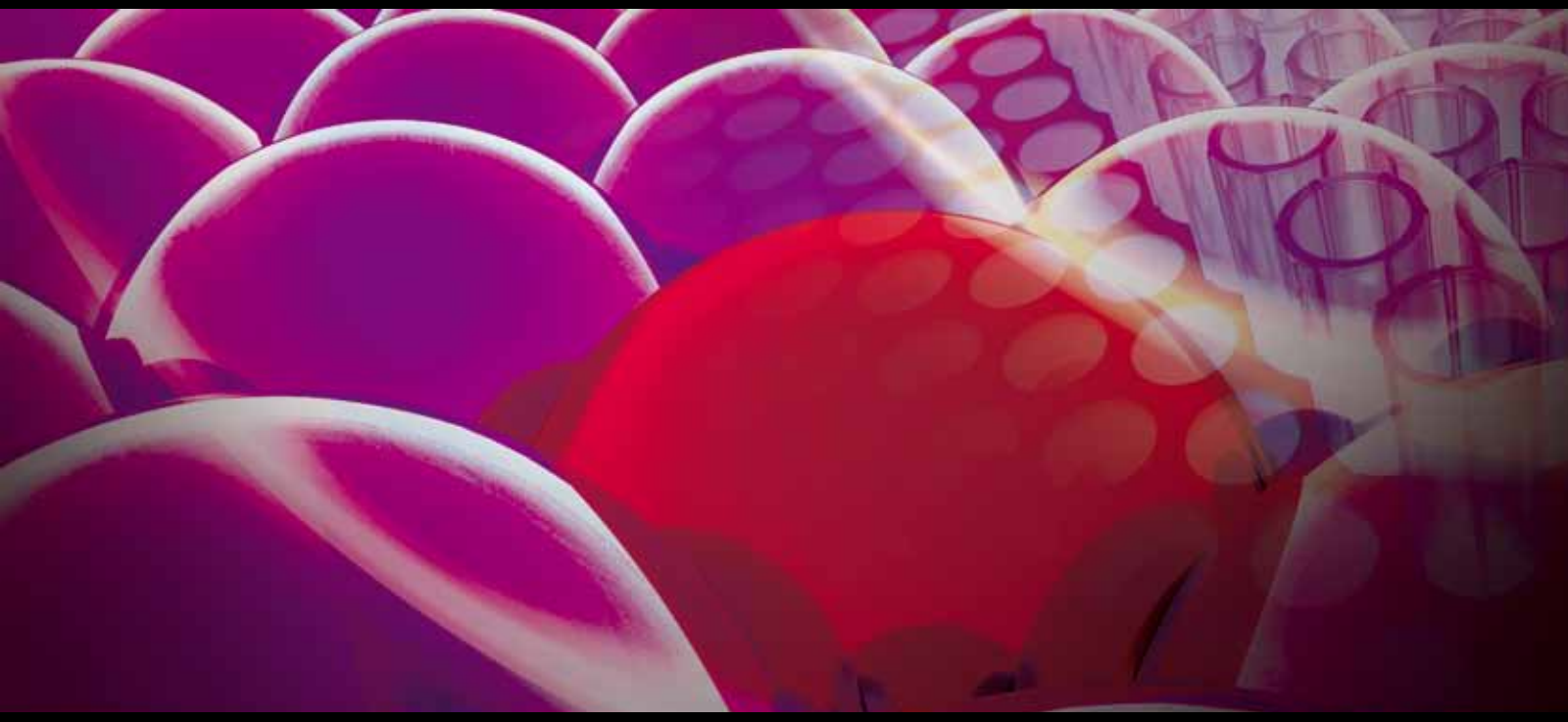

Bioprocess Development for Biofuels and Bioproducts

International Journal of Chemical Engineering

Bioprocess Development for Biofuels and Bioproducts

Guest Editors: Michael K. Danquah, Ravichandra Potumarthi, and Pogaku Ravindra

Editorial Board

Contents

Hindawi Publishing Corporation
International Journal of Chemical Engineering
Volume 2010, Article ID 257873, 2 pages
doi:10.1155/2010/257873

Editorial

Bioprocess Development for Biofuels and Bioproducts

Michael K. Danquah,[1] Ravichandra Potumarthi,[2] and Pogaku Ravindra[3]

[1] *Department of Chemical Engineering, Monash University, Wellington Road, Clayton VIC 3800, Australia*
[2] *Bioengineering and Environmental Centre, Indian Institute of Chemical Technology (CSIR), Tarnaka, Hyderabad 500 607, India*
[3] *Department of Chemical and Bioprocess Engineering, University Malaysia Sabah, Kotakinabalu 88999, Malaysia*

Correspondence should be addressed to Michael K. Danquah, michael.danquah@eng.monash.edu.au

Received 18 April 2010; Accepted 18 April 2010

The increasing pursuit of green technology and renewable resource products has fostered a dramatic interest in biofuels and bioproducts globally. Primarily, this is due to the potentials displayed by biofuels and bioproducts in curbing current global warming issues through sustainable conversions of biomass into valuable consumer products. The development of biofuels and bioproducts creates pathways independent on petroleum but towards a more secure transport and manufacturing future with a lower greenhouse gas signature. In particular, biofuels and bioproducts have demonstrated the capacity to support the growth of agriculture, forestry, and rural economies and to foster major new domestic industries such as biorefineries to make a variety of fuels, chemicals, and other products. Examples of these products include bioethanol, biodiesel, biohydrogen for biofuels, and a range of bioproducts from low volume high value products to high volume low value products such as biopolymers and renewable chemicals including propanediol and lactic acid. Of course, the selected topics and papers are not an exhaustive representation of the area of bioprocess development for biofuels and bioproducts. Nonetheless, they represent the rich and many-faceted knowledge that we have the pleasure of sharing with the readers. We would like to thank the authors for their excellent contributions and patience in assisting us. Finally, the fundamental work of all reviewers on these papers is also very warmly acknowledged.

This special issue contains five papers, where two papers are related to energy and the environment, two papers cover algal resources, and the last one covers conventional biodiesel production and optimization.

In the first paper, Luo et al. present "Energy and environmental performance of bioethanol from different lignocelluloses." The paper deals with the use of cellulosic processing technologies to convert different lignocellulosic biomass to fuel ethanol. Seven different studies were conducted to permit a direct comparison of fuel ethanol from different lignocelluloses in terms of energy use and environmental impact and are summarized in this paper. The work provides an overview on the energy efficiency and environmental performance of using fuel ethanol derived from different biomass feedstocks in comparison with gasoline.

In the second paper, Irvine et al. present "Energy from waste: reuse of compost heat as a source of renewable energy." An in-vessel tunnel composting facility in Scotland was used to investigate the potential for collection and reuse of compost heat as a source of renewable energy. The amount of energy offered by the compost was calculated and seasonal variations analysed. From the report, using the heat of the compost was found to provide the most reliable level of supply at a similar price to competing sources.

In the third paper, Baliga and Powers present "Sustainable algae biodiesel production in cold climates." The paper employs life cycle assessment to determine the most suitable operating conditions for algae biodiesel production in cold climates to minimize energy consumption and environmental impacts. Two hypothetical algae photobioreactor production and biodiesel plants located in Upstate New York (USA) were utilized for the analysis. The results obtained were compared with that of soy biodiesel.

In the fourth paper, Hosikian et al. present "Chlorophyll extraction from microalgae: a review on the process engineering aspects." This review discusses the process engineering of chlorophyll extraction from microalgae. It presents an upstream scenario where microalgal cultivation is used for capturing CO_2 and wastewater treatment and some downstream extraction technologies. Different chlorophyll extraction methods and chlorophyll purification techniques are evaluated. The report suggests supercritical fluid extraction as a promising technology for chlorophyll extraction and high-performance liquid chromatography as a power spectroscopic technique for accurate analysis of chlorophyll molecules.

In the fifth paper, Boulifi et al. present "Process optimization for biodiesel production from corn oil and its oxidative stability." They used response surface methodology (RSM) based on central composite design (CCD) to optimize biodiesel production from corn oil. The process variables, temperature, and catalyst concentration were found to have significant influence on biodiesel yield amongst other variables.

Michael K. Danquah
Ravichandra Potumarthi
Pogaku Ravindra

Hindawi Publishing Corporation
International Journal of Chemical Engineering
Volume 2010, Article ID 740962, 12 pages
doi:10.1155/2010/740962

Review Article

Energy and Environmental Performance of Bioethanol from Different Lignocelluloses

Lin Luo, Ester van der Voet, and Gjalt Huppes

Institute of Environmental Sciences (CML), Leiden University, P.O. Box 9518, 2300 RA Leiden, The Netherlands

Correspondence should be addressed to Lin Luo, luo@cml.leidenuniv.nl

Received 9 November 2009; Accepted 6 March 2010

Academic Editor: Ravichandra Potumarthi

Climate change and the wish to reduce the dependence on oil are the incentives for the development of alternative energy sources. The use of lignocellulosic biomass together with cellulosic processing technology provides opportunities to produce fuel ethanol with less competition with food and nature. Many studies on energy analysis and life cycle assessment of second-generation bioethanol have been conducted. However, due to the different methodology used and different system boundary definition, it is difficult to compare their results. To permit a direct comparison of fuel ethanol from different lignocelluloses in terms of energy use and environmental impact, seven studies conducted in our group were summarized in this paper, where the same technologies were used to convert biomass to ethanol, the same system boundaries were defined, and the same allocation procedures were followed. A complete set of environmental impacts ranging from global warming potential to toxicity aspects is used. The results provide an overview on the energy efficiency and environmental performance of using fuel ethanol derived from different feedstocks in comparison with gasoline.

1. Introduction

Climate change and the wish to reduce the dependence on oil are the incentives for the development of alternative energy sources. In view of the carbon dioxide reduction target agreed upon in the Kyoto protocol, a shift from fossil fuels to renewable resources is ongoing, also to secure the long-term energy supply at both national and international level. The European Commission demonstrated in 2007 that a 20% target for the overall share of energy from renewable sources and a 10% target for energy from renewable sources in transport would be appropriate and achievable objectives [1], though both targets have become subject of dispute since then. In the near term, liquid biofuels will still largely contribute to the target in transport sector due to the limited available technologies for fuels from other renewable sources. Especially bioethanol with its biorenewable nature, optimized production technology, and potential of greenhouse gas (GHG) mitigation already proved itself as an attractive alternative fuel.

Most of the current practice only concerns first-generation ethanol from conventional crops like corn, wheat, sorghum, potato, sugarcane, sugar beet, and so forth. Criticism is expressed on the first-generation bioethanol with regard to land use requirement and competition with food and nature. These issues have become the driving forces for the technology innovation towards second-generation ethanol from lignocellulosic feedstocks, both as agricultural coproducts and wastes and dedicated crops. EC Directive 2009 addressed the importance of commercializing second-generation biofuels [2]. The United States, as one of the leading nations in promoting biofuels, proposed that cellulosic ethanol must achieve 44% of the total biofuel production by 2020 [3].

With the development of the cellulosic technology being able to convert agricultural coproducts of often lower value to ethanol, two major questions are raised when comparing second-generation bioethanol to fossil fuel and first-generation bioethanol. (1) Is second-generation ethanol a better option for energy conservation? (2) What are the environmental benefits of second-generation ethanol? In order to answer the first question efforts were exerted on energy analysis of ethanol from corn stover [4, 5], switchgrass [6–9], and woodchip [7, 10]. Most of these studies yield

a positive net energy value (NEV), which indicates that lignocelluloses are more favourable feedstocks than dedicated crops, that is, corn grain. However, Pimentel and Patzek [7] exceptionally reported negative NEV from switchgrass- and wood-ethanol systems concluding that cellulosic ethanol processes are more energy intensive than ethanol from corn grain. With respect to the second question many life cycle assessment (LCA) studies were conducted on ethanol from lignocelluloses such as corn stover [11–15], Switchgrass [9, 11], Miscanthus and willow [16], sugarcane bagasse [17, 18], cereal straw [19], woodchip and wood wastes [20–22], flax shives [23], and hemp hurds [24]. All these studies, to different extent, show environmental benefits especially in terms of reduced fossil resource depletion and GHG emissions.

However, these studies on both energy analysis and LCA of second-generation bioethanol raise a number of questions. First of all, there is insufficient consistency regarding the definition of system boundaries, with different choices made without explicit arguments. For instance, an ethanol refining system does not include the environmental impact from the production of cellulase enzyme for degrading cellulosic feedstocks [25], leaving out a major energy requiring process. Secondly, in different studies allocation methods are different and not systematic and mostly are unclearly stated. A high sensitivity to the allocation method has been reported for LCA results when evaluating carbon intensity and fossil energy consumption for bioethanol pathways [12, 20, 26, 27]. The differences and ambiguities in the definition of system boundaries and allocation methodology made most of the studies incomparable.

To allow for a direct and meaningful comparison of different analysis, Farrell et al. [6] aligned methods and assumptions for six selected studies [7, 8, 28–30] and removed differences in the underlying data. Their focus, however, is mostly on corn-based ethanol. They indicate that calculations of NEV are highly sensitive to assumptions about both system boundaries and key parameter values and, as to content. They conclude that large-scale use of fuel ethanol certainly requires more sustainable practices in agriculture and advanced technologies, shifting from corn based to cellulosic ethanol production.

In order to have an overview of the energy intensity and environmental performance of bioethanol production from different lignocellulosic feedstocks, we have conducted five LCA studies at CML [12, 18, 23, 24, 31] and two studies on energy analysis [5, 32] of bioethanol from lignocelluloses, in all of which the same technologies were used to convert cellulose and hemicellulose to ethanol and to generate heat and power from lignin and wastes, the same system boundaries were defined, and the same allocation procedures were followed. In all LCA studies a comprehensive set of environmental impacts is used, ranging from abiotic depletion and GHG emissions to acidification and toxicity aspects. The present study summarizes and compares the results obtained from these five LCA studies and the two energy analyses, also in comparison with other studies.

2. Life Cycle Assessment (LCA)

2.1. Methodology. All five case studies compared in the present study focus on LCA of fuel ethanol from lignocellulosic feedstocks, with application of different allocation methods and/or scenario analysis. In all studies advanced cellulosic processing technology is assumed to convert biomass to ethanol, the system boundaries are identical, and the same allocation procedure is applied. Therefore they are well comparable. The feedstocks in these studies are summarized as follows:

(1) corn stover [12],

(2) sugarcane and bagasse [18],

(3) switchgrass [31],

(4) flax shives [23],

(5) hemp hurds [24].

In this section the methodologies used in all five studies are described. It is worth noting that study (2) presents a comparative LCA of ethanol production from solely sugar (current practice) and sugar plus bagasse (future case). As combining sugar and bagasse as feedstock for ethanol production is proposed to be a common practice in Brazil in the future, we did not perform an LCA on ethanol derived solely from bagasse. Thus the future case presented in study (2) is used to compare with other four studies, even though the feedstock includes not only the lignocellulose (bagasse) but also sugar.

2.1.1. Functional Unit and Alternatives. The functional unit in all studies is defined as power to wheels for one kilometre driving of a midsize flexible fuelled vehicle (FFV), which means that engine modification can be left out of account. Four fuel alternatives are considered: (1) conventional gasoline, (2) a blend of 90% gasoline with 10% ethanol by volume (termed E10), (3) a blend of 15% gasoline with 85% ethanol by volume (termed E85), and (4) pure ethanol. In practice pure ethanol is not used as transport fuel; hence it is only a hypothetical case here for easy comparison with gasoline.

2.1.2. System Boundaries. The systems defined in all five studies are based on the "cradle-to-grave" approach, which includes crude oil extraction and refinery, with all transport required, and agriculture production of lignocellulosic biomass, harvest and transport of biomass to ethanol refinery, production of ethanol and its coproducts, blend and transport all fuels to regional storages, and the final use phase of fuels in vehicle driving. The production and transport of chemicals used in all processes are also taken into account. Moreover, emissions from capital goods production and waste management are included. However, emissions and wastes associated with the production and disposal of the FFV are outside the system boundaries.

In all five studies different coproducts are produced from either agricultural production or ethanol refinery, as listed in Table 1. In fact, in study (1), (2), (4), and (5) electricity is also cogenerated from the ethanol refinery; however, it is

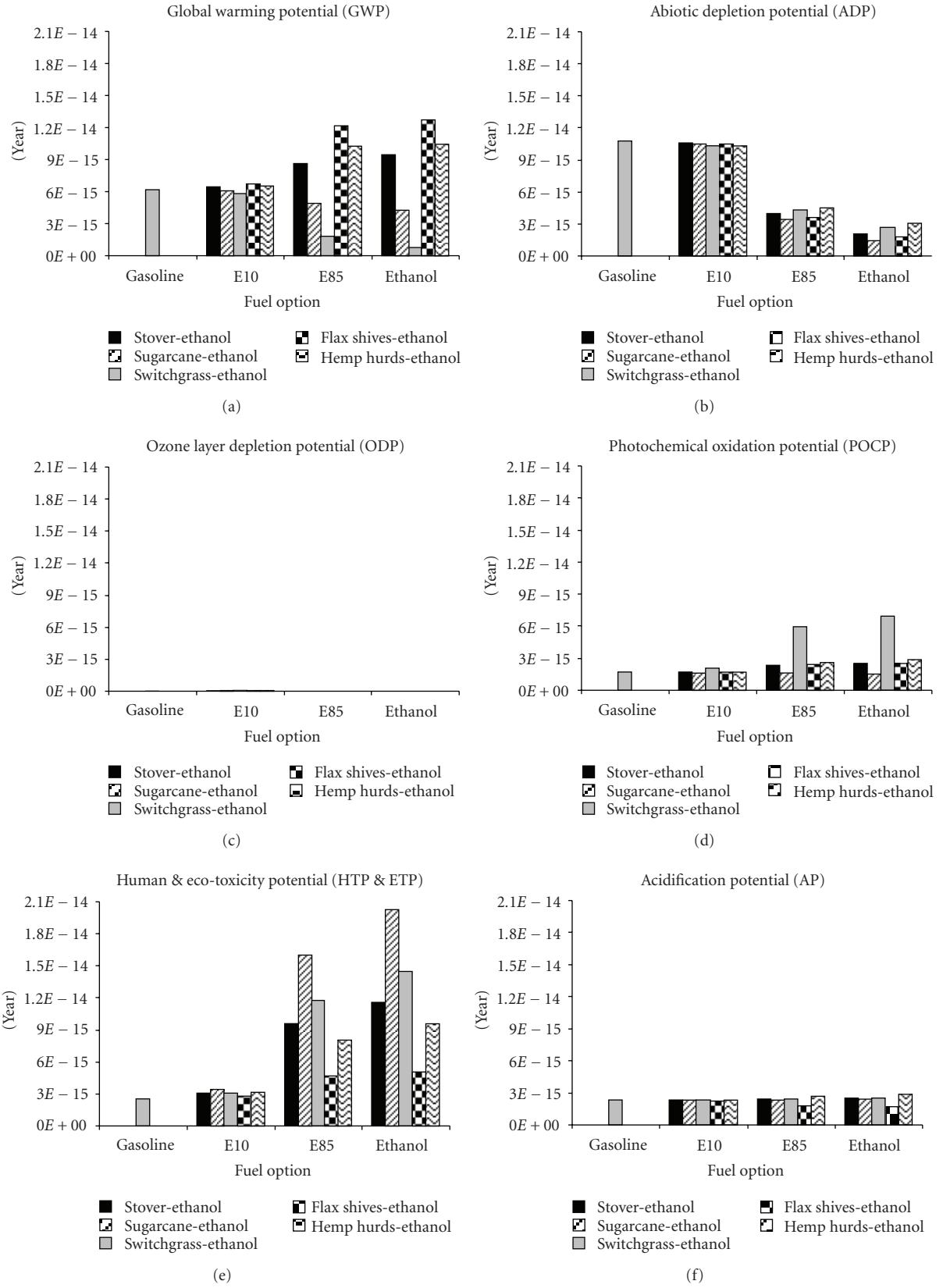

Figure 1: Continued.

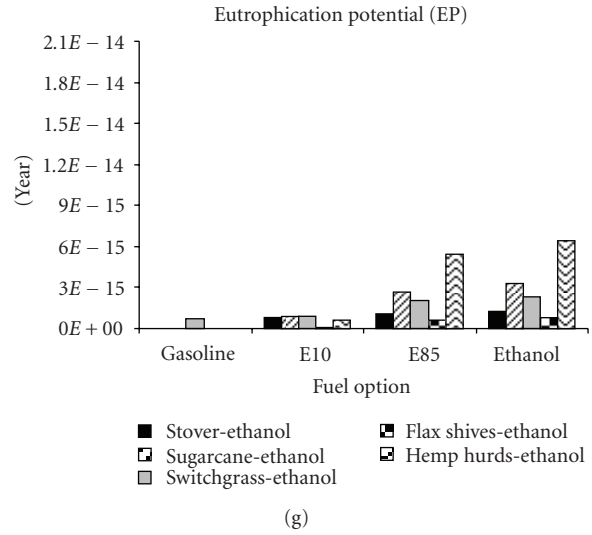

Figure 1: Overall comparison of environmental impact of all fuel options in all studies.

Table 1: Product and coproducts from agriculture and ethanol refinery.

Study	Products			
	Agriculture		Ethanol refinery	
	Product	Coproducts	Product	Coproducts
(1) Luo et al. [12]	Corn	Stover	Ethanol	—
(2) Luo et al. [18]	Sugarcane	—	Ethanol	Sugar
(3) Bai et al. [31]	Switchgrass	—	Ethanol	Electricity
(4) González García et al. [23]	Shives	Fibres & linseed	Ethanol	—
(5) González García et al. [24]	Hurds	Fibres & dust	Ethanol	—

fully utilized by the refinery and no surplus can be considered as co-product. In study (2) extra electricity needs to be purchased from local grid due to the insufficiency of the cogenerated electricity inside the refinery.

2.1.3. Data Sources and Software. Life cycle inventory (LCI) data used in all studies are obtained from different sources, as summarized in Table 2. The completeness of data may differ between sources; therefore, the Ecoinvent database from Swiss Centre of Life Cycle Inventories [33] is used as a standard whenever possible, as this source has long learning experience and involves a very broad range of processes (around 4,000). Software package Chain Management by Life Cycle Assessment (CMLCA) is used for the analysis [34].

2.1.4. Allocation Method. The allocation procedure in multiproduct processes has been always one of the most critical issues in LCA. The ISO 14040 and 14044 [51, 52] recommend a stepwise procedure for allocation. First of all, allocation should be avoided whenever possible through subdivision of certain processes or by expanding system boundaries so as to include the additional functions related to them. If allocation cannot be avoided, methods reflecting underlying physical relationships shall be applied, of how process inputs and outputs change due to a quantitative change in products and functions delivered. This is often filled in as allocation based on mass or energy content of the coproducts. To the extent that physical relations cannot be established, other relevant variables like economic values of the coproducts can be used to allocate. This last option is similar to the cost allocation methods used in managerial accounting [53, 54].

In all five studies, one allocation method is applied, followed by a sensitivity analysis when two or more allocation methods can be applied. In some studies methods based on mass or energy content cannot be applied systematically. For instance, in the case of electricity as a co-product in ethanol refinery, mass allocation is not applicable; in the case of sugar as a co-product, energy content allocation cannot be used. Therefore, in the present study, in order to permit a fair comparison, economic allocation, which is used in all five studies, is applied. In no case the more general ISO requirements on physical allocation have been used or met. The multiproduct processes in these studies are given as follows:

(1) corn agriculture, where corn and stover are produced;

(2) ethanol production from sugarcane and bagasse, where ethanol and sugar are produced;

(3) ethanol production from switchgrass, where ethanol and electricity are produced;

Table 2: Data sources for the life cycle inventories of the five studies.

Subsystem	Data source
Corn agriculture	U.S. Life-Cycle Inventory Database [35]
Sugarcane agriculture	Macedo et al. [36]
Switchgrass agriculture	Bullard and Metcalfe [37]; Nemecek and Kägi [38]
Flax agriculture	Nemecek et al. [39], Hauschild [40], Audsley et al. [41], Arrouays et al. [42], EMEP/CORINAIR [43]
Hemp agriculture	Nemecek et al. [39], Hauschild [40], Audsley et al. [41], Arrouays et al. [42], EMEP/CORINAIR [43]
Biomass transport	Spielmann et al. [44]
Stover-ethanol production	Aden et al. [45]
Sugarcane-ethanol production	Efe et al. [46]
Switchgrass-ethanol production	Guerra Miguez et al. [47]
Flax shives-ethanol production	Aden et al. [45]
Hemp hurds-ethanol production	Aden et al. [45]
Ethanol transport	Spielmann et al. [44]
Gasoline production & transport	Swiss Centre of Life Cycle Inventories [33]
Emissions from capital goods production	EIPRO Database [48]
Emissions from vehicle driving	Kelly et al. [49], Reading et al. [50]
Background processes	Swiss Centre of Life Cycle Inventories [33]

Table 3: Partitioning factors for economic allocation in all five studies.

Study	Multiproducts	Partitioning factor
(1) Luo et al. [12]	Stover/corn	0.118/0.882
(2) Luo et al. [18]	Ethanol/sugar	0.837/0.163
(3) Bai et al. [31]	Ethanol/electricity	0.894/0.106
(4) González García et al. [23]	Shives/fibers/linseed	0.042/0.911/0.047
(5) González García et al. [24]	Hurds/fibers/dust	0.122/0.863/0.015

(4) flax agriculture, where flax fibres, shives, and linseed are produced;

(5) hemp agriculture, where hemp fibres, hurds, and dust are produced.

For the gasoline production, the allocations were taken as currently implemented in the Ecoinvent database by its designers, using different methods for different parts of the product system. This shortcoming is less relevant when comparing different biofuel options. The partitioning factors-based economic values in the five studies are given in Table 3. In study (4) and (5) the authors also conducted sensitivity analysis on the price of shives and hurds. For the comparison in the present study, an average price of flax shives and the price of hemp hurds in the base case scenario are taken.

2.1.5. Impact Assessment. The categories selected for impact assessment in all five studies are as follows:

(i) abiotic depletion potential (ADP),

(ii) global warming potential (GWP),

(iii) ozone layer depletion potential (ODP),

(iv) photochemical oxidation potential (POCP),

(v) human and ecotoxicity potential (HTP & ETP),

(vi) acidification Potential (AP),

(vii) eutrophication Potential (EP).

The environmental impacts addressed here reflect the differences between operations of vehicles fuelled with gasoline, E10, E85, and pure ethanol. The results are normalized to the "world total" in order to compare the importance of each impact. Overall evaluation requires weighting, which has not been applied in this study. The Handbook on Life Cycle Assessment [55] states: "Weighting is an optional step for all non-comparative assertions; there is no best available method and there is no recommended set of weighting factors." Nevertheless, for actual decision making some sort of weighting always is required.

2.2. Results Comparison and Discussion. The LCA results of fuel ethanol from the five different feedstocks compared with gasoline for each impact category are presented in Figure 1. In order to compare the relative size of results in different impact categories, they are normalized to "world total 1995" and are all set to the same scale. This normalised score indicates the percentage the system would contribute to the world total score on that impact, for the reference year taken.

2.2.1. Global Warming Potential (GWP). Global warming has always been considered as the most important category in biofuel LCA studies, a simple type of weighting. The results of GWP always draw special attention also due to the diversity of results between different studies. This stands also true in the present study. When sugarcane and switchgrass are the energy crops, ethanol fuels show better performance than gasoline. The reason for the decrease of GHG emissions is the large amount of CO_2 taken up by the growth of sugarcane and switchgrass. Moreover, switchgrass seems to be a better feedstock than sugarcane because in the ethanol production from switchgrass, there is surplus electricity which is sold to the local grid. However in the sugarcane-ethanol refinery, the cogenerated electricity is not enough to supply the refinery and additional electricity needs to be purchased from the grid. If the electricity supplied by the grid is also biobased in the future, its contribution to GHG emissions could be less.

However, when fuel ethanol is produced from corn stover, flax shives, and hemp hurds, the application of ethanol fuels leads to worse performance. Here the economic allocation applied in agriculture production in these three studies plays an important role. As compared to corn, flax, and hemp, the stover, shives, and hurds have much smaller partitioning factors due their low prices (see Table 3). Hence when economic allocation is applied, most of the CO_2 uptakes in agriculture are allocated on corn, flax, and hemp fibres. Flax shives turned out to be the worst feedstock due to its smallest allocation factor (0.042). The substantial influence of allocation methods on the outcome of GWP is illustrated in Section 2.2.3.

2.2.2. Other Impact Categories. In the other six impact categories, the results of driving on fuel ethanol from different feedstocks are also diverse. The level of ADP is significantly reduced when replacing gasoline with fuel ethanol, irrespective of the feedstock used. Apparently this is due to the replacement of fossil resources by biomass. The levels differ among the five studies insignificantly. The reasons for these differences can be the energy efficiency in agriculture as well as in ethanol refinery. To have a better understanding in which subprocesses are energy intensive, a detailed energy analysis is required.

Normalized ODP shows substantially lower level than other impacts, which means that it contributes relatively less to the world total, negligible in comparison. Among all the ethanol fuels, sugarcane-derived ethanol is the best option regarding ODP. This indicates that less fossil energy is used in the life cycle of sugarcane-ethanol. This result is in accordance with the one of ADP, where ethanol from sugarcane also leads to the lowest impact. The ODP levels of fuel ethanol from other feedstocks do not differ significantly. Overall, the ODP score can be left out of account in decision making. Even a very high weight on this impact could not make it a relevant one.

Regarding POCP level, again sugarcane-derived ethanol shows the best performance, which is slightly lower than gasoline. POCP is mainly contributed by the emissions from production and refining of oil and gas, and the volatile organic compounds in the gasoline and ethanol life cycle, respectively. Thus when shifting gasoline to ethanol fuels, the emissions from fossil resource extraction are reduced; however, the emissions from ethanol production and transport of chemicals are increased. In all ethanol life cycles except the one derived from sugarcane, the level of increase is higher than the one of reduction. Among all switchgrass-derived ethanol is the worst option due the large amount of acetaldehyde emitted from ethanol fermentation, which contributes 77% to its total POCP score [31]. This finding indicates that, although the processes for ethanol product have all been optimized, possibilities for further optimization with better technology need to be investigated to reduce environmental impact.

In the category concerning HTP and ETP, ethanol fuels all have higher impact than gasoline. The main contributors of human and eco-toxicity are the production of chemicals and machineries used in agriculture. Among ethanol fuels from different feedstocks, ethanol from sugarcane and switchgrass perform worse. This does not mean that their agriculture processes are more polluting. The reason for this is again the partitioning factors based on economic allocation in the agriculture of corn stover, flax shives, and hemp hurds. Large amount of emissions in these three cases are allocated on the main crops—corn, flax, and hemp.

The levels of AP increase slightly in all cases except flax shives-derived ethanol when replacing gasoline with ethanol fuels. This level is mainly contributed by ammonia emitted in agriculture, nitrogen oxides (NO_x) emissions from operation of lorries and FFV, and sulphur dioxide (SO_2) from oil refinery. Hence in ethanol life cycles, although less SO_2 is emitted from the oil refinery, ammonia emissions are not negligible. This results in worse performance of most of ethanol fuels. For the adverse results from shives-derived ethanol, the same reasoning as the one for HTP and ETP can be applied. As shives shares only a very small part of environmental burdens in agriculture, the level of AP is decreased.

With regards to EP the trend is similar to AP. The level of EP is mostly attributed to agriculture processes, especially the nitrate to ground water and nitrogen oxides (NO_x) to air from the application of nitrogen fertilizers. As flax shives has a much smaller allocation factor in agriculture than other feedstocks, it gives the best performance, followed by gasoline, and then stover, switchgrass and, sugarcane-derived ethanol. EP of hemp hurds-derived ethanol draws attention due to its significantly higher level compared to other fuel cycles. The main contributor of this is the large amount of nitrate leaching to fresh water.

In order to have a clear overview, the environmental performances per impact category from the best to the worse fuel option are summarized in Table 4.

It can be seen that different fuel options show better performance in different categories. The overall evaluation depends on the importance attached to each impact category. As weighting is not included in this study, it is impossible to draw conclusion on which fuel option is the best. However, as the results are normalized and are set to the same scale, it can

Table 4: Overall results of environmental performance of all fuel options in all studies.

Impact category	Environmental performance					
	Best	→				Worst
GWP	Swi	Sug	Gas	Sto	Hur	Shi
GWP (CO_2-neutral)	Sug	Swi	Shi	Sto	Hur	Gas
ADP	Sug	Shi	Sto	Swi	Hur	Gas
ODP	Sug	Sto	Swi	Shi	Hur	Gas
POCP	Sug	Gas	Sto	Shi	Hur	Swi
HTP & ETP	Gas	Shi	Hur	Sto	Swi	Sug
AP	Shi	Gas	Sug	Swi	Sto	Hur
EP	Shi	Gas	Sto	Swi	Sug	Hur

Gas: gasoline; Sto: stover-based ethanol; Sug: sugarcane-based ethanol; Swi: switchgrass-based ethanol; Shi: shives-based ethanol; Hur: hurds-based ethanol.

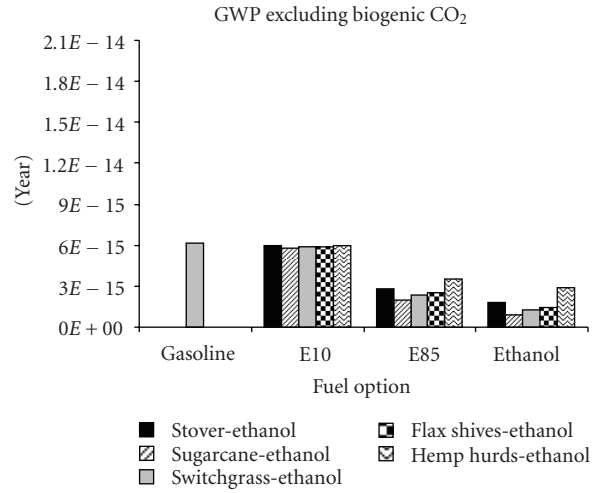

Figure 2: Results of GWP excluding biogenic CO_2 in all studies.

be seen that GWP, ADP, HTP, and ETP contribute relatively more to the world total; thus they deserve more attention when evaluating all the fuel options. POCP, AP, and EP are of less importance, and ODP definitely can be left out of account.

2.2.3. Influence of Methodology Choices. In the studies on stover, shives, and hurds-derived ethanol, sensitivity analyses on allocation methods were conduced. The results show that when allocations reflecting physically relationship (mass or energy content) are applied, GWP levels are significantly reduced. The reason for this outcome is that stover, shives, and hurds are agricultural coproducts which have low market prices when comparing to corn, flax, and hemp. When economic allocation is applied, most of the CO_2 uptake is allocated to the crops due to their large partitioning factors; however, when mass or energy content-based allocation is applied, the amount of CO_2 uptake allocated to stover, shives, and hurds increases due to the large amount produced. For toxic effects of pesticide use, economic allocation similarly leads to a very low share, and allocation by mass would increase the already high human and ecotoxicity scores substantially. This allocation dependency of outcomes has been explained in more details in three of the studies [12, 23, 24]. Therefore allocation issues are of crucial importance in LCA studies applied to biofuels and should be discussed explicitly whenever it is concerned.

In most of the studies the usual allocation procedure is followed dealing with CO_2 uptake and CO_2 emissions—the uptake counts as an extraction from atmosphere; hence the emissions of this biogenic CO_2 at combustion are counted just the same as fossil-based CO_2. In the field of LCA on biofuels, there also is a "CO_2-neutral" approach, which ignores both extractions and emissions of biogenic CO_2. In a straightforward system that does not require allocation; the net result should be the same. However, when allocation is needed, this may no longer be the case. As the allocation methods applied strongly influence the results of GWP scores, a comparative computation for the systems excluding biogenic CO_2 was made, and the results are given in Figure 2.

When biogenic CO_2 is excluded, reduction of GWP is achieved when replacing gasoline with ethanol fuels irrespective of the feedstocks used. As the switchgrass-ethanol system is relatively straightforward with only small amount of electricity cogenerated, its GWP levels do not differ significantly in both approaches (allocation versus CO_2 neutral). For the other four studies, as economic allocation plays an important role, the results turn to be very different in the "CO_2-neutral" approach. In fact, what has happened here by excluding biogenic CO_2 is that CO_2 escapes the selected allocation method. Instead, CO_2 is allocated in all cases on the basis of carbon share of the products. Therefore, implicitly, another way of allocating is introduced in the carbon neutral approach and here then mixed with economic allocation.

The choice of allocation influences the impact category of global warming more significantly, as the other categories refer to more specific process in the chain and, more importantly, do not deal with negative emissions.

3. Energy Considerations

3.1. Methodology. The purpose of this section is to understand whether second-generation bioethanol is more energy efficient compared to the first-generation. We have conducted two energy analyses on bioethanol from corn stover [5] and sugarcane [40]. In both studies the energy inputs of all subprocesses are calculated and the resulting net energy values (NEVs) are compared with literature studies on first-generation bioethanol from corn and sugarcane and second-generation ethanol from switchgrass. In our sugarcane-ethanol system, as the data used are from the same source as the ones in LCA study, two scenarios are considered: base case—ethanol and sugar are produced from the sugar extracted from cane, and bagasse is used for steam and electricity generation; future case—bagasse is also used for

ethanol production, and heat and power are generated from the lignin residues and wastes.

All relevant processes in biomass production and ethanol conversion are included in the system boundaries as well as capital goods production and wastes management. No allocation is involved in the foreground processes, as all the energy used to produce all coproducts is taken into account. Two types of NEV are estimated—with and without accounting for coproduct energy values.

The outcomes of these two studies are compared with the six literature studies on corn-ethanol summarized by Farrell et al. [7, 9, 28–30, 56], one study on switchgrass-ethanol [9] and three studies on sugarcane ethanol [28, 36, 57].

3.2. Results Comparison and Discussion. The net energy summaries excluding and including coproducts compared to the literature values are presented in Tables 5 and 6, respectively.

When coproducts are not included meaning that all the inputs and outputs are 100% allocated to stover, three studies on corn-ethanol result in negative net energy values due to their then seemingly more intensive agriculture practice. The other three studies on corn ethanol yield very small positive NEV values compared to the ones of ethanol from sugarcane and cellulosic feedstocks (stover and switchgrass). However, stover is a relatively bad feedstock due to its intensive agriculture production process. The reason why the energy use in agriculture per litre of ethanol in stover-ethanol case is the highest is that the yield of ethanol from stover is lower than the one from corn. In order to produce 1 litre of ethanol more stover is needed—the average ethanol yield of ethanol from corn is 0.4l/kg, while from stover it is only 0.3l/kg.

When the energy credits (taken as the energy content of the product) are taken into account for all coproducts, all studies yield positive net energy values. The highest NEV of stover-ethanol attributes to the co-product in agriculture—corn. The resulting NEVs from corn-ethanol studies become comparable with those from ethanol derived from switchgrass and sugarcane. In the study conducted by Hadzhiyska et al. [32] sugar is coproduced in the ethanol refinery in both base and future case; the values of net energy are significantly higher than the ones from other studies without sugar coproduction. This indicates that outcomes of net energy calculations depend on whether or not taking the energy values of coproducts into account.

As mentioned earlier, in our sugarcane-ethanol study, the base case demonstrates the current practice in Brazilian ethanol industries—ethanol and sugar are produced from sugar juice after cane milling, and steam and electricity are generated from combustion of bagasse; the future case presents the option that bagasse is also utilized for ethanol production, while heat and power are only generated from the lignin residues and wastes. In the base case 2.6 MJ/litre of surplus electricity is generated and sold to the grid; however, in the future case extra electricity needs to be purchased from the grid to supply the refinery. The results in Table 6 show that from an energy conservation perspective, it is better to use bagasse for electricity generation instead of ethanol production in such a refinery.

4. Conclusions and Recommendations

In the first part of this paper five studies on LCA of ethanol from lignocellulosic feedstocks are summarized. Seven impact categories are used for assessment and the results from different studies are compared per category. One interesting outcome is that ODP scores are quantitatively irrelevant in all cases, even if attributing a very high weight to this impact category. One limitation of the current method for life cycle impact assessment is that it does not reckon with the contribution of N_2O emissions to ODP, as recent findings show that N_2O now has become the major cause of depletion of ozone layer [58].

In terms of GWP when economic allocation is applied, switchgrass is the best energy crop, followed by sugarcane. In both cases significant reductions of GHG emissions are achieved, which attributes to the CO_2 uptake in agriculture. The electricity surplus generated in switchgrass-ethanol refinery also helps reduce the GHG emissions in the life cycle of ethanol fuels. The application of ethanol fuels from stover, shives, and hurds leads to worse performance than gasoline, due to the small partitioning factors based on economic allocation in agriculture. When the "CO_2-netural" approach is applied, reduction of GHG emissions is achieved by ethanol fuels from all feedstocks, compared to gasoline. Sugarcane, in this approach, becomes the most favourable feedstock, followed by switchgrass.

Sugarcane-derived ethanol turns out to be the best option in terms of ADP, ODP, and POCP. Its less energy intensive agriculture and ethanol process lead to less fossil resource extraction and related emissions which contributes POCP significantly. Ethanol derived from corn stover and flax shives shows modest performance, and hemp hurds and switchgrass are unfavourable feedstocks in these three categories.

In the category of HTP and ETP and AP and EP, flax shives-derived ethanol shows the best environmental performance among all the ethanol fuels. As the agriculture practices, especially the production machineries and application of fertilizers, contribute most to these impact, flax shives, sharing only small part of environmental burdens due to its small allocation factor (0.042), becomes the most promising feedstock.

In most of the categories hemp hurds-derived ethanol shows the worst performance due to its intensive agriculture practice. Thus this feedstock is not recommended for ethanol production, which may then be utilized directly for heat and power generation, unless its agriculture process can be significantly improved.

In many impact categories (GWP, POCP, HTP & ETP, AP and EP) ethanol fuels as a whole do not show advantages over gasoline, which means that strong promotion of bioethanol as a transport fuel needs to be carefully considered. More advanced technologies with optimization of energy use and emissions in both agriculture and ethanol refinery still need to be developed to reduce the current relatively high scores.

It is worth noting that in the sugarcane-ethanol study, ethanol is converted from both sugar and bagasse, as it is

Table 5: Net energy summary excluding coproducts, no allocation.

Feedctock		Energy use (MJ/L[a])					
		Agriculture	Biorefinery	Total input	Ethanol[b]	Total output	Net energy value (NEV)
Stover	Luo et al. [5]	10.0	0.5	**10.5**	21.2	**21.2**	**10.7**
Corn	Patzek [56]	9.9	17.0	**26.9**	21.2	**21.2**	**−5.7**
	Pimentel and Patzek [7]	10.0	17.0	**27.0**	21.2	**21.2**	**−5.8**
	Shapouri and McAloon [30]	5.3	15.2	**20.5**	21.2	**21.2**	**0.7**
	Graboski [29]	5.6	16.6	**22.2**	21.2	**21.2**	**−1.0**
	Dias de Oliveira et al. [28]	6.3	14.1	**20.4**	21.2	**21.2**	**0.8**
	Wu et al. [9]	6.6	12.5	**19.1**	21.2	**21.2**	**2.1**
Switchgrass	Wu et al. [9]	2.4	1.0	**3.4**	21.2	**21.2**	**17.8**
Sugarcane	Hadzhiyska et al. (base case) [32]	6.5	0.1	**6.6**	21.2	**21.2**	**14.6**
	Hadzhiyska et al. (future case) [32]	2.7	0.5	**3.2**	21.2	**21.2**	**18.0**
	Pimentel and Patzek [57]	2.6	3.4	**6.0**	21.2	**21.2**	**15.2**
	Diaz de Oliveira et al. [28]	5.6	0.6	**6.2**	21.2	**21.2**	**15.0**
	Macedo et al. [36]	2.0	0.3	**2.3**	21.2	**21.2**	**18.9**

[a]The unit of energy use is MJ per litre of ethanol produced from biorefinery. [b]Normalized energy value for ethanol based on lower heating value (LHV).

proposed to be the common practice in the future in Brazil. In the future research, in order to know whether bagasse is a promising lignocellulosic feedstock, environmental performance of ethanol fuels from bagasse shall be studied.

The choice of allocation methodology is essential for the outcomes especially related to GHG emissions. As this is an important issue and one of the main reasons for considering biofuels as a replacement of fossil fuels, it should be given special attention in life cycle-based studies of biofuels. In order to support decision making, sensitivity analysis shall always be conducted whenever more than one allocation methods can be applied. Furthermore, the results from the "CO_2-neutral" approach seem to be more realistic, as GWP levels are highly affected by the allocation methods applied. It is important that LCA practitioners realize this and deal with it in an appropriate manner.

Although the LCA results from only five studies are compared, these five feedstocks can, to certain extent, represent other lignocelluloses. This paper gives an indication on the environmental performance of second-generation bioethanol as a whole in comparison with gasoline; hence it contributes significantly to the current debate on the importance of biofuels in future energy mix.

LCA methodology as its stands cannot capture all the relevant environmental impacts. Direct and indirect land use and competition with food products do not fit well into the LCA framework. A broader approach to expand LCA studies to include these impacts is required in future research.

The second part of this paper summarizes the NEV results from ethanol from stover and sugarcane and compares them with literature values. Two approaches are considered—excluding and including co-product energy credits. This is in fact similar to the allocation issue which has been extensively discussed in the stover-ethanol study [12]. In order to prevent applying allocation procedure, here "including co-product credits" is similar to the "system expansion" approach LCA studies while "excluding co-product credits" means "cut-off of coproducts/wastes".

When coproducts are not included, three studies on corn-ethanol result in a negative NEV. The others result in positive values with different degrees. Sugarcane and lignocellulosic feedstocks are more favourable due to their less energy intensive agriculture practice and refining process. The low-energy inputs in these ethanol refining processes are due to the steam and electricity cogeneration inside refineries. This suggests that cogeneration of heat and power from process wastes is an important way to increase energy efficiency in the cellulosic ethanol process.

When the energy credits of all coproducts are taken into account, all studies yield positive net energy values with the highest from stover-ethanol case. Accounting for the energy values of coproducts especially corn, stover, and sugar produced in different cases affects strongly the performance of most cases from an energy perspective. This issue of co-product credits is in fact similar to the allocation issue in LCA studies but is only solved here in a different manner.

Table 6: Net energy summary including coproducts, no allocation.

Feedstock		Energy use (MJ/L[a])							
		Agriculture	Biorefinery	Total input	Ethanol[b]	Coproducts in agriculture[c]	Coproducts in bioreinery[d]	Total output	Net energy value (NEV)
Stover	Luo et al. [5]	10.0	0.5	**10.5**	21.2	85.2	0.2	**106.6**	**96.1**
Corn	Patzek [56]	9.9	17.0	**26.9**	21.2	25.9	4.1	**51.2**	**24.3**
	Pimentel and Patzek [7]	10.0	17.0	**27.0**	21.2	25.9	1.9	**49.0**	**22.0**
	Shapouri and McAloon [30]	5.3	15.2	**20.5**	21.2	24.0	7.3	**52.5**	**32.0**
	Graboski [29]	5.6	16.6	**22.2**	21.2	24.6	4.1	**49.9**	**27.7**
	Diaz de Oliveira et al. [28]	6.3	14.1	**20.4**	21.2	24.6	4.1	**49.9**	**29.5**
	Wu et al. [9]	6.6	12.5	**19.1**	21.2	24.6	4.0	**49.8**	**30.7**
Switchgrass	Wu et al. [9]	2.4	1.0	**3.4**	21.2	0.0	4.8	**26.0**	**22.6**
Sugarcane	Hadzhiyska et al. (base case) [32]	6.5	0.1	**6.6**	21.2	0.0	32.7	**53.9**	**47.3**
	Hadzhiyska et al. (future case) [32]	2.7	0.5	**3.2**	21.2	0.0	12.6	**33.8**	**30.6**
	Pimentel and Patzek [57]	2.6	3.4	**6.0**	21.2	0.0	0.0	**21.2**	**15.2**
	Diaz de Oliveira et al. [28]	5.6	0.6	**6.2**	21.2	0.0	1.1	**22.3**	**16.1**
	Macedo et al. [36]	2.0	0.3	**2.3**	21.2	0.0	3.0	**24.2**	**21.9**

[a]The unit of energy use is MJ per litre of ethanol produced from biorefinery.
[b]Normalized energy value for ethanol based on lower heating value (LHV).
[c]In stover-ethanol study it refers to the corn as a coproduct in the agriculture; in the other six studies on corn-ethanol it refers to the harvested stover (60%, dry mass basis) as a coproduct, and the values are estimated in this study.
[d]In stover-ethanol and switchgrass-ethanol study it refers to electricity; in corn-ethanol studies it refers to a range of products from corn milling, such as dried distiller grains, corn gluten feed, and corn oil; in sugarcane-ethanol study it refers to electricity surplus or/and bagasse.

The results of the sugarcane-ethanol cases conducted by us show that it is better to use bagasse for electricity generation instead of ethanol production in such a refinery. Here we assume the "grid" as the average electricity mix from Ecoinvent database. If the electricity supplied by the grid can be produced fully from renewable sources in the future, the outcomes would be different.

The changes occurred after taking all coproducts into account are striking in the case of ethanol derived from corn, stover, and sugarcane [32] due to the large amount of stover (not using corn), corn (not using stover), and sugar coproduced. Literature studies on energy assessment are not conducted in a consistent way when co-product energy credits are concerned. For instance, Pimentel and Patzek in [7, 56, 57] conclude negative NEV without accounting for the energy value of the coproducts which can be produced from the ethanol life cycle. Farrell et al. [6] reckon with the coproducts from corn-ethanol biorefinery for these studies, but not the stover produced from agriculture. Our study shows the importance and urgency of developing a consistent and relevant methodology for energy analysis in biofuel research.

As we account for total energy inputs and outputs, which means that no allocation method is applied, taking all coproducts into account becomes essential. To assess the energy flow of only one main product, an allocation based on energy content may be applied in some cases, that is, between corn and stover, and between ethanol and electricity. Nevertheless, for the combined production of ethanol and sugar, it is difficult as the energy values of sugar and ethanol do not belong to the same category (food versus energy product).

Although we compare studies on only four feedstocks, they are representative in the debate on energy analysis of first- and second-generation bioethanol. Irrespective of the methodology used, switchgrass and sugarcane seem to be good feedstocks for ethanol production due to their low-energy use in agricultural production and good environmental performance.

Acknowledgment

This project is financially supported by The Netherlands Ministry of Economic Affairs and the B-Basic partner organi-

zations (http://www.b-basic.nl/) through B-Basic, a public-private NWO-ACTS program (ACTS: Advanced Chemical Technologies for Sustainability).

References

[1] "Renewable Energy Road Map—Renewable energies in the 21st century," building a more sustainable future. 2007. COM, 848 final, 2006.

[2] "Directive 2009/28/EC of the European Parliament and of the Council," 2009.

[3] DOE/EIA-0383, *Annual Energy Outlook 2008 with Projections to 2030*, U.S. Energy Information Administration, Washington, DC, USA, 2008.

[4] A. Lavigne and S. E. Powers, "Evaluating fuel ethanol feedstocks from energy policy perspectives: a comparative energy assessment of corn and corn stover," *Energy Policy*, vol. 35, no. 11, pp. 5918–5930, 2007.

[5] L. Luo, E. van der Voet, and G. Huppes, "An energy analysis of ethanol from cellulosic feedstock-Corn stover," *Renewable and Sustainable Energy Reviews*, vol. 13, no. 8, pp. 2003–2011, 2009.

[6] A. E. Farrell, R. J. Plevin, B. T. Turner, A. D. Jones, M. O'Hare, and D. M. Kammen, "Ethanol can contribute to energy and environmental goals," *Science*, vol. 311, no. 5760, pp. 506–508, 2006.

[7] D. Pimentel and T. W. Patzek, "Ethanol production using corn, switchgrass, and wood; biodiesel production using soybean and sunflower," *Natural Resources Research*, vol. 14, no. 1, pp. 65–76, 2005.

[8] M. Wang, "Developing and use of GREET 1.6 fuel-cycle model for transportation fuels and vehicle technologies," Tech. Rep. ANL/ESD/TM-163, Argonne National Laboratory, Argonne, Ill, USA, 2001.

[9] M. Wu, Y. Wu, and M. Wang, "Energy and emission benefits of alternative transportation liquid fuels derived from switchgrass: a fuel life cycle assessment," *Biotechnology Progress*, vol. 22, no. 4, pp. 1012–1024, 2006.

[10] C. A. Cardona Alzate and O. J. Sánchez Toro, "Energy consumption analysis of integrated flowsheets for production of fuel ethanol from lignocellulosic biomass," *Energy*, vol. 31, no. 13, pp. 2447–2459, 2006.

[11] S. Kim, B. E. Dale, and R. Jenkins, "Life cycle assessment of corn grain and corn stover in the United States," *International Journal of Life Cycle Assessment*, vol. 14, no. 2, pp. 160–174, 2009.

[12] L. Luo, E. van der Voet, G. Huppes, and H. A. Udo de Haes, "Allocation issues in LCA methodology: a case study of corn stover-based fuel ethanol," *International Journal of Life Cycle Assessment*, vol. 14, no. 6, pp. 529–539, 2009.

[13] E. Searcy and P. C. Flynn, "Processing of straw/corn stover: comparison of life cycle emissions," *International Journal of Green Energy*, vol. 5, no. 6, pp. 423–437, 2008.

[14] J. Sheehan, A. Aden, K. Paustian, et al., "Energy and environmental aspects of using corn stover for fuel ethanol," *Journal of Industrial Ecology*, vol. 7, no. 3-4, pp. 117–146, 2004.

[15] S. Spatari, Y. Zhang, and H. L. Maclean, "Life cycle assessment of switchgrass- and corn stover-derived ethanol-fueled automobiles," *Environmental Science and Technology*, vol. 39, no. 24, pp. 9750–9758, 2005.

[16] D. Styles and M. B. Jones, "Life-cycle environmental and economic impacts of energy-crop fuel-chains: an integrated assessment of potential GHG avoidance in Ireland," *Environmental Science and Policy*, vol. 11, no. 4, pp. 294–306, 2008.

[17] T. Botha and H. von Blottnitz, "A comparison of the environmental benefits of bagasse-derived electricity and fuel ethanol on a life-cycle basis," *Energy Policy*, vol. 34, no. 17, pp. 2654–2661, 2006.

[18] L. Luo, E. van der Voet, and G. Huppes, "Life cycle assessment and life cycle costing of bioethanol from sugarcane in Brazil," *Renewable and Sustainable Energy Reviews*, vol. 13, no. 6-7, pp. 1613–1619, 2009.

[19] B. Gabrielle and N. Gagnaire, "Life-cycle assessment of straw use in bio-ethanol production: a case study based on biophysical modelling," *Biomass and Bioenergy*, vol. 32, no. 5, pp. 431–441, 2008.

[20] T. Beer and T. Grant, "Life-cycle analysis of emissions from fuel ethanol and blends in Australian heavy and light vehicles," *Journal of Cleaner Production*, vol. 15, no. 8-9, pp. 833–837, 2007.

[21] G. Z. Fu, A. W. Chan, and D. E. Minns, "Life cycle assessment of bio-ethanol derived from cellulose," *International Journal of Life Cycle Assessment*, vol. 8, no. 3, pp. 137–141, 2003.

[22] A. J. Kemppainen and D. R. Shonnard, "Comparative life-cycle assessments for biomass-to-ethanol production from different regional feedstocks," *Biotechnology Progress*, vol. 21, no. 4, pp. 1075–1084, 2005.

[23] S. González García, L. Luo, M. T. Moreira, G. Feijoo, and G. Huppes, "Life cycle assessment of flax shives derived second generation ethanol fueled automobiles in Spain," *Renewable and Sustainable Energy Reviews*, vol. 13, no. 8, pp. 1922–1933, 2009.

[24] S. González García, L. Luo, M. T. Moreira, G. Feijoo, and G. Huppes, "Fuel ethanol from hemp hurds: environmental performance," submitted.

[25] J. Sheehan, A. Aden, and C. Riley, "Is ethanol from corn stover sustainable? Adventures in cyber-farming: a life cycle assessment of the production of ethanol from corn stover for use in a flex fuel vehicle," Draft Report for Peer Review, NREL, Golden, Colo, USA, 2002.

[26] S. Kim and B. E. Dale, "Allocation procedure in ethanol production system from corn grain: I. System expansion," *International Journal of Life Cycle Assessment*, vol. 7, no. 4, pp. 237–243, 2002.

[27] J. Malça and F. Freire, "Renewability and life-cycle energy efficiency of bioethanol and bio-ethyl tertiary butyl ether (bioETBE): assessing the implications of allocation," *Energy*, vol. 31, no. 15, pp. 3362–3380, 2006.

[28] M. E. Dias de Oliveira, B. E. Vaughan, and E. J. Rykiel Jr., "Ethanol as fuel: energy, carbon dioxide balances, and ecological footprint," *BioScience*, vol. 55, no. 7, pp. 593–602, 2005.

[29] M. Graboski, *Fossil Energy Use in the Manufacture of Corn Ethanol*, National Corn Growers Association, Washington, DC, USA, 2002.

[30] H. Shapouri and A. McAloon, *The 2001 Net Energy Balance of Corn-Ethanol*, U.S. Department of Agriculture, Washington, DC, USA, 2002.

[31] Y. Bai, L. Luo, and E. van der Voet, "Life cycle assessment of switchgrass-derived ethanol as transport fuel," *International Journal of Life Cycle Assessment*, vol. 15, pp. 468–477, 2010.

[32] D. Hadzhiyska, L. Luo, and E. van der Voet, "An energy analysis of ethanol from sugar cane," CML Report, Leiden, The Netherlands, 2009.

[33] "Swiss Centre of Life Cycle Inventories," June 2007, http://www.ecoinvent.org/.

[34] "Chain Management by Life Cycle Assessment (CMLCA)," May 2007, http://cml.leiden.edu/software/software-cmlca.html.

[35] "U.S. Life-Cycle Inventory Database," June 2007, http://www.nrel.gov/lci/.

[36] I. C. Macedo, M. R. L. V. Leal, and J. E. A. R. da Silva, "Assessment of greenhouse gas emissions in the production and use of fuel ethanol in Brazil," Report, Government of the State of São Paulo and Secretariat of the Environment, São Paulo, Brazil, 2004.

[37] M. Bullard and P. Metcalfe, "Estimating the energy requirement and CO_2 emissions from production of the perennial grasses miscanthus, switchgrass and reed canary grass," Tech. Rep. ETSU B/U1/00645/REP.

[38] T. Nemecek and T. Kägi, "Life cycle inventories of Swiss and European agricultural production systems," Ecoinvent Report 15, Swiss Centre for Life Cycle Inventories, Dübendorf, Switzerland, 2007.

[39] T. Nemecek, A. Heil, O. Huguenin, et al., "Life cycle inventories of agricultural production systems," Ecoinvent Report 15, Swiss Centre for Life Cycle Inventories, Dübendorf, Switzerland, 2004.

[40] M. Z. Hauschild, "Estimating pesticide emissions for LCA of agricultural products," in *Agricultural Data for Life Cycle Assessments*, B. P. Weidema and M. J. G. Meeusen, Eds., vol. 2, pp. 64–79, LCANet Food, The Hague, The Netherlands, 2000.

[41] E. Audsley, S. Alber, R. Clift, et al., "Harmonization of environmental life cycle assessment for agriculture," Concerted Action AIR3-CT94-2028, European Commission. DG VI Agriculture. SRI, Silsoe, UK, 1997.

[42] D. Arrouays, J. Balesdent, J. C. Germon, P. A. Jayet, J.F. Soussana, and P. Stengel, "Contribution à la lutte contre l'effet de serre. Stocker du carbone dans les sols agricoles de France? Expertise scientifique collective," Rapport d'expertise réalisé par INRA à la demande du Ministère de l'Ecologie et du Développement Durable, INRA, Paris, France, 2002.

[43] EMEP/CORINAIR, "Atmospheric emission inventory guidebook," Tech. Rep. 11, European Environment Agency, Copenhagen, Denmark, 2006.

[44] M. Spielmann, T. Kägi, P. Stadler, and O. Tietje, "Life cycle inventories of transport services," Ecoinvent Report 14, Swiss Centre for Life Cycle Inventories, Dübendorf, Switzerland, 2004.

[45] A. Aden, M. Ruth, and K. Ibsen, "Lignocellulosic biomass to ethanol process design and economics utilizing co-current dilute acid prehydrolysis and enzymatic hydrolysis for corn stover," Tech. Rep. NREL/TP-510-32438, 2002.

[46] Ç. Efe, A. J. J. Straathof, and L. A. M. van der Wielen, "Technical and economical feasibility of production of ethanol from sugarcane and sugarcane bagasse," in *B-Basic Internal Report*, 2005.

[47] O. Guerra Miguez, D. Siva Siddarthan, and D. A. Suárez Zuluaga, "Technical and economical feasibility of production of ethanol from switchgrass," in *B-Basic Internal Report*, Delft University of Technology, Delft, The Netherlands, 2009.

[48] A. Tukker, G. Huppes, J. B. Guinée, et al., "Environmental Impact of Products (EIPRO)—Analysis of the life cycle environmental impacts related to the final consumption of the EU-25," 2005.

[49] K. J. Kelly, B. K. Bailey, T. C. Coburn, W. Clark, and P. Lissiuk, "Federal test procedure emissions test results from ethanol variable-fuel vehicle Chevrolet Luminas," in *Society for Automotive Engineers, International Spring Fuels and Lubricants Meeting*, Dearborn, Mich, USA, 1996.

[50] A. H. Reading, J. O. W. Norris, E. A. Feest, and E. L. Payne, "Ethanol emissions testing," AEAT unclassified E&E/DDSE/02/021, Issue 3, 2002.

[51] ISO Norm 14040, "Life cycle assessment: principles and framework," Environmental management, 2006.

[52] ISO Norm 14044, "Life cycle assessment: requirement and guidelines," Environmental management, 2006.

[53] G. Huppes, *Macro-Environmental Policy: Principles and Design*, Elsevier, Amsterdam, The Netherlands, 1993.

[54] J. B. Guinée, R. Heijungs, and G. Huppes, "Economic allocation: examples and derived decision tree," *International Journal of Life Cycle Assessment*, vol. 9, no. 1, pp. 23–33, 2004.

[55] J. B. Guinée, Ed., *Handbook on Life Cycle Assessment—Operational Guide to the ISO Standard*, Kluwer Academic Publishers, Dodrecht, The Netherlands, 2002.

[56] T. W. Patzek, "Thermodynamics of the corn-ethanol biofuel cycle," *Critical Reviews in Plant Sciences*, vol. 23, no. 6, pp. 519–567, 2004.

[57] D. Pimentel and T. Patzek, "Ethanol production: energy and economic issues related to U.S. and Brazilian sugarcane," *Natural Resources Research*, vol. 16, no. 3, pp. 235–242, 2007.

[58] A. R. Ravishankara, J. S. Daniel, and R. W. Portmann, "Nitrous oxide (N_2O): the dominant ozone-depleting substance emitted in the 21st century," *Science*, vol. 326, no. 5949, pp. 123–125, 2009.

Hindawi Publishing Corporation
International Journal of Chemical Engineering
Volume 2010, Article ID 627930, 10 pages
doi:10.1155/2010/627930

Research Article

Energy from Waste: Reuse of Compost Heat as a Source of Renewable Energy

G. Irvine, E. R. Lamont, and B. Antizar-Ladislao

School of Engineering, Institute for Infrastructure and Environment, University of Edinburgh, William Rankine Building, The King's Buildings, Edinburgh EH9 3JL, UK

Correspondence should be addressed to B. Antizar-Ladislao, b.antizar-ladislao@ed.ac.uk

Received 10 December 2009; Accepted 14 April 2010

Academic Editor: Michael K. Danquah

An in-vessel tunnel composting facility in Scotland was used to investigate the potential for collection and reuse of compost heat as a source of renewable energy. The amount of energy offered by the compost was calculated and seasonal variations analysed. A heat exchanger was designed in order to collect and transfer the heat. This allowed heated water of 47.3°C to be obtained. The temperature could be further increased to above 60°C by passing it through multiple tunnels in series. Estimated costs for installing and running the system were calculated. In order to analyse these costs alternative solar thermal and ground source heat pump systems were also designed. The levels of supply and economic performance were then compared. A capital cost of £11,662 and operating cost of £1,039 per year were estimated, resulting in a cost of £0.50 per kWh for domestic water and £0.10 per kWh for spatial heat. Using the heat of the compost was found to provide the most reliable level of supply at a similar price to its rivals.

1. Introduction

Composting is an aerobic process where organic materials are biologically decomposed, producing mainly compost, carbon dioxide, water, and heat. Conventional composting processes typically comprise four major microbiological stages in relation to temperature: mesophilic, thermophilic, cooling, and maturation, during which the structure of the microbial community also changes, and the final product is compost [1]. In recent years, the development and widespread use of more expensive in-vessel systems for the processing of biowastes has resulted from legislative pressures on the safety of the composting process and the subsequent use of the compost product [2]. Such systems allow for much more precise control of the composting process particularly in terms of moisture and temperature control [3]. Thus, current composting approaches and technologies tend to emphasize the use of high temperatures (>70°C) in order to meet regulatory requirements for pathogen control [2].

Compost has been widely used as soil conditioners and soil fertilizers. This practice is recommended, as soil fertility needs more than ever to be sustained. Food demand is increasing rapidly in non-OECD (Organisation for Economic Co-operation and Development) countries, and it is in those countries particularly where organic waste needs to be diverted from landfill sites to composting practices, so compost can enhance soil fertility [4]. In OECD countries, where composting of organic waste is already established, its use as a landfill cover to abate greenhouse gas emissions has shown to be promising [5]. The addition of compost can minimize land degradation and soil erosion. Additionally, composting can contribute to achieve sufficient hygienisation of organic wastes and control soilborn and airborn pathogens by promotion of beneficial micro-organisms and suppression of harmful micro-organisms [6].

As energy demand is increasing rapidly, bionergy is seen as one of the primary possibilities for preventing global warming [7]. At present, the immediate factor impeding the emergence of an industry converting biowastes into bioenergy on a large scale is the high cost of processing, rather than the cost or availability of biomass feedstock [8]. Thus, the challenge is to extend the amount of bioenergy that can be produced sustainably by using biowastes, such as municipal, industrial, and construction waste as biomass feedstocks [9]. Thus, it is suggested that the heat generated during composting processes can be reused as a renewable source of energy.

A limited number of previous studies has investigated the potential energy content of compost. A recent study reports that during high-temperature phases (~60°C) of municipal waste composting, on average 1136 kJ kg^{-1} of heat was released [10]. Similar values (961 kJ kg^{-1}) have been reported earlier with an average compost moisture content of 52.7% [11]. Heat produced during the composting of wheat straw and poultry droppings was approximately 17.06 MJ kg^{-1} [12] and 12.8 MJ kg^{-1} [13], respectively. Additionally, it has been reported that the compost from municipal waste is characterised by fairly low values of thermal conductivity coefficient (0.31 Wm^{-1}K^{-1} for a compost density of 600 kg m^{-3}, 60°C), and that an increase in temperature or density both lead to an increase in the thermal conductivity coefficient [10]. Thus, as the compost ages, and it suffers a reduction in density and temperature, the thermal conduction coefficient will decrease. Klejment and Rosiński (2008) concluded that the low value of heat conductivity coefficients does not allow compost to cool too fast and enables the application of a battery of heat exchangers. A limited number of studies on compost heat reuse has also been reported. Lekic [14] investigated the increase in water temperature between the inlet and the outlet of polyethylene pipes embedded in composting windrows and reported that 73% of the theoretical value of heat energy was transferred to the water. One main limitation of this study was the placement of the pipes within the compost mass. A solution proposed by Seki and Komori [15] involved using a packed column heating tower that transfers the heat from the warm exhaust air of the compost to a volume of water.

From the above, it is fully justified to investigate the potential reuse of compost heat as a source of renewable energy. Our primary objectives were (a) to identify the potential energy available through full-scale in-vessel composting units; (b) to identify potential technological solutions to harnessing/collecting the energy; (c) to identify the optimum alternative use for the energy collected; and (d) to critically evaluate the potential of reusing that heat from compost by comparing the performance with alternative renewable energies.

2. Materials and Methods

2.1. Site Description. This case study was focused upon the Deerdykes Composting Facility located in Scotland, UK. The facility was originally constructed on the site of a decommissioned sewage treatment works, where much of the existing infrastructure was able to be reused for the composting facility. Work was completed in 2006, and the site currently accepts green waste, industrial sludge, and liquid waste [16]. The main components of the site are the site office, the in-vessel composting tunnels, the windrow composting area, and the raw material mixing area (Figure 1).

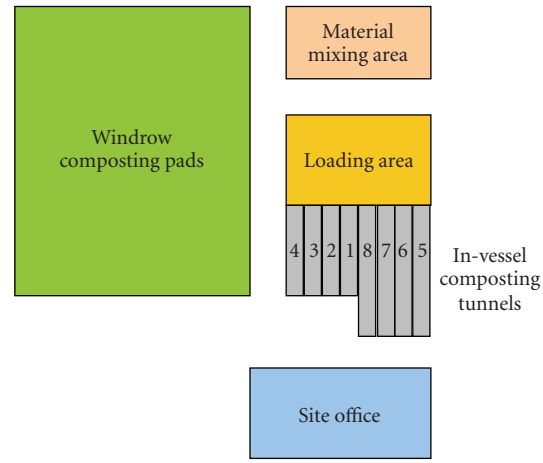

Figure 1: Deerdykes site layout.

2.2. In-Vessel Units' Description and Operation. There are 8 in-vessel composting tunnels that were constructed in the former presettlement tanks [16]. The dimensions of the tunnels varied with tunnels 1–4 being 5 m wide and 25 m long, tunnels 5 and 6 being 5.3 m wide and 35 m long, and tunnels 7 and 8 being 5 m wide and 35 m long. The tunnels were all approximately 5 m in height, however, compost was only loaded to a height of 3 m (Figure 2). Compost was loaded for an average period of 12–17 days, allowing a sanitary and stable condition of compost to be achieved. Air was supplied through small aeration holes in the floor of the tunnel thus ensuring aerobic conditions were maintained throughout the compost mass. The air drawn off from the top was primarily recirculated through the compost with a small portion expelled as exhaust air. Additionally, fresh air was mixed with the recirculated air to ensure oxygen concentrations were maintained at acceptable levels.

The exhaust air was put through two stages of treatment. Firstly, the wet scrubber removed ammonia, hydrogen sulphide, and volatile fatty acids whilst cooling the warm air. Secondly, the biofilter removed any remaining concentrations of the pollutants and provided odour control, allowing the air to be released to the atmosphere. Potential production of methane, a potent green house gas, in anaerobic "pockets" within the composting pile, would have either metabolically oxidized to carbon dioxide while the percolated through the composting pile, or during its passage through the biofilter. Thus emissions of green house gases were not expected.

The in-vessel composting process was completely computer controlled by a software package specifically designed for the process. The air flow rates for all air blowers were varied automatically depending on the current temperature, oxygen, and pressure levels inside the tunnel. A user-defined minimum oxygen content was maintained whilst aiming to maximise the temperature, and thus degradation rate, of the compost [16]. Once the two-week period was complete the degraded compost material was transferred to the neighbouring windrow pads where it was allowed to decompose for a further 6 weeks.

2.3. Temperature Profiles. Temperature values for each batch of compost and in-vessel unit were gathered during January–December 2008 for analysis. The data stated the temperatures measured by each of the 8 temperature probes that were

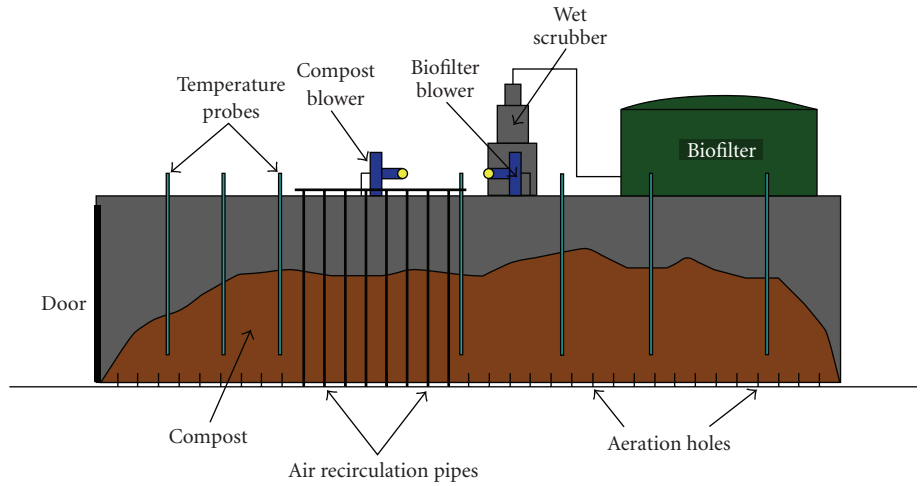

Figure 2: In-vessel unit cross-section.

placed into the mass of compost inside the tunnel. Results were recorded with a regular time step of 15 minutes, with the occasional exception, throughout the whole of the degradation process. The 8 temperature values were averaged for each batch in order to derive an overall time-temperature relationship. Any readings that were clearly incorrect were disregarded.

Individual time-temperature relationships were then accumulated by season allowing overall trends to be analysed. Subsequently an average time-temperature relationship for each of the four seasons could be created.

2.4. On-Site Hot Water Demand. The average value for daily hot water consumption for the Deerdykes composting facility's site office was calculated at 180 L d^{-1}. A medium heating requirement of 12 kW for the site office was estimated, which ranged from poorly isolated buildings with a very high heating load of 22 kW [17] to an Eco-House with a required heating load of 8 kW [18]. It was assumed that the heating would be used on average 980 hours per year.

2.5. Energy Values. Energy values were then calculated for each of the four seasons. The method used was of that described by Haug [1] using the standard heat flow into a substance at constant pressure equation. This equation was also utilised in energy-balanced analyses carried out by other researchers in composting systems [19].

The following equation was used:

$$q_p = m \times c_p \times \Delta T, \quad (1)$$

where q_p is heat energy leaving the system (kJ kg^{-1}), m is mass of product (kg), c_p is specific heat at a constant pressure (kJ $kg^{-1}K^{-1}$), and ΔT is change in temperature (K). This equation assumes a process at constant pressure with a constant specific heat capacity. This assumption is valid for the relatively small changes in pressure and temperature associated with composting [1]. Heat energy values were calculated for each time step using estimated compost material concentrations and standard specific heat capacity values (Table 1). The energy values were then accumulated by day to give the energy stored in kJ $kg^{-1}day^{-1}$. Cumulative energy over the 15-day composting period was also calculated.

Table 1: Estimated material composition for composting at Deerdykes.

Material	% present	c_p (kJ $kg^{-1}K^{-1}$)	Overall c_p (kJ $kg^{-1}K^{-1}$)
Air	10%	1.012	2.844
Water	60%	4.184	
Soil	28%	0.80	
Lignocellulosic material	2%	0.42	

2.6. Heat Exchange and Energy Collection. A heat exchanger was designed for the collection of energy generated during composting. The heat exchanger selected for the purpose of this study was a pipeline made of stainless steel that run suspended from the top of the in-vessel tunnels in the airspace above the composting piles. At the initial calculation stage the length and diameter of pipe required was unknown so the initial pipe layout shown in Figure 3 was investigated. The design of the heat exchanging element of the proposed design was carried out using the principles and methods discussed by Shah and Sekulic [20].

Nomenclature used in the following section is summarized in Table 2. The aim of the design process was to determine the outlet temperature for both the hot and cold fluid for a suggested heat exchanger surface area

2.6.1. Hot Fluid. In this case study, the hot fluid was the warm, moist air that is released by the composting process and circulated throughout the tunnel. The temperature of this air was dictated by the temperature of the compost itself; the majority of the air was recirculated. The temperature of the air approached that of the compost after the process

Table 2: Nomenclature.

Parameter[a]	Description	Unit
$T_{,i}$	Temperature of the fluid entering the system	K
$T_{,o}$	Temperature of the fluid leaving the system	K
$\dot{m}$	Mass flow rate of the fluid	$\mathrm{kg\,s^{-1}}$
c_p	Specific heat capacity of the fluid at constant pressure	$\mathrm{kJ\,kg^{-1}K^{-1}}$
d_i	Inner diameter of the heat exchanger pipe	m
d_o	Outer diameter of the heat exchanger pipe	m
k_w	Thermal conductivity value of the pipe wall material	$\mathrm{W\,m^{-1}K^{-1}}$
h_{AIR}	Heat transfer coefficient of air	$\mathrm{W\,m^{-2}K^{-1}}$
h_{WATER}	Heat transfer coefficient of water	$\mathrm{W\,m^{-2}K^{-1}}$
A	Surface area of the heat exchanger wall	$\mathrm{m^2}$

[a]The subscript h refers to the initially hotter fluid, and the subscript c refers to the initially colder fluid.

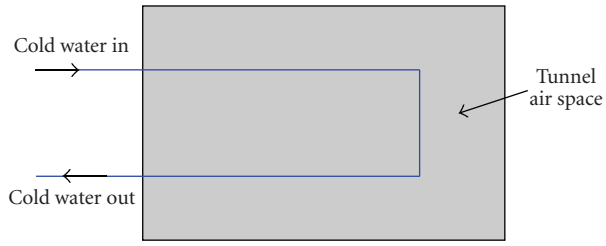

Figure 3: Initial design pipe layout.

has been running for a certain period. The only other effect on the temperature of the air was through heat conductive losses through the concrete walls and roof of the tunnel. The mass flow rate of the air through the tunnel was driven by a centrifugal blower the maximum capacity of which was $8000\,\mathrm{m^3\,hr^{-1}}$. These blowers were controlled in real time by computer to regulate oxygen and moisture levels.

2.6.2. Cold Fluid. It was proposed to use water as the cold fluid that runs through the pipe work of the heat exchanger. This was due to its low cost, ease of availability, and its thermal properties which were optimal for absorbing and storing thermal energy [21]. The mass flow rate of the water was fully controllable by the design team. A pump, pressure, or gravity fed system was designed according to requirements.

2.6.3. Individual Heat Transfer Coefficient. The individual heat transfer coefficient was calculated using

$$h = \frac{\Delta Q}{A \times \Delta T \times \Delta t}, \tag{2}$$

where ΔQ is the heat input or heat lost (J), h is the heat transfer coefficient, $(\mathrm{W\,m^{-2}K^{-1}})$, A is the heat transfer surface area $(\mathrm{m^2})$, ΔT is the temperature difference between the solid surface and surrounding fluid (K), and Δt is the time period (s).

2.6.4. Overall Heat Transfer Coefficient. The overall heat transfer of the pipe was calculated by summing the individual heat transfer coefficients of the acting fluids using [20]

$$\frac{1}{U} = \frac{1}{h_o} + \frac{1}{h_{o,f}} + \frac{d_o \ln(d_o/d_i)}{2k_w} + \frac{d_o}{h_{i,f} d_i} + \frac{d_o}{h_i d_i}, \tag{3}$$

where the subscripts o and i refer to the outside and inside of the pipe wall, respectively, U is the overall heat transfer coefficient $(\mathrm{W\,m^{-2}K^{-1}})$, and $h_{,f}$ is the thermal fouling resistance capacity $(\mathrm{W\,m^{-2}K^{-1}})$.

2.6.5. Design Equations. The heat capacity rates for each fluid were calculated using [20]

$$C = \dot{m}\, c_p. \tag{4}$$

Subsequently the heat capacity ratio, C^*, could be calculated using (5). The heat capacity ratio is simply the smaller-to-larger ratio of the heat capacity rates of the two fluids

$$C^* = \frac{C_{\min}}{C_{\max}}. \tag{5}$$

The next step was to calculate the ratio of the overall thermal conductance to the smaller of the two heat capacities, which is defined as the number of transferred units (NTUs). This was found with the following equation:

$$\mathrm{NTU} = \frac{\mathrm{UA}}{C_{\min}}. \tag{6}$$

Once these values were obtained the exchanger effectiveness, ε, was calculated. The equation for exchanger effectiveness depends on the type and flow direction associated with the particular exchanger being designed. In this case study (7) was used as it is appropriate for the counter-flow conditions that existed in the tunnel [20]

$$\varepsilon = \frac{1 - \exp[-\mathrm{NTU}(1 - C^*)]}{1 - C^* \exp[-\mathrm{NTU}(1 - C^*)]}. \tag{7}$$

Once the exchanger effectiveness was calculated the fluid outlet temperature was found using

$$\varepsilon = \frac{C_h(T_{h,i} - T_{h,o})}{C_{\min}(T_{h,i} - T_{c,i})} = \frac{C_c(T_{c,o} - T_{c,i})}{C_{\min}(T_{h,i} - T_{c,i})}. \tag{8}$$

Table 3: Monthly solar irradiation (kW h m^{-2}) for Glasgow, UK (DGS 2005).

Month	Jan	Feb	Mar	Apr	May	Jun	Jul	Aug	Sep	Oct	Nov	Dec
Irradiance	0.45	1.04	1.94	3.40	4.48	4.70	4.35	3.48	2.33	1.26	0.60	0.32

2.7. Comparison of Waste to Energy with Other Renewable Energies. Compost heat as a source of renewable heat was compared to solar thermal systems and to ground-source heat. The solar thermal system was designed using the good-practice guidelines discussed by DGS [17], which was originally written with a single-family house in mind which proved transferable to the purpose in this case study. Design methods were discussed separately for both domestic hot water supply and spatial heating.

Supplying domestic hot water is the most common use for solar thermal systems. The following sizing calculations allowed a full design to be proposed. Using the calculated value of hot water demand for the site office, V_{HW}, the heat requirement was determined using

$$Q_{HW} = V_{HW} \times c_p \times \Delta T, \tag{9}$$

where Q_{HW} is the daily heat requirement (kWh day^{-1}), V_{HW} is the daily hot water consumption (L day^{-1}), c_p is the specific heat capacity of water (Wh kg^{-1}K^{-1}), and ΔT is the temperature difference between the hot and cold water (K).

In order to calculate the area of the solar collector required the desired solar fraction, SF, and the overall average system efficiency, η_{SYS}, of the solar collector were found. The SF is the ratio of solar heat yield to total energy required by the building and is shown by (10). It showed what percentage of the yearly heat energy demand is to be supplied by solar rather than conventional means

$$\text{SF} = \frac{Q_S}{Q_S + Q_{AUX}} \times 100, \tag{10}$$

where SF is the desired solar fraction, Q_S is the solar heating requirement (kWh), and Q_{AUX} is the auxiliary heating requirement (kWh).

Achieving as high a solar fraction as possible would appear desirable, however due to the variable nature of solar energy throughout the year in temperate zones it is advisable to aim for a solar fraction of around 60% [17]. Aiming for a solar fraction of 60% prevented the supply of hot water becoming overly stressed during the winter months, due to the provision of a backup boiler supply.

If aiming to counter this by using a large area of solar collectors to better cope with winter months, it will result in an oversupply of hot water during the summer months, thus a much less efficient design. For these reasons as the solar fraction increases the system efficiency decreases. When coupled with the high set-up costs associated with a scheme of that kind it proved to be an option that limits the economic attractiveness of solar thermal systems [17].

The average system efficiency is the ratio of solar heat yield to global solar irradiance experienced by the absorber surface and is linked to the solar fraction. Average system efficiencies η_{SYS} take into account losses at the collector, solar circuit, and storage. Guidelines state that initial calculations should assume a η_{SYS} of 0.35 for a flat-plate collector and 0.45 for an evacuated-tube collector [17]. This data was then used to calculate the required area of solar collector using (11). The yearly solar irradiance value, E_G, was calculated for Glasgow (Table 3):

$$A = \frac{365 \text{ days} \times Q_{HW} \times \text{SF}}{E_G \times \eta_{SYS}}, \tag{11}$$

where A is absorber surface area (m^2), Q_{HW} is the daily heat requirement (kWh day^{-1}), SF is the desired solar fraction, E_G is the yearly potential solar irradiance (kWh m^{-2} year^{-1}), and η_{SYS} is the average system efficiency.

In order to calculate the optimal diameter for the piping of the solar circuit it is vital to regulate both the speed of flow and the volumetric flow. In order to minimise noise nuisance and prevent abrasion a flow speed, v, of 0.7 m s^{-1} is to be aimed for [17]. The level of volumetric flow is key in keeping the collector cooling at an efficient rate, preventing overheating and therefore wasting energy. It has been shown that a volumetric flow of about 40 L hr^{-1} per m^2 of collector area is ideal [17]. The volumetric flow was calculated using

$$\dot{m} = \frac{\dot{Q}}{c_p \times \Delta T}, \tag{12}$$

where $\dot{m}$ is the volumetric flow (L m^{-2}hr^{-1}), $\dot{Q}$ is the usable thermal output converted by the collector (W m^{-2}hr^{-1}), c_p is the specific heat capacity of the solar fluid (kJ kg^{-1}K^{-1}), and ΔT is the temperature difference between the feed and the return flows (K).

Subsequently the optimum pipe diameter, D, could be calculated using

$$D = \sqrt{\frac{4\left(\dot{m}/v\right)}{\pi}}. \tag{13}$$

This calculation allowed an appropriate size of commercially available pipe to be proposed. The recommended method for calculating the collector area required to fulfill spatial heating demand is currently far less developed than for domestic hot water supply [17]. This is due to the highly variable nature of the thermal insulation of buildings, individual preferences for the comfortable temperature of a room, and whether the building uses conventional or underfloor heating systems. The calculation method used was of that described by DGS (2005) which is based solely on the living area required to be heated. The relationships presented in Table 4 are valid for a climate with a low solar fraction of 35% such as the UK and were used to calculate the collector surface area and storage volume that would be required [17].

Table 4: Design guidelines for solar thermal spatial heating system.

Parameter	Recommended value
Evacuated tube collector area	0.5–0.8 m^2 of collector area per 10 m^2 heated living area
Storage volume	>50 L per m^2 of collector surface area

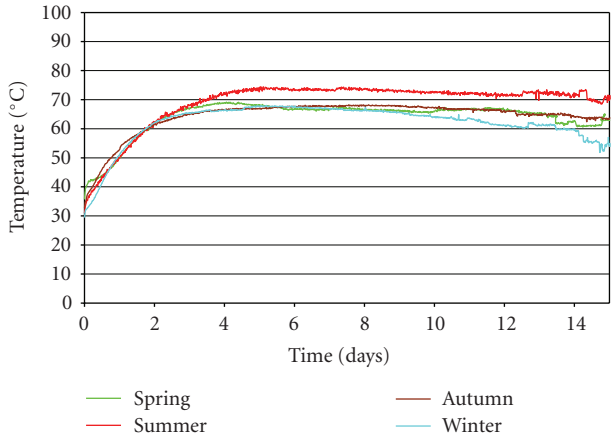

Figure 4: Average temperature temporal profiles: seasonal comparison.

Regarding a ground source heat pump design, generic design guidelines for specifying ground source heat pumps are currently at an underdeveloped stage.

3. Results and Discussion

3.1. Temperature and Energy Values. Figure 4 shows the seasonal average temperature temporal profiles between January and December 2008. The compost reached temperatures above 60°C after two days, and the highest values (~70°C) were recorded during the summer. This time is similar (2–4 days) to that observed when composting with one direction of airflow [22], but higher than that observed (0.63 days) using high recirculation of processed air [19]. Average temperatures at the end of day 12 of composting were above 65°C during spring, summer, and autumn, and about 60°C during the winter, which was close to the values reported by Harper et al. [23] for 1.5–2 m of compost depth and 7 days of composting and by Ekinci et al. [19] for pilot scale 208 L reactors, 0.285 m in radius, and 0.816 m in height.

Energy values were calculated using these average temperature profiles, and they are presented in Figure 5, where Figure 5(a) presents daily energy values and Figure 5(b) presents cumulative energy values. In this study, maximum heat generation rate per initial mass of compost dry matter was ~6000 kJ kg^{-1} day^{-1}. This value was higher than that reported by Harper et al. [23] for straw and poultry manure composting (2791 kJ kg^{-1} day^{-1}), and by Ekinci et al. [19] for paper mill sludge with broiler litter (2435 kJ kg^{-1} day^{-1}). Negative values in Figure 5(a) can be explained by the overall energy losses being greater than the energy emitted on those particular days, as the in-vessel systems were not hermetically closed.

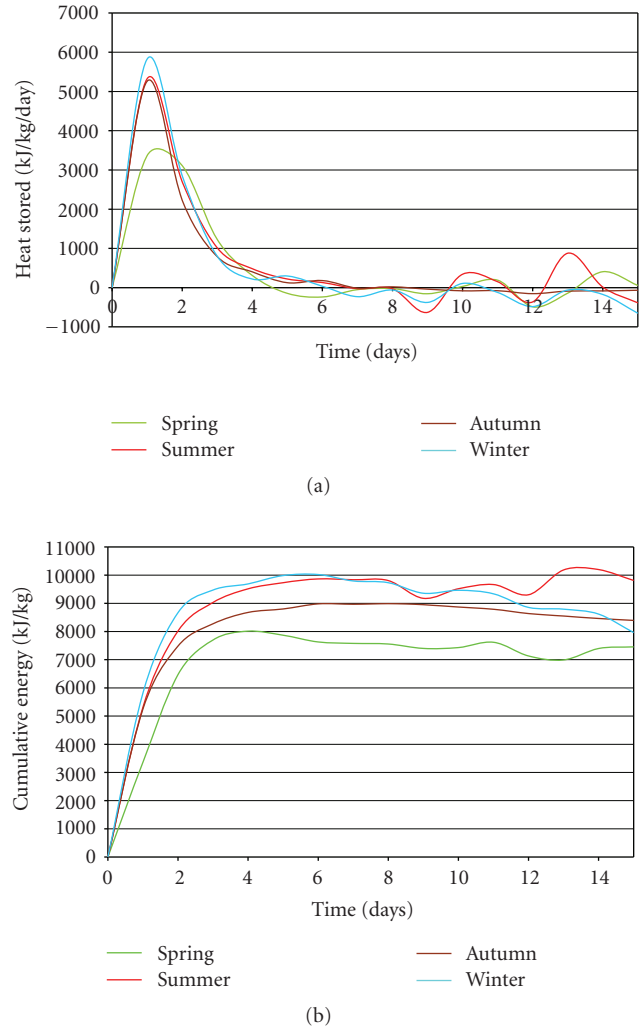

Figure 5: (a) Heat stored in compost, and (b) cumulative heat stored by compost; seasonal values.

Cumulative energy values ranged from approximately 7000 to 10 000 kJ kg^{-1}. These values related well to those reported by Ekinci at al. [19] for biosolids and wood chips (8092 kJ kg^{-1}) and Steppa [24] for organic waste (9000–11 000 kJ kg^{-1}), but were lower than that reported by Sobel and Muck [13] for poultry droppings (12 800 kJ kg^{-1}), and by Stainforth [12] for wheat straw (17 600 kJ kg^{-1}). Additionally, they were greater than that for paper mill sludge and poultry manure compost (3649 kJ kg^{-1}), and that for straw and poultry manure compost (5111 kJ kg^{-1}) [23]. Differences in cumulative energy values are due to differences in decomposition rates under different conditions and heat of combustion values of the different composting substrates, which lead any direct comparisons being difficult to arrive upon and ultimately ineffectual. However, it is clear that, as these values are in line with a section of the existing research, they are reliable figures which may be utilised appropriately for subsequent calculations. The main reason for seasonal variation is likely due to the difference in material that is available during that particular season. For example, there will be less nitrogen rich material such as grass cuttings

Table 5

Inlet temperatures		$T_{c,i}$	0	°C
		$T_{h,i}$	65	°C
Cold fluid flow rate (water pump)		Flow rate	3	L min^{-1}
			0.00005	m^3 s^{-1}
		Density water	999	kg m^3
		Flow rate	0.04995	kg s^{-1}
		m dot c	0.04995	kg s^{-1}
Hot fluid flow rate (blower at average capacity)		m dot h	2000	m^3 hr^{-1}
		Density air	1.2	kg m^3
			2400	kg hr^{-1}
		m dot h	0.66667	kg s^{-1}
Specific heat capacities		$c_{p,c}$	4.19	kJ kg^{-1}K^{-1}
		$c_{p,h}$	1.004	kJ kg^{-1}K^{-1}
Pipe properties (stainless steel)		d_i	0.02465	m
		d_o	0.02667	m
		Thickness	0.00202	m
		k_w	16.3	W m^{-1}K^{-1}
Heat transfer coefficients	$h = \frac{\Delta Q}{A \times \Delta T \times \Delta t}$	h_c	1200	W m^{-2}K^{-1}
		h_h	50	W m^{-2}K^{-1}
Heat capacity rates	$C = \dot{m}\, c_p$	C_c	209.2905	W K^{-1}
		C_h	669.3333	W K^{-1}
Heat capacity ratio	$C^* = \frac{C_{\min}}{C_{\max}}$	$C_{\min}$	209.2905	W K^{-1}
		C^*	0.31269	
Fouling capacity (standard)		$R_{w,f}$	0.002	m^{2}K W^{-1}
Overall heat transfer coefficient	$\frac{1}{U} = \frac{1}{h_o} + \frac{1}{h_{o,f}} + \frac{d_o \ln(d_o/d_i)}{2k_w} + \frac{d_o}{h_{i,f} d_i} + \frac{d_o}{h_i d_i}$	$1/h_h$	0.02	
		$d_o/h_c d_i$	0.0009015	
		Wall	0.0000644	
		Fouling inside	0.0021637	
		Fouling outside	0.002	
		U	39.7936	W m^{2}K^{-1}
Pipe total surface area		A	7.96	M^2
NTU	$\text{NTU} = \frac{\text{UA}}{C_{\min}}$	NTU	1.5135	
E	$\varepsilon = \frac{1 - \exp[-\text{NTU}(1 - C^*)]}{1 - C^* \exp[-\text{NTU}(1 - C^*)]}$	eqn top line	0.6466	
		eqn bottom line	0.8895	
		E	0.7270	
Outlet temperatures	$\varepsilon = \frac{C_h(T_{h,i} - T_{h,o})}{C_{\min}(T_{h,i} - T_{c,i})} = \frac{C_c(T_{c,o} - T_{c,i})}{C_{\min}(T_{h,i} - T_{c,i})}$	$T_{h,i} - T_{h,o}$	14.7750	
		$T_{h,o}$	50.2250	°C
		$T_{c,o} - T_{c,i}$	47.2520	
		$T_{c,o}$	47.2520	°C
Energy balance check		q	9889.3897	kW
		$T_{h,o}$	50.2250	C
Pipe length needed		Surface area	0.0838	m^2 m^{-1}
		Pipe length	95.0036	m

during the autumn and winter months, thus resulting in a lower overall energy content.

3.2. Heat Exchanger and Potential Uses for the Gathered Heat. All design parameters are summarised in Table 5, and the pipe layout in the in-vessel unites shown in Figure 6. These layouts provide enough length whilst managing to avoid contact points such as temperature probe holes and exhaust air outtakes. Using this particular pipe dimension leads to the hot and cold fluid exit temperatures that are presented in Table 6. These have been calculated for varying cold water inlet temperatures, due to the potential seasonal variability,

Table 6: Outlet fluid temperatures at varying inlet temperatures.

Temperature of cold water entering system	0°C	5°C	10°C
Temperature of cold water leaving system	47.3°C	48.6°C	50.0°C
Temperature of hot air leaving system	50.2°C	51.4°C	52.5°C

and an initial air temperature of 65°C in each case. According to these values, the hot water could be transferred to a storage vessel site office and used to supplement the hot water supply. The predicted daily demand of 180 L day^{-1} could be met in full by the heat exchanger, which runs at a flow rate of 3 L min^{-1}. This would remove the need for gas or electricity to provide hot water. However, in order to meet storage legislation [25] the temperature of the stored water must exceed 60°C at all times. Currently the heated water leaving the tunnel heat exchanger system is at a temperature between 47.3°C and 50°C, depending on the temperature of the cold water entering the system. However, if the water exiting a tunnel is put through another tunnel in which degradation is also underway then higher temperatures can be achieved. For example, calculations based on an initial cold water feed of 0°C and initial hot air temperatures of 65°C result in temperatures of 0°C, 47.3°C, 60.2°C, and 63.7°C by passing water through 0, 1, 2, and 3 tunnels in series. Thus, by passing the same volume of water through 2 or 3 in-vessel tunnels, the required storage temperature of 60°C can be achieved. As the hot air is at an approximate temperature of 65°C, then passing the water through more than three in-vessel tunnels has little improved effect and is likely inefficient practice.

The main issue with this use is that it requires at least two tunnels to be operating at the same time. If considering the usage over the past year as an accurate gauge then two or more tunnels are running simultaneously on 91% of days and three or more tunnels are running simultaneously on 78% of days (Calculations and graphical solution behind these statements not shown). It can be suggested therefore that domestic hot water supply, which requires a higher temperature for storage, can be supplied at least 78% of the time whilst underfloor spatial heating, as discussed below, can be provided 91% of the time. Another issue is that this system will require additional infrastructure to facilitate the level of control needed to direct the water into the correct tunnels. Two-way switch valves can be installed which could be controlled manually or by computer if required.

If underfloor heating is provided in the new site office then it may be feasible to provide the hot water for the system. Standard operating procedure for underfloor heating is to have an inlet temperature of 55°C and a return flow at 45°C. The water will therefore have to be passed through two in-vessel tunnels in series and so provide 91% of the yearly demand. Standard underfloor systems require a heated water flow rate in the region of 1.55 L min^{-1} [26]. The heat exchanger element has been designed with a flow rate of 3 L min^{-1} so is capable of meeting demand. Water could be stored thus allowing the pumps to be run for fewer hours each day or the pump could be run at a lower capacity thus improving temperature gain further.

Table 7: Solar thermal domestic hot water supply system specification.

Parameter	Design value
Solar collector type	Evacuated tube
Solar collector area	4.18 m^2
Heat store tank	277 L
Solar circuit piping diameter	8.86 mm
High temperature expansion vessel	18 L

3.3. Solar Thermal System. The level of potential solar energy supply is 860 kWh m^{-2} year^{-1}, while the predicted hot water demand for the site office of the Deerdykes composting facility is 180 L day^{-1} and the hot water energy demand is 6.8 kWh day^{-1}. These supply and demand parameters led to the quantification of the solar thermal system components as shown in Table 7. The predicted performance of this system is to provide 60% of the offices yearly hot water demand. The remaining 40% will have to be provided by an auxiliary conventional boiler system. Regarding the design for spatial heating, for a heated living area of 200 m^2, the evacuated tube surface area chosen for design was 12.53 m^2, and the store volume 700 L.

3.4. Ground Source Design. The method utilised to size and cost a suitable ground source heat pump system is very simplified and will not provide wholly accurate or reliable answers. This process was carried out in order to provide a comparison of typical cost and performance level of alternate renewable sources and is therefore for guidance purposes only. If a more detailed design is to be carried out a full site survey will be required to determine ground conditions and the levels of thermal insulation provided by the site office.

3.5. Cost Benefit Analysis. Table 8 summarises the cost per kWh of energy generated for each of the three possible methods. This cost is based solely on the annual operating cost required to run the system. Capital costs are provided for information and comparative purposes only and are not a factor in the cost per kWh calculation. The fraction of spatial heating provided is based on supplying a standard underfloor heating system with an input temperature of 55°C. Capital costs do not include the underfloor heating system or the heating network itself. These should be similar if not identical for each system.

From this it is clear that reusing the heat offered by the compost is an economically attractive option when compared to alternate possible renewable sources. It is able to provide the highest proportion of the total hot water requirement of the three systems. Although comparative costs per kWh are greater than for solar thermal regarding domestic hot water supply and greater than ground source heat pump regarding spatial heating, these supplies will have

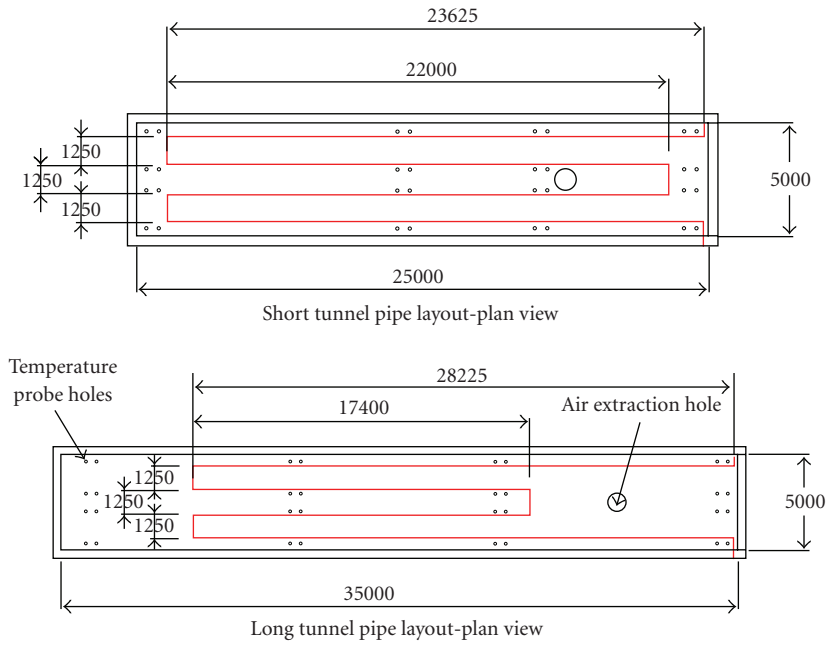

Figure 6: Suggested pipe layout for short and long in-vessel units.

Table 8: Costs benefit analysis.

Method	Compost heat		Solar thermal		Ground source heat pump	
	Domestic hot water supply	Spatial heating	Domestic hot water supply	Spatial heating	Domestic hot water supply	Spatial heating
Capital cost (£)	11 662		4180	13 415	5413	
Operating Cost (£ yr^{-1})	1039		625	940	840	
Fraction Provided	78%	91%	60%	35%	50%	100%
kWh yr^{-1} required	2667	11 760	2667	11 760	2667	11 760
Cost per kWh (£)	0.4994	0.0971	0.3905	0.2284	0.6298	0.0714

to be boosted to a greater degree by additional conventional boiling.

The capital cost of using the heat from the compost, although large, is also attractive when compared to its competitors. Although the ground source heat pumps capital cost is lower, this initial gain will soon be lost with the high level of additional hot water heating required to provide domestic hot water supply. This cost assumes all 8 tunnels will have a heat exchanger element installed, thus increasing reliability. A cost that has not been included is the valve control system that directs the water into the correct tunnels. This could be controlled manually, but an appropriate computer controlled system will guarantee a reliable supply of water. The expenditure of such a product has not been included.

4. Conclusions

The amount of energy that could be obtained from composting at the Deerdykes composting facility near Glasgow has been calculated as between 7000 and 10 000 kJ kg^{-1} for a 15-day composting period. The variations were likely due to seasonal differences in conditions and raw material supply. The results were in line with alternate existing investigations into material of similar composition. This showed that the compost contained a usable amount of energy if it could be gathered.

Methods of extracting the heat were fully researched. A solution of absorbing the heat contained in the expelled air in the tunnel space above the compost was put forward. A bespoke air-water heat exchanger utilising stainless steel piping was designed and specified. The outlet temperature of the water was shown to be 47.3°C. This can be shown to rise to above 60°C if the water is passed through multiple tunnels in series.

Several usable purposes were suggested for this heated water, including contributing to the site offices hot water demand and process optimisation. Adequate levels of heated water were shown to be provided for the domestic hot water and spatial heating supplies for 78% and 91% of the time, respectively.

Installing this system was submitted to preliminary costing in order to calculate a cost per kWh of energy that could be displaced by using the heat of the compost. This cost was then compared with that of specially designed solar

thermal and ground source heat pump systems. From this the heat exchanger system could be put into a real world context. The system was found to provide the most reliable supply of the three systems, and to do so at a very competitive price of £0.499 and £0.097 per kWh for domestic hot water supply and spatial heating, respectively. It can therefore be concluded that collecting the waste heat of compost through a heat exchanger is a realistic solution to contributing to energy demand.

Further investigations to maximize the production of heat from in-vessel units are ongoing.

Acknowledgments

The authors are grateful to Andrew Meldrum and Donald MacBrayne (Deerdykes Composting Facility), for providing data and information required for the completion of this paper. They are also grateful to Paul Steen (Ramboll UK), for providing advice on particular aspects of this paper. They also thank Paolo Pironi (University of Edinburgh) for providing access to thermocouples for further collection of temperature readings outside the composting vessels.

References

[1] R. T. Haug, *Compost Engineering: Principles & Practice*, Ann Arbor Science Publishers, Ann Arbor, Mich, USA, 1980.

[2] EC, *EU Animal By-Products Regulations (2003/31/EEC)*, European Commission, 2003.

[3] B. Antizar-Ladislao, A. J. Beck, K. Spanova, J. Lopez-Real, and N. J. Russell, "The influence of different temperature programmes on the bioremediation of polycyclic aromatic hydrocarbons (PAHs) in a coal-tar contaminated soil by in-vessel composting," *Journal of Hazardous Materials*, vol. 144, no. 1-2, pp. 340–347, 2007.

[4] L. Allievi, A. Marchesini, C. Salardi, V. Piano, and A. Ferrari, "Plant quality and soil residual fertility six years after a compost treatment," *Bioresource Technology*, vol. 43, no. 1, pp. 85–89, 1993.

[5] M. Chapman and B. Antizar-Ladislao, "Biotic landfill CH_4 emission abatement using bio-waste compost as a landfill cover," in *Landfill Research Focus*, E.C. Lehmann, Ed., Nova Science Publishers, New York, NY, USA, 2007.

[6] H. Insam, N. Riddech, and S. Klammer, *Microbiology of Composting*, Springer, Berlin, Germany, 2002.

[7] K. Sipilä, A. Johansson, and K. Saviharju, "Can fuel-based energy production meet the challenge of fighting global warming—a chance for biomass and cogeneration?" *Bioresource Technology*, vol. 43, no. 1, pp. 7–12, 1993.

[8] EEA, "State of renewable energies in Europe 2006," 2008, http://www.energies-renouvelables.org/observer/stat/baro/barobilan/barob-ilan6.pdf.

[9] B. Antizar-Ladislao and J. L. Turrión-Gómez, "Second-generation biofuels and local bioenergy systems," *Biofuels, Bioproducts and Biorefining*, vol. 2, no. 5, pp. 455–469, 2008.

[10] E. Klejment and M. Rosiński, "Testing of thermal properties of compost from municipal waste with a view to using it as a renewable, low temperature heat source," *Bioresource Technology*, vol. 99, no. 18, pp. 8850–8855, 2008.

[11] N. Guljajew and M. Szapiro, "Determining of heat energy volume released by waste during biothermal disposal," in *Sbornik Naucznych Robot*, pp. 135–141, Akademija Kommunalnowo Chozjajstwa, Moskow, Russia, 1962.

[12] A. Stainforth, *Cereal Straw*, Clarendon, Oxford, UK, 1979.

[13] A. T. Sobel and R. E. Muck, "Energy in animal manures," *Energy in Agriculture*, vol. 2, pp. 161–176, 1983.

[14] S. Lekic, *Possibilities of Heat Recovery from Waste Composting Process*, Centre for Sustainable Development, Department of Engineering, University of Cambridge, Cambridge, UK, 2005.

[15] H. Seki and T. Komori, "Packed-column-type heating tower for recovery of heat generated in compost," *Journal of Agricultural Meteorology*, vol. 48, pp. 237–246, 1992.

[16] S.D. Last, D. MacBrayne, and A. J. MacArthur, "Deedykes Composting Facility: a case study of the conversion of a conventional activated sludge sewage works to in-vessel composting, with slude co-composting facility," in *Proceedings of Kalmar Eco-Tech and The 2nd Baltic Symposium on Environmental Chemistry*, Kalmar, Sweden, 2005.

[17] DGS, *Planning and Installing Solar Thermal Systems: A Guide for Installers, Architects and Engineers*, James & James, London, UK, 2005.

[18] P. S. Doherty, S. Al-Huthaili, S. B. Riffat, and N. Abodahab, "Ground source heat pump—description and preliminary results of the Eco House system," *Applied Thermal Engineering*, vol. 24, no. 17-18, pp. 2627–2641, 2004.

[19] K. Ekinci, H. M. Keener, and D. Akbolat, "Effects of feedstock, airflow rate, and recirculation ratio on performance of composting systems with air recirculation," *Bioresource Technology*, vol. 97, no. 7, pp. 922–932, 2006.

[20] R. K. Shah and D. P. Sekulic, *Fundamentals of Heat Exchanger Design*, John Wiley & Sons, Hoboken, NJ, USA, 2003.

[21] R. D. Heap, *Heat Pumps*, E. & F.N. Spon, London, UK, 1979.

[22] K. Ekinci, *Theoretical and Experimental Study on the Effects of Aeration Strategies on the Composting Process*, Department of Agricultural Engineering, The Ohio State University, Columbus, Ohio, USA, 2001.

[23] E. Harper, F. C. Miller, and B. J. Macauley, "Physical management and interpretation of an environmentally controlled composting ecosystem," *Australian Journal of Experimental Agriculture*, vol. 32, pp. 657–667, 1992.

[24] M. Steppa, " Two options for energy recovery from waste biomass," *Maszyny i Ciagniki Rolnicze*, no. 3, 1988.

[25] HSE, "Legionnaires disease: essential information for providers of residential accommodation," Health and Safety Executive, 2003.

[26] Oxyvent, "The Oxyvent Tank: Underfloor heating / Radiant heating," 2009, http://www.oxyvent.com/underfloorheating.php.

Hindawi Publishing Corporation
International Journal of Chemical Engineering
Volume 2010, Article ID 102179, 13 pages
doi:10.1155/2010/102179

Research Article

Sustainable Algae Biodiesel Production in Cold Climates

Rudras Baliga and Susan E. Powers

Center for the Environment, Clarkson University, 8 Clarkson Aveue, Potsdam, NY 13699-5700, USA

Correspondence should be addressed to Susan E. Powers, sep@clarkson.edu

Received 30 November 2009; Accepted 1 April 2010

Academic Editor: Michael K. Danquah

This life cycle assessment aims to determine the most suitable operating conditions for algae biodiesel production in cold climates to minimize energy consumption and environmental impacts. Two hypothetical photobioreactor algae production and biodiesel plants located in Upstate New York (USA) are modeled. The photobioreactor is assumed to be housed within a greenhouse that is located adjacent to a fossil fuel or biomass power plant that can supply waste heat and flue gas containing CO_2 as a primary source of carbon. Model results show that the biodiesel areal productivity is high (19 to 25 L of BD/m^2/yr). The total life cycle energy consumption was between 15 and 23 MJ/L of algae BD and 20 MJ/L of soy BD. Energy consumption and air emissions for algae biodiesel are substantially lower than soy biodiesel when waste heat was utilized. Algae's most substantial contribution is a significant decrease in the petroleum consumed to make the fuel.

1. Introduction

In 1998, an amendment to the U.S. Energy Policy Act (EP Act) of 1992 triggered the rapid expansion of the US biodiesel industry. This act required that a fraction of new vehicles purchased by federal and state governments be alternative fuel vehicles. The U.S. Energy Independence and Security Act (EISA) of 2007 further mandated the production of renewable fuels to 36 billion gallons (136 billion liters) per year by 2022, including biodiesel. Crops such as soybeans and canola account for more than three quarters of all biodiesel feedstocks in the U.S. [1].

About 14% of U.S. soybean production and 4% of global soybean production were used by the U.S. biodiesel industry to produce fuel in 2007 [1]. The use of oil crops for fuel has been criticized because the expansion of biodiesel production in the United States and Europe has coincided with a sharp increase in prices for food grains and vegetable oils [2]. The production of biodiesel from feedstocks that do not use arable land can be accomplished either by using biomass that is currently treated as waste or by introducing a new technology that allows for the development of new feedstocks for biodiesel that utilize land that is unsuitable for food production.

Microalgae have the potential to displace other feedstocks for biodiesel owing to its high vegetable oil content and biomass production rates [3]. The vegetable oil content of algae can vary with growing conditions and species, but has been known to exceed 70% of the dry weight of algae biomass [4]. Microalgae could have significant social and environmental benefits because they do not compete for arable land with food crops and microalgae cultivation consumes less water than other crops [5]. Algae also grow in saline waters that are unsuitable for agricultural practices or consumption. This makes algae well suited for areas where cultivation of other crops is difficult [6, 7]. High biomass productivities may be achieved with indoor or outdoor photobioreactors (PBRs) [8]. In cold climates, PBRs have been used successfully, when housed within greenhouses and provided with artificial lighting

Microalgae biodiesel has received much attention in news media. Considerable progress has been made in the field of algae biomorphology [9–11]. In recent decades, however, little quantitative research has been done on the energy and environmental impacts of microalgae biodiesel production on a life cycle basis. The life cycle concept is a cradle to grave systems approach for the study of feedstocks, production, and use. The objective of this work was to assess the feasibility

Table 1: Life cycle sustainability metrics for biodiesel.

Environmental Impact	Sustainability Metrics
Energy and Resource Consumption	– Total energy consumed (MJ/L BD)
	– Fossil fuel energy consumed (MJ/L BD)
	– Petroleum consumed (MJ/L BD)
	– Land required (m^2/L of BD)
	– Water required (L water/L BD)
Climate Change	– Net green house gas emissions (g CO_2 equivalents/L of BD)
Acidification	– Acidification potential (g SO_2 eq./L BD)
Toxic Emissions	– Particulate matter emissions (PM_{10}, $PM_{2.5}$)
	– Carbon monoxide emissions
	– Volatile organic carbon emissions

of algae biodiesel production in New York State (USA) based on life cycle energy and environmental impact parameters. Upstate NY was chosen as a challenging case for algae biodiesel production due to shorter days and cold temperatures during winter months. The productivity, energy consumption, and environmental emissions associated with the algae/BD production lifecycle were quantified in order to identify the best growing conditions and assess its impacts relative to soybean biodiesel.

2. Methodology

2.1. System Boundary and Scope. The life cycle concept is a cradle to grave systems approach for the study of feedstocks, production, and use. The concept revolves around the recognition of different stages of production starting from upstream use of energy to cultivation of the feedstock, followed by the different processing stages. A life cycle inventory assessment allows for the quantification of mass and energy streams such as energy consumption, material usage, waste production, and generation of coproducts. A summary of the sustainability assessment metrics used for this life cycle inventory of microalgae feedstock for biodiesel production is presented in Table 1.

Figure 1 provides an overview of the system boundary used in this analysis, which includes the production of algae and biodiesel via a transesterification reaction. The boundary includes all upstream mass and energy flows that are required to make the chemical and energy resources required for the processing. The production of biodiesel from algae and direct energy consumption is characterized by four distinct stages: cultivation, dewatering/drying, oil extraction, and transesterification (Figure 1). The energy consumed and subsequent emissions for fuel production, electricity generation, and chemical production comprise the upstream energy consumption and emissions. Biodiesel and algae meal are the products leaving the system boundary. The use of these products is not directly included within the analysis.

The hypothetical algae and biodiesel production processing facilities considered are located in upstate placeStateNew York. The facilities are assumed to be adjacent to a biomass or fossil fuel electricity generation plant for access to the carbon dioxide in their flue gas and waste heat in order to maximize the utilization of waste resources within this system. Waste heat is considered to have no value as an energy product; so it is not counted as part of the total energy resources consumed by the facility.

Two different locations were considered for the microalgae biodiesel facility: Syracuse, NY (43°2′ N, 76°8′ W) and Albany, NY (42°7′ N, 73°8′ W). Although these locations are at approximately the same latitude and have very similar hours of daylight, the Syracuse area is colder and cloudier throughout the year due to its proximity to the Great Lakes. Albany offers more intense natural lighting and less severe winter temperatures (Figure 2). Three specific cases were considered for each of these locations:

(i) greenhouse structure to maximize natural lighting; natural gas used to maintain the system temperature;

(ii) greenhouse structure to maximize natural lighting; waste heat used to maintain the system temperature;

(iii) a well-insulated facility that allows for no natural lighting but requires substantially less heat.

The PBRs are assumed to operate continuously, using artificial lighting when natural lighting is not sufficient. In all cases, it was assumed that *Phaeodactylum tricornutum* algae would be grown for biodiesel production. This algae species has a relatively high oil content (about 30% by dry weight), is resistant to contamination, and has been previously utilized to produce biodiesel [12, 13].

Estimating the environmental and energy lifecycle impacts requires quantification of the mass and energy flows through this system. A mathematical model for the algae production process was developed in the work presented here. As shown in Figure 3, the mass and energy flows estimated with the algae production model were used in conjunction with the Greenhouse gases, Related Emissions, and Energy use in Transportation (GREET) model 1.8a developed at the Argonne National Laboratories [14]. GREET provided the general framework and structure for the lifecycle inventory, especially aspects of the transesterification process and energy and emissions related to the upstream production of chemicals and energy resources. BD production from soybeans, which is used here as a benchmark for comparison, was taken directly from the GREET model. GREET is a widely accepted model and many studies and analyses have been based upon it because of its vast data on energy sources and the associated emissions (e.g., [15–17]). The default values for soybean production, oil extraction, and transesterification were taken as GREET default values [14], which are representative of the Midwestern region of the United States where most soybeans are grown. These were based initially on an LCA completed at the National Renewable Energy Lab [18] and updated to keep the GREET

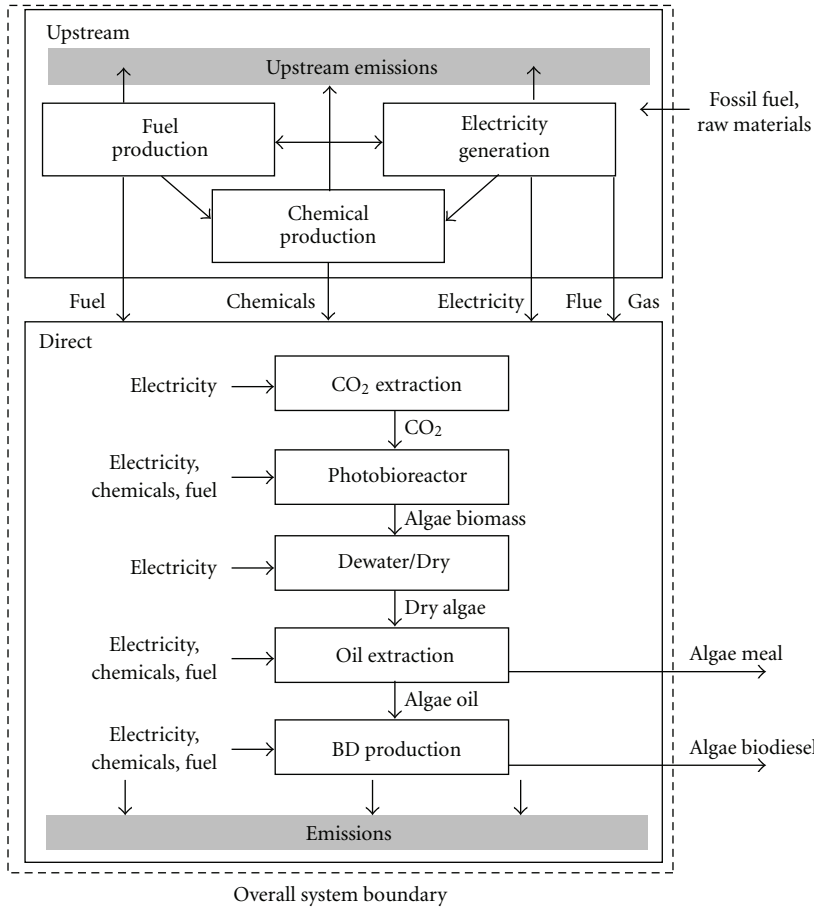

Figure 1: Flowchart depicting system boundary for life cycle inventory of biodiesel from microalgae.

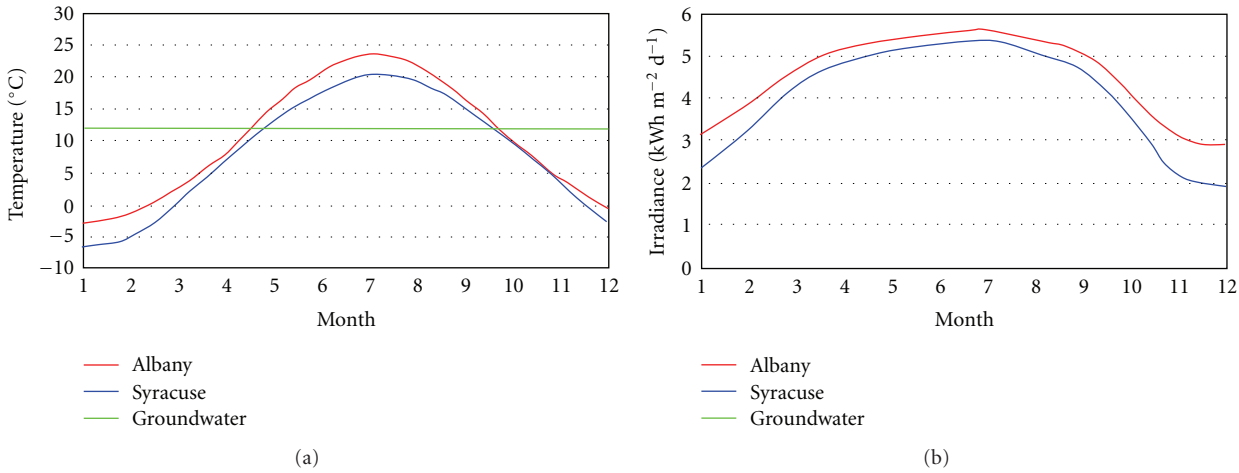

Figure 2: Monthly average temperature (a) and total monthly solar irradiance (b) for Syracuse, NY, and Albany, NY.

model as current as possible (e.g., [17]). There is only a small production of soybeans in NY State, with yields well below the average yield in the Midwest. Thus, no attempt was made to match the geographic system boundaries for biodiesel from algae to that of soybeans.

Uncertainty in the data was addressed by utilizing Monte Carlo simulations to input a range of values for parameters. For a given assumption or variable with a distribution as input, the commercially available software, Crystal Ball was utilized to determine a forecast or range of possible outputs.

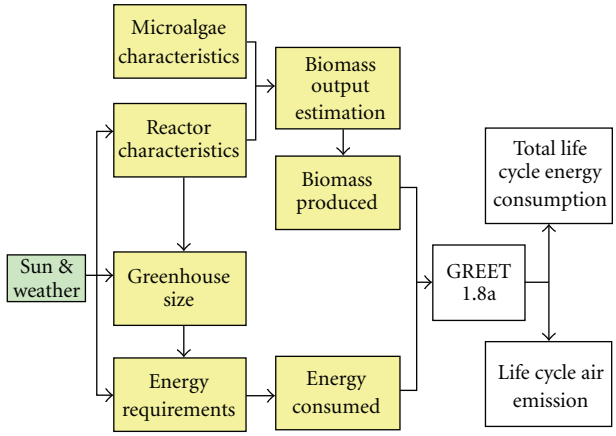

Figure 3: Overview of microalgae biomass LCA model. The yellow boxes represent the contributions of the work presented here. The soybean LCA results were taken almost entirely from GREET.

Standard error bars were created utilizing the mean value of the forecast and 95% certainty.

2.2. Algae Production Models. The biomass production model utilizes solar data and a biological growth rate to estimate actual yields for algae biomass for a photobioreactor system [13, 19].

2.2.1. Microalgae Plant Setup. Hypothetical tubular closed photobioreactors (PBRs) were modeled in this case to predict algae production and account for energy consumption and emissions in Syracuse and Albany NY. The PBR plant setup is illustrated in Figure 4. It was assumed that processes such as dewatering and transesterification could be carried out on site, thus eliminating the need for transportation.

The various dimensions and parameters for the PBR were taken from recommendations of previous studies in order to depict a realistic setup [12, 13]. The PBR setup was designed for a maximum of 30 hours detention time. The maximum effluent concentration (C_e) was fixed at 3.4 kg/m^3 with a recycle ratio of 0.35 [13, 20] and an allowable superficial fluid velocity of 0.3 m/s [21]. Since a long tubular length is required to meet these constraints (32,400 m), the PBR is split up into 6 units each of which is 61 m^3 (5,400 m long, 0.12 m diameter). Stacking of tubes reduces the total foot print area of the greenhouse. All tubes are connected and algae broth passes through all six units.

The floor area or foot print area of the greenhouse house was determined from the volume of the reactor and type of cultivation (annual/seasonal operation) and the specific processes. The diameter of tubes was set at 0.12 m for all cases since it is a widely reported size for PBRs [3, 13, 22, 23]. The spacing of tubes was set at 0.3 m. This is an important factor since it defines the total floor size, which in turn influences heating and lighting requirements. The various parameters related to plant setup are summarized in Table 2.

2.2.2. Estimating Biomass Output. Microalgae productivity is estimated from the location, reactor specifications, and microalgae data. It is assumed that CO_2 and nutrients are provided in excess to the microalgae culture through the media, thereby making light the only limiting factor for cell growth and decay [12]. If adequate lighting is available, the specific growth rate μ is determined from the average irradiance available I_{avg} (μE/m^2-s) [19]:

$$\mu = \mu_{max} \frac{I_{avg}^n}{K_I^n + I_{avg}^n}, \quad (1)$$

where K_I is the half saturation constant (i.e., I_{avg} for which half of μ_{max} is attained), and the exponent n is a unitless empirical constant. Both K_I and n are constant for a given species of algae. Note that decay of algae cells during the hours with light is incorporated into the maximum specific growth rate (μ_{max}) (h^{-1}) since values provided by Molina Grima et al. [22] and Fernandez et al. [23] were determined from the net growth rate. I_{avg} is determined from the Beer-Lambert equation:

$$I_{avg} = \frac{I}{\varphi_{eq} K_a C_i} \left[1 - \exp\left(-\varphi_{eq} K_a C_i\right)\right], \quad (2)$$

where C_i (kg/m^3) is the influent biomass concentration. The path length of light within the reactor is given by φ_{eq}, which is the ratio of the tube diameter to the cosine of the solar zenith angle. The photosynthetically active irradiance (I) (μEm^{-2}s^{-1}) is a function of various solar angles and the total solar irradiance. Hourly solar data were available from NREL's solar database [24], and thus, algae cell growth was determined at an interval of an hour. The analysis of the solar data to estimate I and φ_{eq} is included in the appendix.

The PBR is modeled as a series of plug flow reactors where the effluent concentration of each reactor is the influent concentration for the next. It is assumed that steady-state conditions prevail for each hour since irradiance is taken as a constant over that time period. Utilizing a Monod reaction rate for substrate utilization [22], the resulting steady-state plug flow reactor equation for each segment can be written as

$$u \frac{dC}{dz} = \mu_{max} \frac{I_{avg}^n}{K_I^n + I_{avg}^n} C, \quad (3)$$

where C is the biomass concentration and u is the fluid velocity. Integrating this expression can provide the effluent concentration for each reactor segment "j" that represents one hour of residence time at an average irradiation rate for that hour:

$$\ln\left(\frac{C_{j+1}^k}{C_j^k}\right) = \mu_{max} \frac{\left(I_{avg(j+1)}^k\right)^n}{K_I^n + \left(I_{avg(j+1)}^k\right)^n} \left(\frac{L}{u}\right), \quad (4)$$

where j and $j+1$ indicate the start and end location along the reactor length of the one hour segment. C_{j+1} is calculated in series to determine the reactor effluent concentration, C_e, for each hour k. The growth rate during that hour is defined

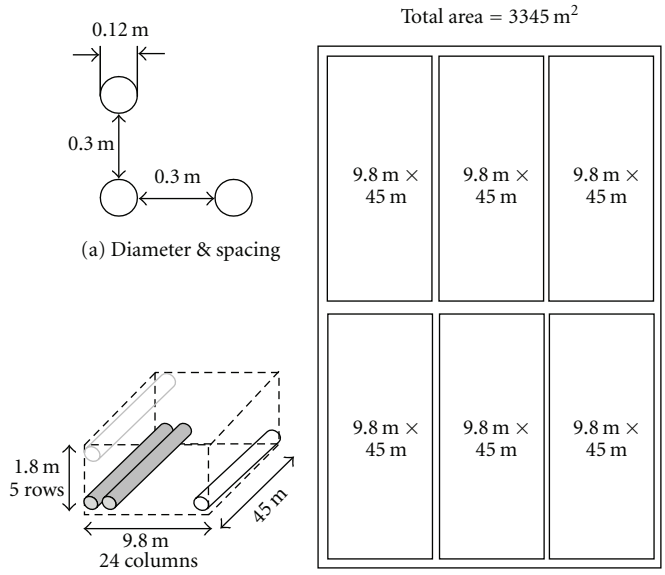

Figure 4: Photobioreactor system layout (not to scale).

Table 2: Summary of photobioreactor and greenhouse parameters.

Parameter	Value	Depends upon	Reference
Diameter of tubes	0.12 m	Larger diameter pipes can cause cell shading	[3]
Spacing of tubes	0.3	Greater spacing is desirable to avoid shading	[13]
Flow rate (Q)	3.4×10^{-3} m^3/s	Algae species and tube diameter	[21]
Recycle Ratio (r)	0.35		[20]
Total volume of reactor (V)	366 m^3	Maximum residence time (30 hrs)	[12]
Influent concentration (C_i)	1.2 kg/m^3		
Max. Effluent concentration (C_e)	3.4 kg/m^3	Growth rate, PBR set up	[13]

by the average irradiance for that hour of the day. The total biomass produced per day (M_{BM}) (kg d^{-1}) is estimated from the flow rate (Q) (m^3 hr^{-1}), recycle ratio (r), and the effluent concentration C_e (kg m^{-3}):

$$M_{\mathrm{BM}} = \sum_{k=1}^{24} Q\left(C_e^k\right)(1-r). \tag{5}$$

The total microalgae biomass produced can be determined from (2), (4), and (5) along with algae growth parameters and solar irradiation data.

The temperature requirements for algae differ by species. In general, faster growing algae species favor higher media temperatures of about 20–30°C [10]. The algae-related constants used for *P. tricornutum* in the model are included in Table 3. This species was selected because it has been used in the past to produce microalgae biodiesel and all relevant data were available [22].

2.3. Energy Consumed during Microalgae Cultivation. Cultivating microalgae in closed systems is an energy intensive process, especially in regions with low temperatures and limited natural lighting [13]. The algae growth and harvesting stage involve a large number of intermediate processes for which estimates of the energy consumption were developed here. Energy consumption requirements for extraction and transesterification are already provided in the GREET model [14]. It was assumed that the processes for transesterification of algae oil are identical to that of soy oil. Thus, the chemical (methanol and sodium hydroxide) and energy consumption and the energy and emissions associated with their production were taken directly as the default parameters in GREET.

Water Heating. Energy requirements for a natural gas water heating system were determined by using the specific heat of water and the efficiency rating of the heater as provided by the manufacturer (EF = 0.82 [26]). It was assumed that groundwater, at an initial temperature (T_{inlet}) of 12°C [27], would be heated to a thermostat set point (T_t) of 25°C.

Media Circulation. Electric pumps are used to circulate the media through the entire length of the reactor. The input

Table 3: *P. tricornutum* growth parameters.

Parameter	Value	Reference
$\mu_{\max}$	0.063 (h^{-1})	[22]
B	0.0018 (h^{-1})	[25]
K_I	3426 ($\mu E\ m^{-2}s^{-1}$)	[22]
n	1–1.34	[25]
E_f	$1.74 \pm 0.09\ \mu E\ J^{-1}$	[22]
X_p	2–4%	[25]
Oil Content (%dry weight)	30%	[13]
Water Content of algae	40%	[13]
Cultivation temperature	25°C	[10]

electrical power required to operate the pumps (P_p) (W) can be given by [28]

$$P_p = \frac{3.91 \times 10^{-6} \mu_1^3 \mathrm{Re}^{2.75}}{\eta_p d^3} A_a, \quad \text{where } \mathrm{Re} = \frac{\rho u d}{\mu_1}, \tag{6}$$

where μ_1 ($kg\,m^{-1}\,s^{-1}$) is the dynamic viscosity of water, Re is the Reynolds number, d (m) is the diameter of the pipes, u is the superficial velocity of flow (m/s), η_p and η_{elec} are the pump efficiency ($\eta_p = 0.7$), and A_a (m^2)is the tube aperture area. The pumps operate continuously.

Artificial Lighting. Natural algae cultivation inherently revolves around the diurnal and seasonal cycles. To compensate for these cycles and to maximize the production of biomass, artificial lighting is used to allow 24-hour cultivation. Lights are turned on from dusk to dawn. Monthly averages of daylight hours are used to define the time the lighting system is in operation each day. The power (P_a) (W) consumed for artificially lighting the greenhouse area is calculated as [29]

$$P_a = A' \left(\frac{I_{\text{avg}}}{L_w C_f} \right). \tag{7}$$

The intensity of the artificial lighting provided was set equal to the naturally available lighting in the month of July (I_{avg} = 1.7 $\mu E/m^2$-s) over the entire greenhouse region (A' = 3345m^2). Specifications for high-efficiency fluorescent GRO lights [29] were used to estimate the power required for artificial lighting. The light intensity of the bulbs is expressed as L_w = 220 Lu/W and the conversion factor (C_f) to convert between micromoles of photons (mE) and lux is 0.29.

CO_2 Purification. Carbon dioxide acts as the only source of carbon for the biomass. Flue gases from power plants provide an inexhaustible source of CO_2. However, flue gases also contain varying levels of other gases such as SO_x and NO_x which are detrimental to microalgae culture beyond certain concentrations [30]. The monoethanolamine (MEA) absorption process can be used to separate pure CO_2 from flue gas for microalgae production. Kadam [31] determined that if about 18% of the total carbon dioxide consumed is taken directly from flue gases and the rest is purified through the MEA process, then, the toxic flue gases will be sufficiently low concentration for algae growth.

Molina Grima [19] determined that in order to make light the only limiting factor, CO_2 must be provided in excess and the ratio of the aqueous CO_2 concentration (kg/m^3) to influent biomass concentration C_i (kg/m^3) should be 0.63. Since growth rates for this system are lower than those in Molina's Grima study [19] due to reduced sunlight, this CO_2 represents a conservative estimate. The mass of carbon dioxide required was estimated based on this ratio, the media flow rate, and the influent biomass concentration. Although carbon dioxide has a high solubility in water, and it is likely that all CO_2 in the gas bubbled through the reactor would dissolve over the length of the reactor, a factor of safety of 2 was used here as an overestimate of the mass of CO_2 that would be required. The MEA CO_2 extraction process has been modeled and studied previously in context with algae production. Kadam [31, 32] reports that the process to extract CO_2 from flue gas and recover the MEA for reuse consumes 32.65 kWh per ton of CO_2 for algae cultivation. Details are not provided in these references to specifically quantify which of the steps in the MEA process consume the most electrical energy.

Greenhouse Heating. Temperature control within the greenhouse is essential for algae cultivation in cold weather conditions. The energy consumed for greenhouse heating depends upon the total surface area exposed, insulation material, and temperature inside and outside the greenhouse. For a given greenhouse with surface area (A_g) (m^2) the heat loss per second (Q_L) (J/s) is given by [33]

$$Q_L = 1.05 \left(\frac{1}{R} \right) \left(T_{\text{req}} - T_{\text{out}} \right) A_g, \tag{8}$$

where R ($1.9\,m^2\,°C\,s\,J^{-1}$) is the R-value of the greenhouse insulating material; T_{req} (25°C) and T_{out} (°C)are the temperatures required within the greenhouse and outside the greenhouse, respectively. The greenhouse was assumed to be insulated with 10 mm twinwall polycarbonate with an R-value of 1.9. The R-value of insulated and windowless cultivation scenario was set at 30. The outside temperature T_{out} is taken from monthly averages for Syracuse and Albany and is input as normal distributions for that month [34].

Steam Drying and Dewatering. Algae are suspended in a dilute broth from photobioreactors [13]. Dewatering and drying of algae is necessary to reduce the water content to 5% [35] before the hexane oil extraction process. For algae with high vegetable oil content, it is suggested that continuous nozzle discharge centrifuges provide the best reliability and consume the least amount of energy. Centrifugation consumes 3.24 MJ/m^3 of effluent media [36]. After centrifugation, algae water content is 70% (by weight).

Steam is utilized to further dry microalgae before oil extraction process. The natural gas consumed to provide the required steam energy was calculated based on the heat of vaporization of water, the mass of water that needed to be vaporized to reduce the water content from 0.70 to 0.05, and

the efficiency of the boiler (0.93 [37]) and dryer (0.8 [26]) utilized. In the scenarios that utilize waste heat, it is assumed that because of the colocation of the algae production facility near a power plant, there is sufficient heat to dry the algae.

2.4. Water Consumption. The consumption of water for the production of biofuels has recently been identified as a significant limitation to the development of an expanded biofuel economy. Water consumption occurs almost entirely in the feedstock production step for most biofuels. The average U.S. production biodiesel from soybeans requires 6,500 liters of water for evapotranspiration per liter of biodiesel produced [38]. Water consumption for algae biodiesel was calculated by a mass balance. The total water flowrate through the bioreactor is the sum of freshwater, water included in the algae recycle stream (35% recycle), and water recovered through the centrifuge dewatering process to increase the algae concentration from 0.34% to 30%. With this mass balance, 848 m^3 make up water is required annually or approximately 4 L water per L of biodiesel for the feedstock production stage. This represents approximately 99% of water recovery and reuse. In the transesterification and biodiesel cleaning processes, 1–3 L of water are required per L of biodiesel produced [39].

2.5. Fertilizer Consumption. The microalgae culture media acts as the primary source of nutrients and carbon dioxide and a means of expelling excess oxygen. The minimum amount of nutrients consumed was defined based on the molecular formula of algae—$CO_{0.48}H_{1.83}N_{0.11}P_{0.01}$ [40]. N and P account for 6.5% and 1.3% of the algae mass. Assuming that maximum possible biomass concentration of algae cells is 4 kg /m^3 [13, 22] in a tubular PBR, the N and P consumed from the algae media would be 0.26 kg N/m^3 and 0.052 kg P/m^3. Excess fertilizer that passes through the bioreactor as part of the broth is assumed to be recovered in the centrifuge dewatering step for reuse. Since nearly all of the water is recycled, it is assumed that nearly all of the nutrients that are not consumed are also recycled.

2.6. Utilizing GREET for Life Cycle Analysis. The GREET model was modified and used to calculate the energy use and emissions generated from algae production, oil extraction, and transesterification stages of biodiesel production as well as the upstream chemical and energy production processes. For a given fuel system GREET evaluates natural gas, coal, and petroleum use as well as the emissions of carbon dioxide equivalent greenhouse gases, volatile organic compounds, carbon monoxide, nitrogen oxides, particulates, and sulfur oxides from all lifecycle stages [14]. The GREET results are presented as primary energy consumed and emissions per million BTU fuel produced. The low heating value of the BD was used to convert to the functional unit used here—liters BD produced.

The GREET model is written in an MS Excel workbook and includes soy biodiesel production energy consumption and emissions pathways. A new spreadsheet page based on the soy biodiesel calculations was added to the GREET workbook and adapted for algae BD production. Default parameters for transesterification were used directly, but other input parameters including energy consumption for the various processes, biomass yield, nutrient requirements, carbon dioxide consumed were modified for algae biodiesel production based on the mass and energy flows presented above. The mix of electricity generation within New York State was used to define the primary energy consumed to generate electricity [41].

The extraction of oil from algae was assumed to be carried out by hexane oil extraction. The procedure is similar to soybean oil extraction, although significantly less hexane is required to recover oil from algae (0.030 kg of hexane/kg of dry algae) [11] than is required for soybeans (1.2 kg hexane/kg dried and flaked soy bean) [18]. During this process, algae meal is produced as a coproduct that can be used as an animal feed in the same manner that soy meal is used as a coproduct from soy biodiesel. GREET uses the displacement method to determine how much of the biomass production and extraction steps can defined as a credit for the biodiesel due to the production of a coproduct. The protein content of soy meal is 48% [42], as compared to 28% in algae meal [13] and 40% in soy beans [42]. Thus, 1 kg of algae meal displaces about 0.7 kg of soybean, whereas 1 kg of soy meal displaces about 1.2 kg of soy bean for animal feed. The credits for not having to produce 0.7 kg soy beans for every kg algae meal produced are subtracted from the total energy use and emissions associated with the algae production, oil extraction, and their associated upstream processes.

An additional credit was also attributed to the algae to represent the carbon dioxide sequestered from the power plant flue gas. Algae cell elemental composition was used to estimate the mass of carbon that was consumed by the algae growth within the PBR (0.51 kg of CO_2 consumed/kg algae grown).

3. Results

3.1. Biomass Production. Biomass output is an important factor for determining life cycle energy analysis of microalgae biodiesel production. When natural lighting is used to minimize electricity consumption for artificial lighting, algae production rises steadily between the months of February and April (Figure 5). Biomass production is the highest between the months of May to July and is followed by a gradual decline in the months of August to October. Production is the lowest in the winter months due to low natural irradiance. The uncertainty bars included represent 95% confidence intervals from Monte Carlo simulation outputs.

The annual biomass productivity in Albany is about 12% greater than that in Syracuse (Table 4). These cities are at very similar latitudes, but the actual irradiance in Albany is higher due to less cloud cover. Biomass and subsequent biodiesel production in the windowless (artificial lighting only) scenario is much higher than greenhouse cases because

Table 4: Comparison of different locations and scenarios by biodiesel production.

Location	Biomass Produced	(tonnes/year)	Biodiesel produced (L m^{-2} y^{-1})
Syracuse NY	Greenhouse Base Case	202	19
	Greenhouse w/waste heat	202	19
	Windowless Cultivation	263	25
Albany NY	Greenhouse Base Case	225	21
	Greenhouse w/waste heat	225	21

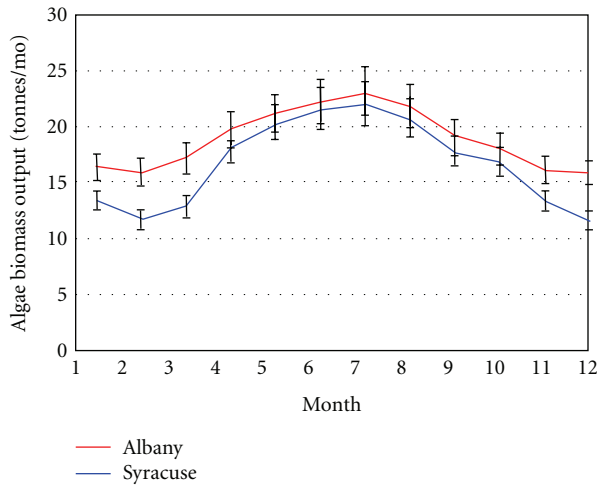

Figure 5: Algae Biomass production for Syracuse and Albany, NY, with natural lighting supplemented by artificial lighting for continuous algae production.

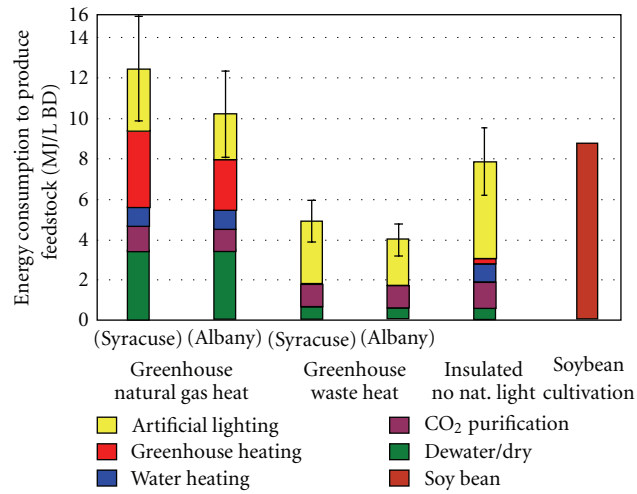

Figure 6: Energy consumption for microalgae and soy bean feedstock production. The error bars represent 95% confidence intervals on the total energy consumption for feedstock production.

illumination is maintained throughout the year at the highest level achieved naturally (noon in the month of July).

3.2. Energy Consumption for Microalgae Biodiesel Production. The energy consumed for biodiesel production was estimated by modeling individual processes in the algae cultivation stage. Energy required for the transesterification process is accounted directly by the GREET 1.8a model. The energy required for feedstock production through the drying process is illustrated in Figure 6. This does not include oil extraction and transesterification processes. Three variables can be assessed with this graph: location (Syracuse versus Albany), use of natural lighting versus solely artificial lighting and algae versus soybean production.

Heating needs consume well over half of the total energy required for algae growth, dewatering, and drying. When no waste heat is available, dewatering and steam drying accounts for the greatest fraction—about 28–32% of the energy required for feedstock production. With the availability of waste heat, this component is reduced to about 13% of the total, which represents the electricity required for centrifugation. Greenhouse heating consumes a similar proportion of the total energy for algae production—about 25–30%. Water heating for cultivation consumes about 7–12% for feedstock production. Both locations have similar water heating requirements because groundwater temperature is assumed to be equal for both cases.

When natural lighting is utilized to the extent possible artificial lighting, it consumes about a quarter of the total energy required for algae cultivation. However, in the windowless cultivation case where there is no natural light available, the artificial lighting cost is almost doubled. However, the total energy requirements in this scenario are still less (35%) than the scenarios requiring natural gas to heat a greenhouse.

Among the design choices and trade-offs considered here, the growth and drying of algae with the utilization of waste heat is the only scenario that is substantially better than growing soybeans from the perspective of process energy consumed. These results clearly show the value of colocating an algae facility near a source of waste heat.

Overall, microalgae cultivation in Albany, NY, consumes about 18–21% less energy than Syracuse, NY, because greenhouse heating energy requirements are lower and higher natural lighting intensity yields about 12% higher biomass output.

Figure 7 illustrates the total lifecycle energy, which now also includes biodiesel production and credits for CO_2 consumption and algae/soy meal produced during the oil extraction phase. For most cases, the energy required for feedstock production is similar to the energy required for oil

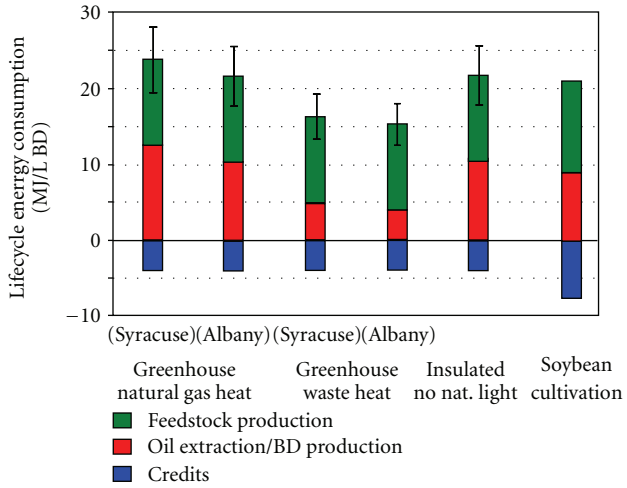

Figure 7: Total life cycle energy consumption by life cycle stage. The error bars represent 95% confidence intervals on the total lifecycle energy consumed.

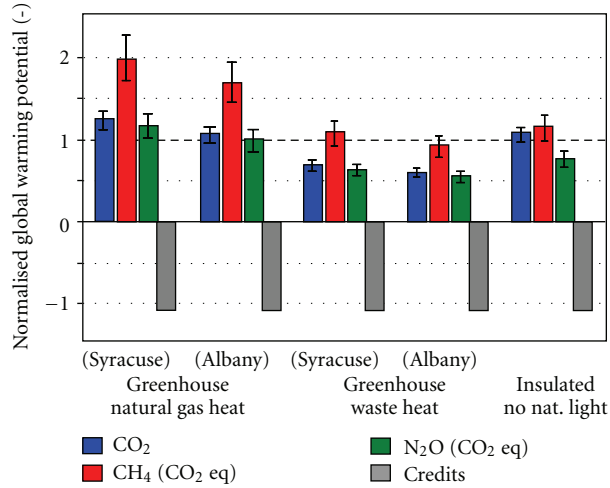

Figure 8: Global warming potential of microalgae biodiesel—mass emissions normalized by dividing by the corresponding emissions for soy biodiesel for comparison.

extraction and transesterification. Thus, the savings associated with the utilization of waste heat in the greenhouse also represent significant savings when the entire lifecycle energy consumption is considered. Greenhouse algae cultivation with waste heat in Albany consumes the least energy on a life cycle basis; however total energy consumption is very similar to that of the corresponding Syracuse case.

The importance of the coproduct and carbon dioxide consumption credits are apparent from the data presented in Figure 7. Soy meal credits are higher than algae meal credits because of higher protein content and higher fraction of soy meal produced per liter of biodiesel (1 kg of algae meal displaces about 0.7 kg of soybean, whereas 1 kg of soy meal displaces about 1.2 kg of soy bean for animal feed). Adding the higher credits for the soy bean BD case to the energy required for production reduces the net energy for this case to a level below the well-insulated and windowless algae production scenario. The greenhouse scenarios utilizing waste heat are still the best option for minimizing the consumption of energy that has value for other uses.

Natural gas accounts for 65–80% of the total energy consumed on a life cycle basis for algae biodiesel production when waste heat is not available (data not shown). The high consumption of natural gas can be attributed to heating processes, the high fraction of natural gas in NY electricity mix (about 22%), and upstream consumption for process fuel and fertilizer production. In contrast, soy biodiesel requires substantially more petroleum (~5x) than microalgae consumes due to the extensive use of tractors and feedstock transportation when BD is made from soybeans. Thus, algae as a BD feedstock has a significant benefit over soybeans in terms of reducing our dependence on imported oil. Algae biodiesel production requires a significant amount of electricity and thus coal accounts for about 6–19% of the total life cycle energy consumption. Insulated cultivation has the highest coal consumption, about 19% of the total life cycle energy consumption, because of increased artificial lighting and electricity consumption. In comparison, for the greenhouse with waste heat case, only 7% the total lifecycle energy is derived from coal.

The processing of soybeans to prepare for oil extraction also requires some heating to dry the beans. Arguably, waste heat could be considered to reduce the fossil fuel consumption for soybean biodiesel too. However, whereas the algae feedstock could be grown at the same location where waste heat is available, the soybeans require a much more dispersed geographical region. Soybeans are typically transported 75 miles or less to a soybean crushing facility. Thus, the probability that soybean production and crushing facilities can be colocated with a waste heat source is significantly less than for algae. If this can be achieved, the lifecycle energy production for the feedstock production (green bar for soybean BD, Figure 7) would be less.

3.3. Global Warming Potential. Global warming potential can be described as the impact of additional units of greenhouse gases to the atmosphere. The global warming potential for the different scenarios and gases is estimated in terms of carbon dioxide equivalents (Figure 8). All algae scenarios are allocated the same CO_2 credits because the carbon dioxide consumed per unit of algae produced is constant.

Most CO_2 emissions for algae biodiesel originate from upstream usage of energy use for heating, transportation fuel use, and coal combustion for electricity. The extraction and utilization of natural gas for heating use, electricity generation, and fertilizer production is accompanied by high methane emissions. Natural gas extraction has a very high methane emission factor. Overall, the emission of carbon dioxide is relatively low compared to methane due to the high natural gas use relative to petroleum or coal. Natural gas utilization has a much lower carbon dioxide emission factor than coal.

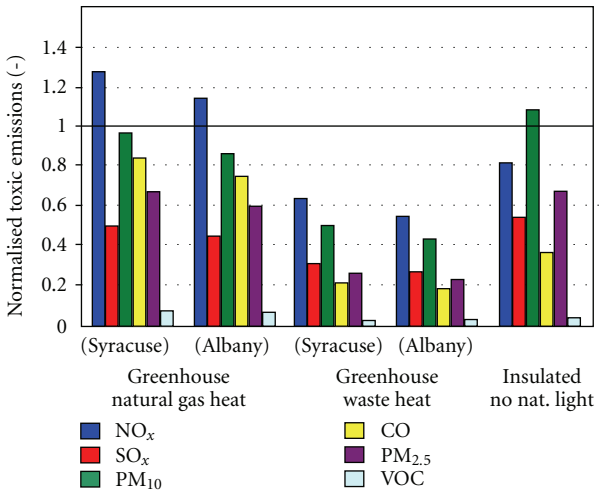

Figure 9: Toxic air emissions from microalgae biodiesel production—mass emissions normalized by dividing by the corresponding emissions for soy biodiesel for comparison.

In cold climates, the production of algae biodiesel with the utilization of waste heat rather than natural gas consumption is the only approach that reduces greenhouse gas emissions relative to soy biodiesel.

3.4. Other Air Emissions. The exposure of humans to air pollutants is increasingly associated with increased mortality and reduction in life expectancy [43]. Figure 9 presents the lifecycle air emissions for algae biodiesel production normalized to the corresponding air emissions estimated by GREET for soybean biodiesel. The microalgae biodiesel air emissions follow a trend similar to the total life cycle energy consumption. The high NO_x emissions can be traced to high emission factors of equipment used to produce natural gas and the flaring of natural gas in refineries. The increased use of artificial lighting for the cultivation of algae in a windowless and well-insulated facility results in high particulate emissions, particularly in comparison to cases where natural lighting is used. These PM emissions originate mainly from coal and residual oil combustion use for electricity production.

VOC emissions from microalgae biodiesel production are much lower than soy biodiesel, because of low utilization of petroleum and hexane. The VOC emission factors for transportation fuels like gasoline are far greater than any other source. Thus, since algae is locally produced for biodiesel and transportation minimal, the VOC emissions from algae biodiesel are much less than soy biodiesel, primarily because only a minimal amount of hexane is required for extraction compared with soy beans.

Overall, the most important source of air emissions for microalgae is the upstream emissions associated with fuel and electricity generation. Yet, these emissions are still relatively low compared to soy biodiesel. The primary factor contributing to this apparent anomaly is the comparison of algae biodiesel produced in New York State to soy biodiesel produced nationally. NY State has a high percentage of hydroelectric (17%) and nuclear (29%) power production and relatively small amounts of electricity generated from coal (15%) [41]. This difference in upstream electricity generation has significant repercussions throughout the lifecycle energy emission estimates for any electricity-intensive manufacturing system: manufacturing in New York State benefits from relatively clean energy resources.

The acidification of soils and water bodies occurs mainly due to the transformation of gaseous pollutants (SO_x, NO_x) into acids. The acidification potential of the different cases is estimated in SO_2 equivalents. All cases of microalgae biodiesel are better than soy biodiesel in terms of acidification emissions. The total SO_2 equivalents follow a trend that resembles the total energy usage.

3.5. Summary of Results. A summary of the lifecycle sustainability assessment metrics for the various algae biodiesel production scenarios and soy biodiesel production is presented in Table 5. The most sustainable biodiesel production for all cases requires the colocation of the algae and BD production facility in the vicinity of a source of waste heat. "Free" heat greatly reduces the fossil fuel consumption and all related green house gas and other air pollutants. At a similar latitude, choosing a location that maximizes sunlight helps somewhat to increase the algae production rate and, therefore, reduce the impacts when the results are compared on a per BD-produced basis. These effects are small, however, compared to the benefits of utilizing waste heat. Similarly, a well-insulated facility can help reduce heating needs, but the consequences of increased electricity use for artificial lighting decrease the benefits of reduced heating fuel required. In most regions of the U.S., where a higher fraction of the electricity mix is generated from fossil fuels, the well insulated windowless scenario would be worse in terms of most sustainability metrics due to the increased dependence on fossil fuels.

4. Conclusions

Cultivation of microalgae in NY State is an energy intensive process owing to temperature control and steam drying process. Colocating microalgae cultivation with a power plant is highly desirable. Annual production of microalgae requires the utilization of waste heat for steam drying, water heating, and greenhouse heating in order to be substantially better than soy biodiesel in terms of energy consumption and emissions. When waste heat is utilized, microalgae biodiesel production consumes less energy than soy biodiesel.

Microalgae consumes less than one third the petroleum fossil fuel required for soy biodiesel and only a small fraction of the water. The feasibility of microalgae biodiesel production at a given location is greatly dependent on availability of waste heat and natural lighting conditions. The availability of either one or both makes algae biodiesel production process cleaner in terms of air emissions and consumes much less energy than soy biodiesel. However if both natural

Table 5: Summary of average sustainability metrics to compare algae and soy BD production.

Environmental Impact		Scenario					
		Greenhouse Nat. Gas, Syracuse	Greenhouse Nat. Gas, Albany	Greenhouse w/waste heat, Syracuse	Greenhouse w/waste heat, Albany	Insulated, no nat. light	Soy biodiesel production
Total life cycle energy Consumption* (MJ/L of BD)		23	21	**16**	**15**	22	21
Land utilization (m^2/L of BD/yr)		0.053	0.048	0.053	0.048	**0.040**	22.2
Water Consumption (L water/L BD)		**5–7**	**5–7**	**5–7**	**5–7**	**4–6**	6,500
Greenhouse gas emissions (g CO_2 equiv/L of BD)		1350	1150	**740**	**630**	910	925
Acidification potential (g SO_2 eq./L of BD)		4.9	4.6	**2.8**	**2.5**	3.4	4.0
Toxic Emissions (g /L of BD)	PM 10	5.1	4.6	**2.6**	**2.3**	5.7	5.3
	PM 2.5	1.8	1.6	**0.7**	**0.6**	1.8	2.7
	VOC	0.22	0.20	**0.06**	**0.05**	0.09	3.4
	CO	2.4	2.1	**0.6**	**0.5**	1.0	2.8

*does not include credits.

lighting and waste heat are absent, algae biodiesel production consumes more energy than soy biodiesel production and emits an equal or more amount toxic air emissions.

Coproducts produced during algae biodiesel production process have less protein content than soy meal and, thus, are less valuable. The production of high value coproducts allows for increased energy allocation for soy biodiesel and thus emissions or energy consumption of both the feedstocks is very close and comparable.

Most microalgae biodiesel production scenarios have low or very similar emissions as compared to soy biodiesel. Green house gas emissions for algae biodiesel are generally higher than soy biodiesel except when waste heat is utilized, in which case emissions are equal. The emission of volatile organic compounds for soy biodiesel is much higher than that for algae biodiesel. Emissions from microalgae production originate mainly from upstream fossil fuel energy consumption. Reducing needs for unit processes like greenhouse heating, lighting, and other systems will have significant benefits.

Appendix

Estimation of Average Light Intensity

A model is used to estimate the growth rate as a function of light for a geographic location and day of the year for tubular photobioreactors [12] that takes into account various solar angles, cloudiness, and reactor geometry. The model accounts for weather conditions and relates them to the growth of biomass.

The photosynthetically active irradiance (I) ($\mu Em^{-2}s^{-1}$) used in (2) is a function of various solar angles (ω, ω_s), total solar irradiance (H) ($J\,m^{-2}d^{-1}$), and photosynthetic efficiency (E_f) (μEJ^{-1}). The total photosynthetically active irradiance (I) over a horizontal culture surface can be determined from the total solar irradiance (H) ($kWhm^{-2}d^{-1}$) directly by utilizing the following equation [22, 44]:

$$I = \frac{\pi H E_f}{24}(a + b\cos\omega)\left|\left(\frac{\cos\omega(\cos\omega_s)}{\sin\omega_s - \omega_s(\cos\omega_s)}\right)\right|, \quad \text{(A.1a)}$$

where

$$a = 0.409 + 0.502\sin(\omega_s - 60), \quad \text{(A.1b)}$$

$$b = 0.661 + 0.477\sin(\omega_s - 60). \quad \text{(A.1c)}$$

The photosynthetic efficiency (E_f) is the ratio of the photosynthetically active radiation to the total incident radiation (H). E_f for *P. tricornutum* algae varies as ($1.74 \pm 0.09 \times 10^{-6}$ EJ^{-1}) [22]. It is substituted as a normal distribution with mean 1.74×10^{-6} and standard deviation 0.09×10^{-6} for Monte Carlo simulations.

The total extraterrestrial irradiance incident on the earth (H_o) ($kWh\,m^{-2}d^{-1}$) varies seasonally. Some of the incoming solar irradiance is lost due to varying atmospheric transmissivity (K_h) associated with cloud cover. The atmospheric transmissivity, which is also known as the clearness index, is the ratio of the total daily radiation (H) ($kWh\,m^{-2}d^{-1}$) at ground level to the total daily extraterrestrial radiation (H_o) ($kWh\,m^{-2}d^{-1}$). K_h, a unitless parameter, varies by month. For this study, NREL's solar data [24] were used as monthly averages for H_o and K_h values [24]. The total irradiance incident that makes it to the earth surface (H) surface was calculated as the product of H_o and K_h. Values for H in Syracuse NY are shown in Figure 10.

Seasonal variations in solar irradiance may be attributed to changes in the solar declination angle. The solar declination angle varies throughout the year and is a function of the day number of the year (N). N takes on values from 1 (January 1) to 365. The solar declination angle (δ) is constant

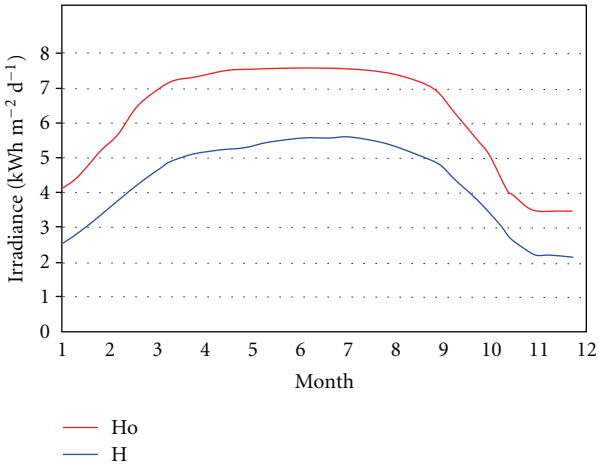

Figure 10: Solar irradiance for Syracuse, NY.

for all locations in the northern hemisphere and can be calculated for each day as follows [45]

$$\delta = 23.45 \sin\left(\frac{360}{365}(284 + N)\right). \quad (A.2)$$

Note. 23.45° is the angle at which the axis of the earth is tilted and 360° and 284 are conversion factors from radians to degree. 365 denotes the number of days taken to complete one revolution by the earth around the sun.

The solar angle at sunrise (ω_s) incorporates seasonal variations in solar declination angle with the latitude (Φ) (degrees) of the area being considered:

$$\cos \omega_s = -(\tan \delta)(\tan \Phi). \quad (A.3)$$

The solar hour angle (ω) (degrees) for a location on earth is zero when the sun is directly overhead and negative before noon and positive in the afternoon [46]. Similarly, hourly changes in the solar irradiance depend upon solar hour angle (ω), which is a function of the solar hour (h). The solar hour h varies from 24 to 1 [43]:

$$\omega = 15(12 - h). \quad (A.4)$$

Equations (A.2)–(A.4) can be used in conjunction with (A.1a)–(A.1c) to find photosynthetically active irradiance at any given latitude and time.

Acknowledgment

This work was supported by United States Department of Agriculture Grant no. NRCS-68-3A75-6-512. Publication of this work does not imply endorsement by the funding agency.

References

[1] DOE Alternative Fuels and Advanced Vehicles Data Center, Biodiesel Production. October, 2009, http://www.afdc.energy.gov/afdc/fuels/biodiesel_production.html.

[2] D. Pimentel, S. Williamson, C. E. Alexander, O. Gonzalez-Pagan, C. Kontak, and S. E. Mulkey, "Reducing energy inputs in the US food system," *Human Ecology*, vol. 34, no. 4, pp. 459–471, 2008.

[3] C. U. Ugwu, H. Aoyagi, and H. Uchiyama, "Photobioreactors for mass cultivation of algae," *Bioresource Technology*, vol. 99, no. 10, pp. 4021–4028, 2008.

[4] A. Banerjee, R. Sharma, Y. Chisti, and U. C. Banerjee, "Botryococcus braunii: a renewable source of hydrocarbons and other chemicals," *Critical Reviews in Biotechnology*, vol. 22, no. 3, pp. 245–279, 2002.

[5] Y. Li, M. Horsman, N. Wu, C. Q. Lan, and N. Dubois-Calero, "Biofuels from microalgae," *Biotechnology Progress*, vol. 24, no. 4, pp. 815–820, 2008.

[6] E. Ono and J. L. Cuello, "Feasibility assessment of microalgal carbon dioxide sequestration technology with photobioreactor and solar collector," *Biosystems Engineering*, vol. 95, no. 4, pp. 597–606, 2006.

[7] M. Olaizola, "Commercial development of microalgal biotechnology, from the test tube to the marketplace," *Biomolecular Engineering*, vol. 20, no. 4–6, pp. 459–466, 2003.

[8] A. Richmond, "Microalgal biotechnology at the turn of the millenniumml: a personal view," *Journal of Applied Phycology*, vol. 12, no. 3–5, pp. 441–451, 2000.

[9] S. Hirata, M. Hayashitani, M. Taya, and S. Tone, "Carbon dioxide fixation in batch culture of Chlorella sp. using a photobioreactor with a sunlight-collection device," *Journal of Fermentation and Bioengineering*, vol. 81, no. 5, pp. 470–472, 1996.

[10] J. Sheehan, T. Dunahay, J. Benemannm, and P. Roessler, "A look back at the U.S. Department of Energy's Aquatic Species Program-Biodiesel from Algae," Tech. Rep. TP-580-24190, NREL, Golden, Colo, USA, 1998, http://www.fuelandfiber.com/Athena/biodiesel_from_algae_es.pdf.

[11] H. Xu, X. Miao, and Q. Wu, "High quality biodiesel production from a microalga Chlorella protothecoides by heterotrophic growth in fermenters," *Journal of Biotechnology*, vol. 126, no. 4, pp. 499–507, 2006.

[12] E. Molina, J. Fernandez, F. G. Acién, and Y. Chisti, "Tubular photobioreactor design for algal cultures," *Journal of Biotechnology*, vol. 92, no. 2, pp. 113–131, 2001.

[13] Y. Chisti, "Biodiesel from microalgae," *Biotechnology Advances*, vol. 25, no. 3, pp. 294–306, 2007.

[14] M. Wang, "Overview of GREET model development at Argonne," in *Proceedings of the GREET User Workshop*, Center for Transportation Research, Argonne National Laboratory, Sacramento, Calif, USA, March 2008, http://www.transportation.anl.gov/pdfs/TA/468.pdf.

[15] A. Lavigne and S. E. Powers, "Evaluating fuel ethanol feedstocks from energy policy perspectives: a comparative energy assessment of corn and corn stover," *Energy Policy*, vol. 35, no. 11, pp. 5918–5930, 2007.

[16] J. Hill, S. Polasky, E. Nelson, et al., "Climate change and health costs of air emissions from biofuels and gasoline," *Proceedings of the National Academy of Sciences of the United States of America*, vol. 106, no. 6, pp. 2077–2082, 2009.

[17] CARB, "Detailed California-GREET Pathway for Biodiesel (Esterified Soyoil) from Midwest Soybeans, Ver. 2.1," Tech. Rep., California Air Resources Board Stationary Source Division, 2009, http://www.arb.ca.gov/fuels/lcfs/022709lcfs_biodiesel.pdf.

[18] J. Sheehan, V. Camobreco, J. Duffield, M. Graboski, and H. Shapouri, "Life cycle inventory of biodiesel and petroleum

diesel for use in an urban bus," Tech. Rep. SR-580-24089, NREL, Golden, Colo, USA, 1998.

[19] E. Molina Grima, E.-H. Belarbi, F. G. A. Fernandez, A. R. Medina, and Y. Chisti, "Recovery of microalgal biomass and metabolites: process options and economics," *Biotechnology Advances*, vol. 20, no. 7-8, pp. 491–515, 2003.

[20] G. L. Rorrer and R. K. Mullikin, "Modeling and simulation of a tubular recycle photobioreactor for macroalgal cell suspension cultures," *Chemical Engineering Science*, vol. 54, no. 15-16, pp. 3153–3162, 1999.

[21] M. Barbosa, *Microalgal photobioreactors: scale up and optimization*, Ph.D. Dissertation, van Wageningen University, Wageningen, The Netherlands, 2003.

[22] E. Molina Grima, F. G. A. Fernandez, F. G. Camacho, and Y. Chisti, "Photobioreactors: light regime, mass transfer, and scaleup," *Journal of Biotechnology*, vol. 70, no. 1–3, pp. 231–247, 1999.

[23] F. G. A. Fernandez, F. G. Camacho, J. A. S. Perez, J. M. F. Sevilla, and E. M. Grima, "Modeling of biomass productivity in tubular photobioreactors for microalgal cultures: affects of dilution rate, tube diameter, and solar irradiance," *Biotechnology and Bioengineering*, vol. 58, no. 6, pp. 605–616, 1998.

[24] National Renewable Energy Laboratory, "National solar radiation database 1991–2005 update: user's manual," Tech. Rep. TP-581-41364, NREL, Golden, Colo, USA, 2007.

[25] L. A. Meireles, A. C. Guedes, C. R. Barbosa, J. L. Azevedo, J. P. Cunha, and F. X. Malcata, "On-line control of light intensity in a microalgal bioreactor using a novel automatic system," *Enzyme and Microbial Technology*, vol. 42, no. 7, pp. 554–559, 2008.

[26] American Council for Energy Efficient Economy. Water Heating, January 2009, http://www.aceee.org/consumerguide/waterheating.htm.

[27] Noritz America Corporation. US Average Groundwater Temperature, November, 2008, http://www.noritz.com/u/US_ground_temperature%5B1%5D.pdf.

[28] G. Burgess, J. G. Fernandez-Velasco, and K. Lovegrove, "Materials, geometry, and net energy ratio of tubular photobioreactors for microalgal hydrogen production," in *Proceedings of the World Hydrogen Energy Conference (WHEC '06)*, vol. 16, Lyon, France, June 2006.

[29] OSRAM Sylvania Corp, "Photosynthetically Active Radiation Units," October, 2009, http://openwetware.org/images/e/e8/Conversion_lux.pdf.

[30] M. H. Reddy, *Application of algal culture technology for carbon dioxide and flue gas emission control*, Master of Science Thesis, Arizona State University, 2002, http://www4.eas.asu.edu/pwest/Theses_Diss/Madhu_Thesis-%20Algae%20Photosynthesis.pdf.

[31] K. L. Kadam, "Microalgae production from power plant flue gas: environmental implications on a life cycle basis," Tech. Rep. TP-510-29417, National Renewable Energy Laboratory, Golden, Colo, USA, 2001.

[32] K. L. Kadam, "Power plant flue gas as a source of CO_2 for microalgae cultivation: economic impact of different process options," *Energy Conversion and Management*, vol. 38, supplement 1, pp. S505–S510, 1997.

[33] ACF Greenhouses, September, 2008, http://www.littlegreenhouse.com/heat-calc.shtml.

[34] Weather.com, Syracuse monthly average temperatures, November, 2008, http://www.weather.com/wxclimatology/monthly/graph/13201? from=month_bottomnav_driving.

[35] J. M. Lidell, "Extraction of triglycerides from microorganisms," US Patent no. 6180376, 2001, http://www.patentstorm.us/patents/6180376/description.html.

[36] E. M. Grima, E.-H. Belarbi, F. G. A. Fernandez, A. R. Medina, and Y. Chisti, "Recovery of microalgal biomass and metabolites: process options and economics," *Biotechnology Advances*, vol. 20, no. 7-8, pp. 491–515, 2003.

[37] S. Sanford, "Greenhouse unit heaters: types, placement, and efficiency," 2008, http://learningstore.uwex.edu/pdf/A3784-15.pdf.

[38] R. Dominguez-Faus, S. E. Powers, J. G. Burken, and P. J. Alvarez, "The water footprint of biofuels: a drink or drive issue?" *Environmental Science and Technology*, vol. 43, no. 9, pp. 3005–3010, 2009.

[39] National Research Council, *Water Implications of Biofuels Production in the United States*, National Academies Press, Washington, DC, USA, 2008.

[40] J. U. Grobbelaar, "Algal nutrition," in *Handbook of Microalgal Culture: Biotechnology and Applied Phycology*, A. Richmond, Ed., Blackwell Publishing, Israel, 2004.

[41] DOE Energy Information Agency, New York Electricity Profile, 2007, http://www.eia.doe.gov/cneaf/electricity/st_profiles/new_york.html.

[42] H. Huo, M. Wang, C. Bloyd, and V. Putsche, "Life-cycle assessment of energy and greenhouse gas effects of soybean-derived biodiesel and renewable fuels," *Environmental Science and Technology*, vol. 43, no. 3, pp. 750–754, 2008.

[43] Environmental Protection Agency. Health and Environmental Effects of Particulate Matter, December, 2008, http://www.epa.gov/ttncaaa1/naaqsfin/pmhealth.html.

[44] J. A. Duffie and W. A. Beckman, *Solar Engineering of Thermal Processes*, Wiley, New York, NY, USA, 1980.

[45] B. Y. H. Liu and R. C. Jordan, "The interrelationship and characteristic distribution of direct, diffuse and total solar radiation," *Solar Energy*, vol. 4, no. 3, pp. 1–19, 1960.

[46] Sunlit Design, Solar Hour Angle, October, 2008, http://www.sunlit-design.com/infosearch/hourangle.php.

Hindawi Publishing Corporation
International Journal of Chemical Engineering
Volume 2010, Article ID 391632, 11 pages
doi:10.1155/2010/391632

Review Article

Chlorophyll Extraction from Microalgae: A Review on the Process Engineering Aspects

Aris Hosikian, Su Lim, Ronald Halim, and Michael K. Danquah

Bio Engineering Laboratory (BEL), Department of Chemical Engineering, Monash University, Victoria 3800, Australia

Correspondence should be addressed to Ronald Halim, ronald.halim@eng.monash.edu.au

Received 1 February 2010; Accepted 30 March 2010

Academic Editor: Ravichandra Potumarthi

Chlorophyll is an essential compound in many everyday products. It is used not only as an additive in pharmaceutical and cosmetic products but also as a natural food colouring agent. Additionally, it has antioxidant and antimutagenic properties. This review discusses the process engineering of chlorophyll extraction from microalgae. Different chlorophyll extraction methods and chlorophyll purification techniques are evaluated. Our preliminary analysis suggests supercritical fluid extraction to be superior to organic solvent extraction. When compared to spectroscopic technique, high performance liquid chromatography was shown to be more accurate and sensitive for chlorophyll analysis. Finally, through CO_2 capture and wastewater treatment, microalgae cultivation process was shown to have strong potential for mitigation of environmental impacts.

1. Background

Microalgae are microscopic unicellular organisms capable to convert solar energy to chemical energy via photosynthesis. They contain numerous bioactive compounds that can be harnessed for commercial use. Marine microalgae in particular have unique biochemical characteristics not found in higher plants [1]. Microalgae are usually cultivated in open ponds or photobioreactors. The cultivation process requires carbon dioxide, light, water and other nutrients which facilitate the photosynthetic process. Microalgal cultivation captures greenhouse gas CO_2 while simultaneously produces biomass containing high-value consumer products.

Chlorophyll is one of the valuable bioactive compounds that can be extracted from microalgal biomass. It is used as a natural food colouring agent and has antioxidant as well as antimutagenic properties. The process of extracting chlorophyll from marine microalgae begins with dewatering and desalting the highly dilute microalgal culture (biomass concentration = 0.1–1% w/v). Chlorophyll is then extracted from the dried biomass by organic solvent extraction or supercritical fluid extraction. This process is followed by a fractionation step to separate the chlorophyll pigments and derivatives. Many studies have been carried out to optimize chlorophyll extraction and fractionation from microalgae. This review focuses on the entire chlorophyll production process beginning from microalgae cultivation to chlorophyll fractionation and purification.

1.1. Chlorophyll Classification. There are two main types of chlorophyll, chlorophyll *a* and chlorophyll *b*. However, exposure of chlorophyll molecules to weak acids, oxygen or light accelerated their oxidation and resulted in the formation of numerous degradation products [2, 4, 5]. Figures 1, 2, and 3 shows the structures of the chlorophyll compounds. The skeleton of chlorophyll molecule is the porphyrin macrocycle, which comprises of four pyrrole rings [6, 7]. An attachment of a single isocyclic ring to one of the pyrrole rings gives rise to the phorbin structure [6]. Each pyrrole ring contains four carbon atoms and one nitrogen atom. All of the nitrogen atoms face inward creating a central hole where an Mg^{2+} metal ion easily binds [7]. In chlorophyll *b*, the methyl group in ring II of chlorophyll *a* is replaced by a formyl group [5, 7]. This structural difference results in chlorophyll *a* being a blue/green pigment with maximum absorbance from 660 to 665 nm and chlorophyll *b* being a green/yellow with maximum absorbance from 642 to 652 nm [2].

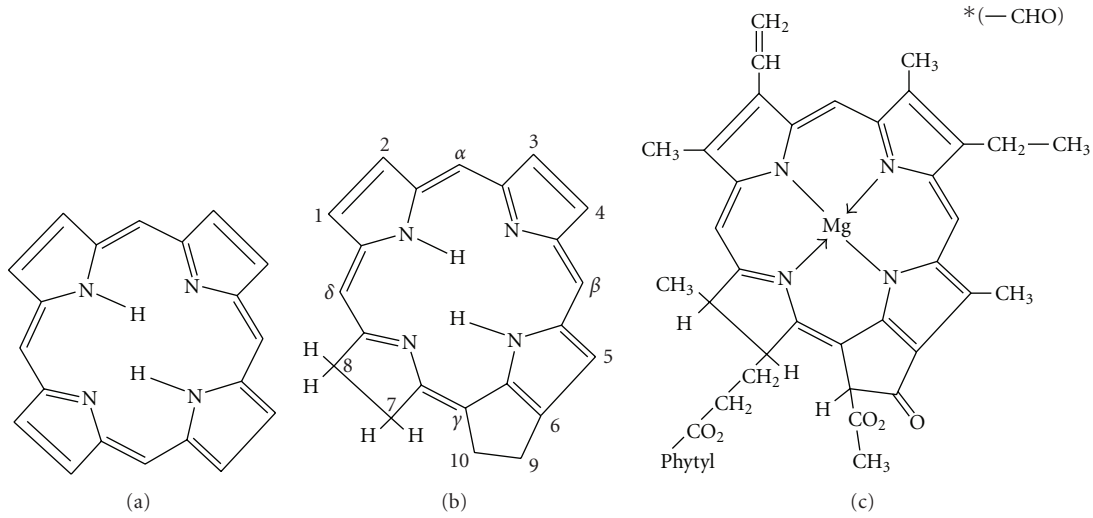

Figure 1: Chemical structures of chlorophyll and its constituents, extracted from [2]. (a) porphyrin macrocycle. (b) phorbin. (c) chlorophyll *a*, chlorophyll *b* is a variant with the methyl group in position 3 being replaced by a formyl group.

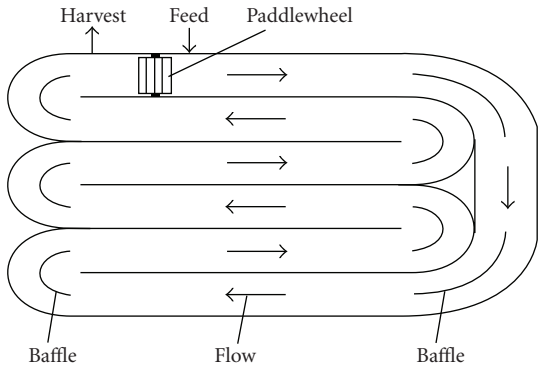

Figure 2: Raceway pond for open-air microalgae cultivation, extracted from [3].

1.2. Uses of Chlorophyll. Chlorophyll is present abundantly in nature and, due to its critical "light harvesting" role in photosynthesis, is vital to the survival of both the plant and animal kingdoms [6]. Chlorophyll selectively absorbs light in the red and blue regions and therefore emits a green colour. Photosynthesis is a process which uses this harvested light energy together with water and carbon dioxide to produce oxygen and carbohydrates; as such, it converts solar energy into chemical energy. The products from this chemical process reflect its significance, with carbohydrates being the primary building block for plants and oxygen being necessary for the survival of animal kingdom [6]. The importance of photosynthesis for life on earth is further highlighted by plants forming the basis of all food chains. Chlorophyll is a compound that is decomposed and reproduced continuously in significant amounts both terrestrially and in the oceans. It is estimated that 1.2 billion tons of chlorophyll are produced annually in the planet [6].

Chlorophyll is used as a colouring agent due to its selective absorbance of light of certain wavelengths and its consequent green colour. Changes in market demands and legislation have resulted in the requirement of natural colouring agents to be used in food products in preference to artificial colourings [8]. Colouring is essential for both consumers and manufacturers, as many foods lose their original colours due to chemical processes they undergo. Consumers demand products of original appearance, while manufacturers desire uniformity for all products [8, 9]. Chlorophyll in plants is confined in chloroplasts where it is not only complexed with phospholipids, polypeptides and tocopherols but also protected by a hydrophobic membrane [6]. When chlorophyll is removed from this protective environment, its magnesium ion becomes unstable and may easily be displaced by a weak acid. In order to overcome this problem, the magnesium ion is often substituted with a copper ion to form a highly stable blue/green complex [6, 9].

Although chlorophyll is a natural food colouring agent, there are disadvantages associated with its use. Its pigment content is not precisely known and it tends to be unstable under the different pH conditions of the foods to which it is added. Additionally, it is more expensive than artificial colourings [8] and it must undergo a chemical modification by replacing the magnesium centre with a copper ion in order to improve its stability as a food colouring agent. Since the copper complex is not absorbed by the body and is removed in its entirety as an excretion product, it is considered to be safe and is permitted to be used in most countries as a food additive. However, the concentration of free ionisable copper in the colouring must be kept below 200 ppm under current regulations [2, 9].

Chlorophyll and its derivatives are also used widely in pharmaceutical products. Chlorophyll has been found to accelerate wound healing by more than 25% in some studies. Since chlorophyll stimulates tissue growth, it prevents the advancement of bacteria and speeds up the wound healing process [10, 11]. Chlorophyll is similar in chemical structure to haemoglobin and, as such, is predicted to stimulate tissue

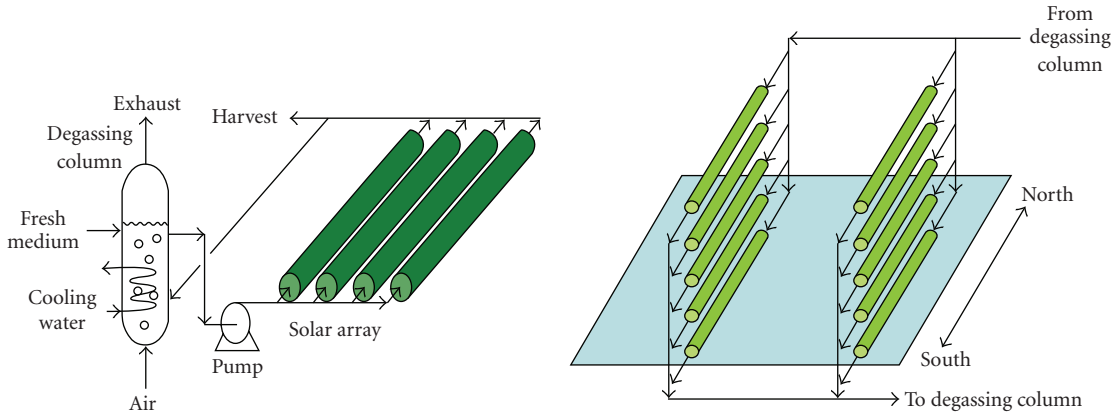

Figure 3: Different configurations of tubular photobioreactors, extracted from [3]. (a) parallel run horizontal tubes. (b) fence-like tubular array.

growth in a similar fashion through the facilitation of a rapid carbon dioxide and oxygen interchange [12]. Because of this property, chlorophyll is used not only in the treatment of ulcers and oral sepsis but also in proctology.

Chronic ulcer is a significant health problem in society, with lengthy periods required for its treatment [13]. Chlorophyll's ability to increase the rate of healing is a breakthrough for ulcer sufferers. The application of ointments containing chlorophyll derivatives was found not only to eliminate pain after several days but also to improve the appearance of the affected tissues [13]. The discharge from the ulcer and its characteristic odour also improved significantly after a few days of chlorophyll treatment [13].

The same properties which make chlorophyll a key compound in the treatment of ulcers also make it vital in the treatment of post-operative wounds from rectal surgery. When proctologists remove large areas of tissue, healing can be difficult and the area of the removed tissue tends to be painful [12]. The stimulation of cells in the host and the consequent acceleration in the tissue formation upon chlorophyll application increase the rate of healing in many cases by 25% [12]. Additionally, chlorophyll was found to remove odours from the wound after a few applications [12]. Its non-toxic nature, antibacterial property and deodorising function make chlorophyll a key product in the treatment of oral sepsis [14].

Chlorophyll *a* and its derivatives also have profound antioxidant properties [15]. Chlorophyll derivatives such as pheophorbide *b* and pheophytin b have always been known as strong antioxidants. However, these derivatives exist in very low concentrations in fruits and vegetables [15].

Fruit and vegetable consumption has been associated with decreasing the risks of cancer. Phytochemicals present in these foods, particularly chlorophyll and its derivatives, have been suggested to play a key role in cancer prevention due to their high displays of antioxidant and antimutagenic activities [15, 16]. The most significant activity of chlorophyll derivatives in the prevention of cancer is the trapping of mutagens in the gastrointestinal tract [16].

2. Capturing CO_2 with Microalgae

Over the past several decades, global warming has become a serious threat to both humans and nature [17]. The increase of Earth's surface temperature can bring about extreme weather occurrences, rise in sea levels, extinction of species, retreat of glaciers and many other calamities. The rise in global temperature is attributed to the high amount of carbon dioxide (CO_2) gases in the atmosphere [18, 19]. CO_2 is emitted from the burning of fossil fuels for electricity, transport, and industrial processes [17, 18, 20]. Due to the serious threat of global warming, the Kyoto Protocol in 1997 proposed a reduction of greenhouse gases by 5.2% based on the emissions in 1990.

Since then, many CO_2 mitigation options have been considered to meet the proposed target [17]. The various strategies suggested can be classified into two main categories: chemical reaction-based approaches and biological mitigation. Chemical reaction-based strategy captures CO_2 by reaction with other chemical compounds before the CO_2 is released to the atmosphere. The disadvantage of this method is that the chemical reactions are very energy-intensive and costly. Furthermore, both CO_2 and the wasted chemical compounds need to be disposed of. On the other hand, biological mitigation is deemed to be more favourable as it not only captures CO_2 but also generates energy through photosynthesis [19]. This method will be much simpler than physical CO_2 sequestration [21].

Photosynthesis is carried out by all plants and any photosynthetic microorganisms. Even though the use of plants to capture CO_2 is viable, it is by no means efficient owing to its slow growth rate. On the other hand, microalgae as photosynthetic microorganisms are able to capture solar energy and CO_2 with an efficiency of 10 to 50 times greater than that of higher plants [19]. Microalgae includes both prokaryotic cyanobacteria and eukaryotic unicellular algae [17]. The structural and functional simplicity of these microorganisms makes them a better choice for research purposes than any other terrestrial plants [22]. In addition,

microalgae have rapid growth rates and higher productivities than any other plant systems. Microalgae can also grow in variable environmental conditions [19, 20, 23].

Apart from CO_2 and sunlight, microalgae also need nutrients, trace metals and water to grow [24]. In short, biomass from microalgae cultivation is produced based on the following reaction:

$$CO_2 + H_2O + \text{nutrients} + \text{light energy} \longrightarrow \text{biomass} + O_2 \quad (1)$$

see [25].

Unlike plants, microalgae can be cultivated with waste or brackish water despite its abundance of heavy metals and pathogens. The nitrogen and phosphorous in waste water can be directly used by the microalgae as nutrients. Hence, use of chemicals and freshwater needed for algal cultivation can be reduced. It also means that it is entirely feasible to incorporate wastewater treatment process with microalgal cultivation [17, 19].

There are over 30,000 species of microalgae in existence on the Earth and they contain a variety of chemicals that have commercial values [26]. Thus, the biomass produced from microalgal cultivation has numerous uses [17]: (1) a source of biofuels (biodiesel and bioethanol); (2) a nutritional supplement for humans in the form of tablets, capsules, powders and liquids; (3) a natural food colorant; (4) a natural food source for many aquacultural species; (5) a nutritional supplement for animals to improve immune response and fertility; (6) for cosmetic supplements; (7) a source of high-value functional ingredients like polyunsaturated fatty acids, ω-3 fatty acids, pigments, and stable isotope biochemicals; (8) a raw material for the formation of 'biochar' through pyrolysis that can be used as biofertiliser and for carbon sequestration [17, 27]; (9) a source of renewable hydrogen [28].

Microalgae can capture CO_2 from the atmosphere, from industrial gases (i.e., power plant flue gases) and in the form of soluble carbonates (i.e., Na_2CO_3 and $NaHCO_3$) [19, 20]. Generally, CO_2 concentration from power plants is higher than the atmosphere. The low CO_2 concentration in the atmosphere can slow down the growth of microalgae due to mass transfer limitation. Efficiency of CO_2 capture by microalgae increases with power plant flue gases that have up to 15% of CO_2 [19] and studies have shown that microalgal species (such as *Scenedesmus sp*. and *Chlorella sp.*) can tolerate 10% to 30% CO_2 in its gas supply [29]. Therefore microalgal cultivation can be synergistically located adjacent to a power plant where the CO_2 emitted from such a plant can be conveniently sequestered by the algae as a source of their nutrients [17].

3. Microalgal Cultivation System

There are two main microalgal large-scale cultivation systems: (1) open air-system and (2) photobioreactors [30]. The selection of a cultivation system depends on several factors: the type and the biology of the algal species, the availability of sunlight, the cost of land, the water supply, the availability of nutrients, the desired final product, the climate conditions and the supply of CO_2 [25, 30]. The amount of nutrients and certain metals (i.e., iron and magnesium) must be optimum as they are important for the growth of microalgae and CO_2 fixation efficiency [19]. Research from an outdoor mass cultivation in New Mexico showed that with the right levels of nutrients, CO_2 fixation by microalgae could be increased [23]. A well-designed cultivation system can improve the effectiveness of CO_2 capture by microalgae [19]. Another important factor when deciding on a cultivation system is the likelihood of contamination by other microorganisms [19]. For example, algal species like *Chlorella, Dunaliella*, and *Spirulina* can grow only in specific environments, hence are not likely to be contaminated by other microalgae when cultivated in an open-air system. In contrast, some marine microalgae such as *Tetraselmis*, *Skeletonem*, and *Isochrysis* are susceptible to foreign invasion and must be grown in closed photobioreactors [30].

3.1. Open-Air System. There are many kinds of open-air systems with each having its own set of advantages and disadvantages. The four common types of open-air systems are shallow big ponds, tanks, circular ponds, and raceway ponds [30]. Open-air systems are less complex to construct and operate than photobioreactors [31]. They are considered as low cost methods to cultivate microalgae if compared to closed systems [19]. Nevertheless, open-air systems have many disadvantages, including diffusion of CO_2 back to the environment, requirement for a large area of land, evaporative water losses, and poor light utilization [31]. Besides that, open systems are exposed to many elements in the atmosphere. Hence, they give low biomass yields as it is difficult to control the culture conditions. The depth of the ponds also presents a problem. It needs to be shallow enough for the sunlight to reach the microalgal cells and, at the same time, deep enough for sufficient mixing. Thus, the maximum biomass that can be achieved from most microalgae is roughly between 0.1 to 0.5 g dry weight/L culture [30].

Among the many types of open-air systems, the most common design is the raceway pond as shown in Figure 2 [19]. The raceway pond is made up of a closed loop recirculation channel that includes a paddle wheel. The paddle wheel provides the circulation and the mixing, while the baffles placed in the channel guide the flow. To ensure that the light reaches the microalgal cells, the raceway pond is only about 0.3 m in depth. This design has been around since the 1950s. The raceways ponds are made from concrete or compacted earth that can be lined with plastics [3]. The continuous mixing that occurs within the pond enables high growth rate and minimises contamination risk by foreign microalgae [30].

Even though this open-air cultivation method is not ideal, there are several companies using the design, such as Aquaflow Bionomics and Live Fuels based respectively in New Zealand and the United States. Both of these companies are using alternative techniques to deal with the presence of unwanted microorganisms [32].

Table 1: Previous studies on organic solvent extraction of microalgal chlorophyll.

Study	Algae species	Solvent	Cell disruption	Key results
Jeffrey et al. [4]	Phytoplankton	Methanol (90%), ethanol (90%), ethanol (100%), DMF	All	DMF is superior to all the other solvents used and cell lysis improves extraction in all cases.
Macías-Sánchez et al. [33]	*Dunaliella Salina*	DMF Methanol	Ultrasound	DMF was found to be more efficient methanol.
Sartory & Grobbelaar [34]	*Scenedesmus quadricauda, Selenastrum capricornutum, Microcystysis aeruginosa*	Ethanol (95%), methanol, acetone (90%)	Homogenisation, sonication, boiling	(1) Methanol and 95% ethanol were superior to 90% acetone. (2) Boiling the algae in either methanol or 95% ethanol for 5 minutes and allowing extraction for 24 hours resulted in the complete extraction of pigments without any formation of degradation products.
Schuman et al. [35]	*Stichococcus, Chlorella*	Acetone, DMF	Grinding, Ultrasoun, bead beater	(1) DMF was found to be the most efficient solvent. (2) Acetone extracted 56-100% of the amount of chlorophyll *a* extracted by DMF. (3) DMF does not require cell disruption. (4) Freeze drying before analysis aids extraction
Simon & Helliwell [36]	Freshwater algae *Selenastrum obliquus*	Methanol and acetone	Probe sonication, bath sonication, tissue grinding, mortar and pestle	Under sonication, methanol removed 3x more pigment than acetone. Under tissue grinding, methanol removed 20% more than acetone.

3.2. Photobioreactor System. The photobioreactor system maximises photosynthesis by circulating the microalgal cells, nutrients, and CO_2 in a narrow enclosed transparent vessel exposed to ample illumination [32]. Its high-surface-area-to-volume ratio enables optimal light utilisation leading to higher biomass productivity. Furthermore, the photobioreactor's closed design facilitates high sterility, robust control of temperature, and good management of culture conditions. All these advantages allow the photobioreactor system to culture a variety of microalgal species without any contamination and to produce a high quality biomass. The photobioreactors are also continuously well-mixed to improve gas diffusion into the microalgal cells. Even though the photobioreactor system gives control over most cultivation parameters and achieves a higher CO_2 fixation rate than open-air system, it requires large amount of energy for its operation and construction [19, 30].

The photobioreactor system comes in several designs like flat-plate, tubular, bubble-sparged vertical column, and airlift. Of those designs, tubular photobioreactors are the most popular [19, 31]. Table 2 shows the comparison between raceway ponds and tubular photobioreactors. Tubular photobioreactors is made up of an array of clear straight tubes. These tubes are made of either glass or plastic and are usually less than 0.1 m in diameter in order to allow for light penetration. The tubes are arranged either horizontally where they are placed parallel to each other flat on the ground or vertically where they are configured to form fence-like structures. Figure 3 shows the two different configurations of tubular photobioreactors [3].

Flat-plate photobioreactors are frequently used for its large illumination surface area. Like the tubular design, flat-plate photobioreactors are also made out of transparent materials for maximum penetration of sunlight. This design can also achieve high CO_2 fixation efficiency and mass cultivation of microalgae. In fact, there is less build-up of oxygen in the flat-plate design compare to the tubular design. However, the design suffers from the following drawbacks: (1) difficulty in controlling culture temperatures; (2) scale-up requires more compartments and support materials; (3) stronger hydrodynamic stress on microalgal cultures [31].

Apart from the four primary designs, there are other types of photobioreactor systems that are currently used. The basics of the systems are the same with some modficiations to maximise the efficiency. One such example is a 450 ft long by 50 ft wide photobioreactor made up of twin transparent plastic algal waterbeds patented by a company called A2BE Carbon Capture LLC. Another company, Green Shift Corporation based in New York has produced a pilot-scale photobioreactor that is incorporated with an ethanol producing facility to capture the CO_2 emitted from power plants [32].

4. Chlorophyll Extraction Methods

4.1. Organic Solvent Extraction. In order to quantify the amount of chlorophyll in a particular species, the intracellular chlorophyll must first be extracted. The traditional method that has been employed is organic solvent extraction [4, 36]. The extraction process involves the organic solvent

Table 2: Comparison between microalgal cultivation systems [19].

System	Raceway ponds	Tubular photobioreactors
Light efficiency	Fairly good	Excellent
Temperature control	None	Excellent
Gas transfer	Poor	Low - high
Oxygen production	Low	High
Accumulation	Low	Low - high
Hydrodynamic stress on algae	Difficult	Easy
Species control	None	Achievable
Sterility	Low	High
Cost to scale-up	Low	High
Volumetric productivity	High	Low

penetrating through the cell membrane and dissolving the lipids as well as the lipoproteins of chloroplast membranes [4]. It has been found that cell disruption, achieved through grinding, homogenisation, ultrasound or sonication, significantly improves the effectiveness of chlorophyll extraction using organic solvents [4, 33, 34, 36]. Simon and Helliwell [36] found that, without cell disruption, only a quarter of the potential chlorophyll *a* was able to be extracted by an optimal method. In addition to cell disruption, there are other parameters which affect the efficiency of organic solvent extraction, including the storage conditions of the filtered microalgae prior to the analysis, the organic solvents used, the duration of the extraction and the number of extraction steps employed in the analysis [4, 34, 35]. Since chlorophyll is highly reactive, the yield of a particular extraction procedure is also affected by the formation of degradation products. Degradation products of chlorophyll are formed when their molecules are exposed to excess light, oxygen/air, high temperatures and acidic or basic conditions [4, 5].

Table 1 shows previous studies on organic solvent extraction of microalgal chlorophyll. Simon and Helliwell [36], Sartory and Grobbelaar [34], and Jeffrey et al. [4] found methanol and ethanol to be superior extraction solvents to acetone. Simon and Helliwell [36] conducted their sonication-assisted chlorophyll extractions in an ice bath and in dark conditions to prevent degradation products from forming. They found that, with sonication, methanol removed three times more pigment than 90% acetone. Additionally, when tissue grinding was used, methanol removed 20% more pigment than 90% acetone. Sartory and Grobbelaar [34] similarly found that 90% acetone was an inefficient organic solvent compared to methanol or 95% ethanol. However, it has been shown that the use of methanol as an extraction solvent resulted in an unstable solution and lead to the formation of chlorophyll *a* degradation products [4, 37]. Although 100% acetone was found not to yield the highest amount of chlorophyll from any particular species, its use as an extracting solvent strongly inhibited the formation of degradation products [4]. In studies carried out by Jeffrey et al. [4] and Macías-Sánchez et al. [33], dimethyl formamide (DMF) was found to be a superior extraction solvent to methanol, 90% ethanol, 100% ethanol and 90% acetone. Extraction using DMF did not require cell disruption as pigments were completely extracted after a few steps of soaking. Additionally, the pigments remained stable for up to twenty days when stored in the dark at 5°C [4, 35]. However, DMF toxic nature decreased its appeal as an efficient solvent [4]. It was also found that storage of the microalgae at low temperatures after filtration (−18°C or −20°C) assisted cell disruption and promoted the extraction of chlorophyll [4]. Schumann et al. [35] found freezing the biomass in liquid nitrogen followed by lyophilisation and then storage at −18°C to be the optimal storage procedure.

Sartory and Grobbelaar [34] found the efficiency of chlorophyll extraction from fresh water microalgae to be optimal when the filtered microalgae and solution were refluxed at the solvent's boiling point. It was shown that boiling for 3 to 5 minutes in methanol or 95% acetone prior to 24-hour extraction led to the complete isolation of chlorophyll *a* without the formation of any degradation products. However when the mixture was subjected to temperatures of 100°C, degradation products started to form [34]. Such findings are contradictory to the general assumption that chlorophyll degraded upon slight temperature elevation.

The amount of chlorophyll extracted from a particular algal species was found to be highly dependent on its growth stage. Microalgae extracted in the stationary growth phase were shown to have significantly higher amount of chlorophyll *a* compared to the same species obtained in the logarithmic phase [35].

4.2. Supercritical Fluid Extraction (SFE). The use of organic solvents for lipophilic extraction posts a serious threat to the environment. The Montreal Protocol in 1987 proposed to restrict or to eliminate the manufacture and the use of ozone depleting solvents such as chlorofluorocarbons (CFCs). From then on, the Montreal Protocol has evolved and most solvents that are damaging to the environment have been restricted. As a result, more industries are looking into a new sustainable process that does not involve environmentally damaging solvents [38]. Supercritical fluid extraction (SFE) is a popular method to replace organic solvent extraction.

Supercritical fluid extraction was first introduced as an alternative extraction method in 1879 by Hannay and

Table 3: Comparison between organic solvent extraction and $SCCO_2$ extraction, modified from [40].

No.	Organic solvent extraction	$SCCO_2$ extraction
1	Solvent presence is unavoidable. The amount of solvent depends on the type of solvent used. Solvent removal requires extra unit operations and increases operational cost.	$SCCO_2$ extraction produces solvent-free extracts.
2	Heavy metal and inorganic salt contents are also unavoidable. Their levels depend on the solvent, the method of solvent recycling, the source of the raw material, and the materials used to construct the contact parts of the machinery.	Extract is completely free of heavy metals and inorganic salts since they are not extractable by the $SCCO_2$ even if they are present in the raw material. No heavy metals are present in the CO_2 extractant or the SFE system.
3	Polar substances get dissolved along with the lipophilic substances from the raw material due to poor selectivity of the solvent. During solvent removal operations, these polar substances may form polymers which lead to discoloration of the extract.	Due its nonpolar nature, $SCCO_2$ will not extract any polar substance.

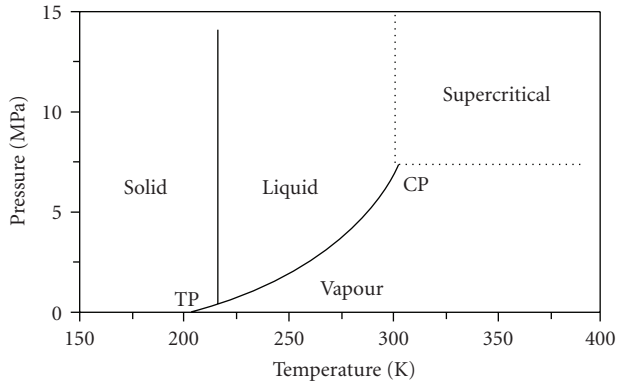

Figure 4: P-T phase diagram for carbon dioxide [42].

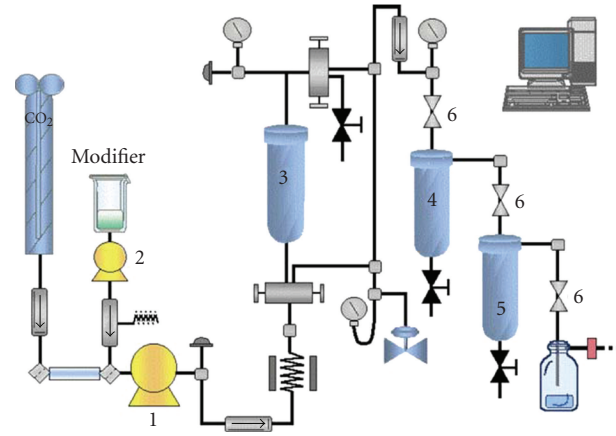

Figure 5: Schematic diagram of supercritical fluid extraction system, extracted from [45]. (1) CO_2 pump, (2) modifier pump, (3) extraction cell, (4) fractionation cell I, (5) fractionation cell II, (6) valve.

Hogarth. However, it was not until around 1960 that this extraction method started to be thoroughly investigated [39]. SFE has many advantages over organic solvent extraction. One of the major advantages is the high purity of the extract. In addition to requiring less processing steps, SFE is significantly safer than organic solvent extraction and can be operated at moderate temperatures to minimize extract degradation. Table 3 shows the comparison between the two extraction methods [40].

The supercritical state is achieved when a substance is exposed to conditions exceeding its critical temperature (T_c) and pressure (P_c). In this state, the substance has liquid-like densities with the viscosities of a gas. The solvent power of supercritical fluids is the highest for slightly polar or non-polar components and is lower for analytes with higher molecular weights. The fluid is easily removed from extract through expansion to atmospheric pressure [41].

CO_2 is the most commonly used fluid for SFE as it is cheap, non-flammable, readily available, and somewhat inert. Figure 4 shows the phase diagram for CO_2 with its supercritical region. The critical temperature and pressure of CO_2 are 304.1 K and 7.38 MPa, respectively. The moderate T_c of CO_2 yields higher quality extracts because it avoids excessive heating which often leads to degradation. This allows for supercritical carbon dioxide ($SCCO_2$) to be used in the extraction of thermolabile compounds [42, 43]. $SCCO_2$ is also preferred due to its high diffusivity and the ease in manipulating its solvent strength. This can be done by adding a substance or modifier which has volatility between the supercritical fluid and the analyte that is to be extracted. For example, the addition of a polar solvent like methanol or water to supercritical CO_2 allows it to extract polar compounds [39, 42]. Studies have shown that addition of ethanol to supercritical fluid increases the yield of lipids from *Arthrospira maxima* [44].

$SCCO_2$ extraction is applicable in many different fields such as food and natural products extraction, environmental science and pharmaceuticals [39]. This review will focus on $SCCO_2$ extraction of chlorophyll from microalgae. Chlorophyll is mainly used in food technology, so there are stringent regulations regarding its quality. By using $SCCO_2$ extraction, a solvent-free highly pure extract can be achieved. Upon decompression, the supercritical CO_2 is removed from the extract as it evaporates to the ambiance in its gaseous state [45].

Table 4: Previous studies on HPLC fractionation of chlorophylls extracted from phytoplanktons.

Study, Chromatography	Mobile phase	Stationary phase	Key results
Jeffrey [49], TLC	First dimension: 0.8% n-propanol in light petroleum (by volume) Second dimension: 20% chloroform in light petroleum (by volume)	Sucrose	In this two dimensional chromatography, there was complete separation of chlorophylls and carotenoids.
Jeffrey et al. [4], HPLC	90 : 10 (v/v) methanol : acetone for 8 min at a flow rate 1 mL/min Preinjection mix of sample 3 : 1 (v/v) sample: 0.5 M ammonium acetate	3 μm C18 Pecosphere	This simple isocratic protocol was able to separate only chlorophyll *a* from other pigments and compounds.
Jeffrey et al. [4], HPLC	Solvent A is 80 : 20 (v/v) methanol : 0.5M ammonium acetate Solvent B is 90 : 10 methanol: acetone Elution order: 0–3 min: solvent A 3–17 min: solvent B flow rates: 1 mL/min Pre-injection mix of samplee 3 : 1 (v/v) sample: 0.5 M ammonium acetat	3 μm C18 Pecosphere	This step-isocratic protocol was found to successfully separate the three chlorophylls (*a*, *b* and *c*) and ten other derivative products.
Jeffrey et al. [4], HPLC	Solvent A is 80 : 20 (v/v) methanol: 0.5 M ammonium acetate Solvent B is 90 : 10 (v/v) acetonitrile : water Solvent C is ethyl acetate Elution order: 0–4 min: linear gradient from 100% A to 100% B 4–18 min: linear gradient to 20% B and 80% C 18–21 min: linear gradient to 100% B 21–24 min: linear gradient to 100% A 24–29 min: isocratic flow of 100% A	3 μm C18 Pecosphere	This ternary gradient protocol was found to separate over 50 pigments. The resolution of this protocol is higher than that of Wright and Shearer [51]. Additionally no ion pairing reagent is required, as in Mantoura and Llewellyn [37].
Lynn Co and Schanderl [52], TLC	Three different solvent systems were experimented. **Solvent system 1** (modified Bauer solvents): First dimension is benzene: petroleum ether: acetone (10 : 2.5 : 2 v/v/v) Second dimension is benzene: petroleum ether: acetone: methanol (10 : 2.5 : 1 : 0.25 v/v/v) **Solvent system 2:** First dimension is benzene: petroleum ether: acetone: methanol (10 : 2.5 : 1 : 0.25 v/v/v) Second dimension is petroleum ether: acetone: n-propanol (8 : 2 : 0.5 v/v/v) **Solvent system 3:** First dimension is benzene: petroleum ether: acetone (10 : 2.5 : 2 v/v/v) Second dimension is petroleum ether: acetone: n-propanol (8 : 2 : 0.5 v/v/v)	Silica Gel	Two dimensional chromatography was carried out on silica gel. Eight major pigments as well as eight to ten minor derivatives were successfully separated with these solvent systems.
Madgwick [50], TLC	30 mL of 1: 1 (v/v) diethyl ether : petroleum spirit	Glucose	(1) One dimensional ascending thin layer chromatography was used. (2) Spectrophotometric analysis was found to overestimate chlorophyll *c* by up to 22% and to underestimate chlorophyll *b* by 10–20%. Chlorophyll *a* was, however, correctly quantified.

Table 4: Continued.

Study, Chromatography	Mobile phase	Stationary phase	Key results
Mantoura and Llewellyn [37], HPLC	Solvent P (ion pairing reagent) is made of 1.5 g tetrabutyl ammonium acetate and 7.7 g of ammonium acetate dissolved in 100 mL of water. Primary eluant is solvent P : water : methanol (10 : 10 : 80 v/v/v) Secondary eluant is 20 : 80 (v/v) acetone: methanol 0–10 min: linear gradient from primary eluant to secondary eluant 10–22 min: isocratic flow of secondary eluant	Four different columns: C3 Zorbax, C8 Zorbax, C18 Zorbax, Shandon Hypersil ODS	High resolution separation of chlorophylls and all major pigments were achieved. The method obtained a high recovery (over 90%) of pigments.
Riley and Wilson [53], TLC	Petroleum ether : ethyl acetate : diethyl amine (58 : 30 : 12 v/v/v)	Silica gel	All plant pigments were separated except for some minor components.
Sartory [48], HPLC	Solvent A is 97% methanol Solvent B is 97% acetone Elution order: 0–15 min: 100% solvent A 15–20 min: linear gradient to 77% solvent A: 23% solvent B Then isocratic flow of 77% solvent A: 23% solvent B Flow rate: 1 mL/min	Sep-Pak C18 Bondapak	(1) HPLC was found to be a rapid, sensitive, and selective method that successfully separated chlorophylls and its derivatives to high resolutions. Recovery of total pigments by HPLC is greater than 96%. (2) Spectrophotometric analysis overestimated chlrophyll *a* and underestimated chlorophyll *b*.
Wright and Shearer [51], HPLC	Linear gradient from 90% acetonitrile to ethyl acetate for 20 mins at a flow rate of 2 mL/min	C18 octadecyl silica.	Carotenes, chlorophylls, xanthophylls, and their degradation products were successfully separated with high resolutions.

4.2.1. SFE Apparatus. There are two supercritical fluid extraction systems: analytical and preparative. In the analytical system, SFE is directly combined with a chromatographic system. The preparative system is used to extract compounds from samples for example chlorophylls from microalgal biomass. SFE can process either liquid or solid samples.

Figure 5 shows a pilot-scale preparative SFE system. It is made up of a solvent (in this case the solvent is CO_2) pump, a modifier pump, an extraction cell, valves and two fractionation cells. The extraction cell is for solids whilst packed columns are used for liquids [45]. The microalgal biomass is placed in the extraction cell [42]. The extract is collected and solvent is depressurized in the fractionation cells which are equipped with temperature and pressure controllers. This configuration allows different compounds to be obtained in each fractionation cell based on their differential solubility in the supercritical fluid [45].

4.2.2. Effect of SFE Operating Conditions. The $SCCO_2$ extraction of chlorophyll from microalgae depends on the fluid density which is a function of operating pressure and temperature. Studies have been conducted on $SCCO_2$ extraction of chlorophyll *a* from at least two microalgal species *Nannochloropsis gaditana* and *Synechococcus sp*. Optimum extraction conditions were found to be 60°C and 400 bar for *Nannochloropsis gaditana* and 60°C and 500 bar for *Synechococcus sp*.

At constant temperature, an increase in pressure will increase the fluid density. Even though this will increase the solvating power of the supercritical fluid, it will decrease its diffusion coefficient. The increase in temperature at constant pressure also has a double effect. Increasing temperature raises the vapour pressures of the pigments and hence gives better solubility. However, it will also decrease the density of the supercritical fluid which leads to a lower solvating power. Therefore, the chlorophyll yield on each operating condition will depend on which effect predominates [43, 46].

5. Chlorophyll Fractionation and Purification on Chromatographic Adsorbents

The traditional method for the quantification of chlorophyll and other pigments in a particular extract is spectrophotometric analysis [34]. The different chlorophyll compounds and other pigments are quantified by measuring the absorbance of a sample at particular wavelengths and using formulated simultaneous equations to calculate the concentrations of particular pigments. It has been found that this method of quantification is often inaccurate as absorption and emission bands of chlorophyll *b* and other pigments overlap with those of chlorophyll *a*. Chlorophyll degradation products are not detected and studies conducted by different authors provided different simultaneous equations [37, 47–50].

In order to overcome the flaws associated with the spectrophotometric analysis, chromatographic techniques are used to fractionate and to quantify chlorophyll and its derivative products. The three types of chromatography

that have been widely used are paper chromatography, thin layer chromatography (TLC) and high pressure liquid chromatography (HPLC). Paper chromatography was mostly used in the 1950s and 1960s during the early stages of the development of chromatographic techniques. This method was found to effectively separate chlorophyll into its three fractions (*a*, *b*, and *c*), pheophytins, carotenes and other derivative products [54]. However, TLC was found to be a preferable technique to paper chromatography due to the ease in quantitatively recovering the pigments from its adsorbents. In paper chromatography, recovery was shown never to exceed 80% [49, 50, 53]. Additionally, TLC requires less sample, is less tedious, and produces chromatograms with sharper resolutions [52, 53].

Organic adsorbents such as sucrose and cellulose were found to be the most efficient stationary phases for use in two dimensional thin layer chromatography [49]. Riley and Wilson [53] and Lynn Co and Schanderl [52] utilised silica gel as their stationary phase and managed to completely separate all of the plant pigments except for some minor components. However, Jeffrey [49] found that use of silica gel promoted the formation of degradation products and resulted in multiple chlorophyll zones.

HPLC is superior to TLC because it requires even less sample for analysis, is faster and features automatic detection system [37, 51]. In addition to these, HPLC is more precise and has a higher degree of sensitivity [55]. Reverse phase HPLC is preferred to normal phase as the latter does not separate polar compounds and its polar stationary phase promotes pigment degradation [37, 51]. An additional drawback of the normal phase HPLC is that it is not compatible with aqueous samples, whereas many of the solvents used for chlorophyll extraction from microalgae are aqueous-based [37]. Several HPLC configurations have been employed, with each providing separation of pigments to varying extents and different resolutions [4]. There are different types of detectors that may be used to measure the concentrations of separated pigments as they exit the column. The most commonly used detectors rely on fluorescence and absorbance analyses. Jeffrey et al. [4] states that fluorescence detection is more sensitive and more selective than absorbance detectors when used to analyze chlorophylls amongst carotenoids. Table 4 summarizes previous studies on chromatographic fractionation of phytoplankton pigments.

6. Conclusions

This review article shows that chlorophyll has a wide range of applications due to its colouring effect, tissue growth stimulating effect, antioxidant and antimutagenic properties. Chlorophyll is best extracted from microalgae by supercritical fluid extraction method. High performance liquid chromatography was found to be the most accurate and sensitive technique to fractionate and to quantify chlorophyll along with its derivatives. Furthermore, biological CO_2 mitigation with microalgal cultivation helps to minimise the global warming impact. Microalgae seem to be a promising alternative source for chlorophyll.

References

[1] R. S. Rasmussen, M. T. Morrissey, and L. T. Steve, "Marine biotechnology for production of food ingredients," in *Advances in Food and Nutrition Research*, pp. 237–292, Academic Press, Boston, Mass, USA, 2007.

[2] A. M. Humphrey, "Chlorophyll," *Food Chemistry*, vol. 5, no. 1, pp. 57–67, 1980.

[3] Y. Chisti, "Biodiesel from microalgae," *Biotechnology Advances*, vol. 25, no. 3, pp. 294–306, 2007.

[4] S. W. Jeffrey, R. F. C. Mantoura, and S. W. Wright, Eds., *Phytoplankton Pigments in Oceanography: Guidelines to Modern Methods*, UNESCO, Paris, Farnce, 1997.

[5] C. Cubas, M. Gloria Lobo, and M. González, "Optimization of the extraction of chlorophylls in green beans (*Phaseolus vulgaris* L.) by N,N-dimethylformamide using response surface methodology," *Journal of Food Composition and Analysis*, vol. 21, no. 2, pp. 125–133, 2008.

[6] A. M. Humphrey, "Chlorophyll as a color and functional ingredient," *Journal of Food Science*, vol. 69, no. 5, pp. 422–425, 2004.

[7] H. Scheer, J. L. William, and M. D. Lane, "Chlorophylls and carotenoids," in *Encyclopedia of Biological Chemistry*, pp. 430–437, Elsevier, New York, NY, USA, 2004.

[8] K. Spears, "Developments in food colourings: the natural alternatives," *Trends in Biotechnology*, vol. 6, no. 11, pp. 283–288, 1988.

[9] C. F. Timberlake and B. S. Henry, "Plant pigments as natural food colours," *Endeavour*, vol. 10, no. 1, pp. 31–36, 1986.

[10] L. W. Smith and A. E. Livingston, "Wound healing: an experimental study of water soluble chlorophyll derivatives in conjunction with various antibacterial agents," *The American Journal of Surgery*, vol. 67, no. 1, pp. 30–39, 1945.

[11] E. B. Carpenter, "Clinical experiences with chlorophyll preparations: with particular reference to chronic osteomyelitis and chronic ulcers," *The American Journal of Surgery*, vol. 77, no. 2, pp. 167–171, 1949.

[12] B. Horwitz, "Role of chlorophyll in proctology," *The American Journal of Surgery*, vol. 81, no. 1, pp. 81–84, 1951.

[13] J. B. Cady and W. S. Morgan, "Treatment of chronic ulcers with chlorophyll: review of a series of fifty cases," *The American Journal of Surgery*, vol. 75, no. 4, pp. 562–569, 1948.

[14] S. L. Goldberg, "The use of water soluble chlorophyll in oral sepsis: an experimental study of 300 cases," *The American Journal of Surgery*, vol. 62, no. 1, pp. 117–123, 1943.

[15] U. M. Lanfer-Marquez, R. M. C. Barros, and P. Sinnecker, "Antioxidant activity of chlorophylls and their derivatives," *Food Research International*, vol. 38, no. 8-9, pp. 885–891, 2005.

[16] M. G. Ferruzzi and J. Blakeslee, "Digestion, absorption, and cancer preventative activity of dietary chlorophyll derivatives," *Nutrition Research*, vol. 27, no. 1, pp. 1–12, 2007.

[17] L. Brennan and P. Owende, "Biofuels from microalgae—a review of technologies for production, processing, and extractions of biofuels and co-products," *Renewable and Sustainable Energy Reviews*, vol. 14, no. 2, pp. 557–577, 2010.

[18] G. A. Florides and P. Christodoulides, "Global warming and carbon dioxide through sciences," *Environment International*, vol. 35, no. 2, pp. 390–401, 2009.

[19] B. Wang, Y. Li, N. Wu, and C. Q. Lan, "CO_2 bio-mitigation using microalgae," *Applied Microbiology and Biotechnology*, vol. 79, no. 5, pp. 707–718, 2008.

[20] J. R. Benemann, "CO_2 mitigation with microalgae systems," *Energy Conversion and Management*, vol. 38, supplement 1, pp. 475–479, 1997.

[21] P. Schenk, S. Thomas-Hall, E. Stephens, et al., "Second generation biofuels: high-efficiency microalgae for biodiesel production," *BioEnergy Research*, vol. 1, no. 1, pp. 20–43, 2008.

[22] E. W. Becker, *Microalgae : Biotechnology and Microbiology*, Cambridge University Press, Cambridge, UK, 1994.

[23] K. G. Zeiler, D. A. Heacox, S. T. Toon, K. L. Kadam, and L. M. Brown, "The use of microalgae for assimilation and utilization of carbon dioxide from fossil fuel-fired power plant flue gas," *Energy Conversion and Management*, vol. 36, no. 6–9, pp. 707–712, 1995.

[24] M. Packer, "Algal capture of carbon dioxide; biomass generation as a tool for greenhouse gas mitigation with reference to New Zealand energy strategy and policy," *Energy Policy*, vol. 37, no. 9, pp. 3428–3737, 2009.

[25] J. Masojídek, G Torzillo, J. Sven Erik, and F. Brian, "Mass cultivation of freshwater microalgae," in *Encyclopedia of Ecology*, pp. 2226–2235, Academic Press, Oxford, UK, 2008.

[26] Z. Cohen, Ed., *Chemicals from Microalgae*, Taylor & Francis, London, UK, 1999.

[27] P. Spolaore, C. Joannis-Cassan, E. Duran, and A. Isambert, "Commercial applications of microalgae," *Journal of Bioscience and Bioengineering*, vol. 101, no. 2, pp. 87–96, 2006.

[28] M. L. Ghirardi, L. Zhang, J. W. Lee, et al., "Microalgae: a green source of renewable H2," *Trends in Biotechnology*, vol. 18, no. 12, pp. 506–511, 2000.

[29] N. Hanagata, T. Takeuchi, Y. Fukuju, D. J. Barnes, and I. Karube, "Tolerance of microalgae to high CO_2 and high temperature," *Phytochemistry*, vol. 31, no. 10, pp. 3345–3348, 1992.

[30] M. A. Borowitzka, "Commercial production of microalgae: ponds, tanks, tubes and fermenters," *Journal of Biotechnology*, vol. 70, no. 1–3, pp. 313–321, 1999.

[31] C. U. Ugwu, H. Aoyagi, and H. Uchiyama, "Photobioreactors for mass cultivation of algae," *Bioresource Technology*, vol. 99, no. 10, pp. 4021–4028, 2008.

[32] G. Marsh, "Small wonders: biomass from algae," *Renewable Energy Focus*, vol. 9, no. 7, pp. 74–78, 2009.

[33] M. D. Macías-Sánchez, C. Mantell, M. Rodríguez, E. M. de la Ossa, L. M. Lubián, and O. Montero, "Comparison of supercritical fluid and ultrasound-assisted extraction of carotenoids and chlorophyll a from *Dunaliella salina*," *Talanta*, vol. 77, no. 3, pp. 948–952, 2009.

[34] D. P. Sartory and J. U. Grobbelaar, "Extraction of chlorophyll a from freshwater phytoplankton for spectrophotometric analysis," *Hydrobiologia*, vol. 114, no. 3, pp. 177–187, 1984.

[35] R. Schumann, N. Häubner, S. Klausch, and U. Karsten, "Chlorophyll extraction methods for the quantification of green microalgae colonizing building facades," *International Biodeterioration and Biodegradation*, vol. 55, no. 3, pp. 213–222, 2005.

[36] D. Simon and S. Helliwell, "Extraction and quantification of chlorophyll a from freshwater green algae," *Water Research*, vol. 32, no. 7, pp. 2220–2223, 1998.

[37] R. F. C. Mantoura and C. A. Llewellyn, "The rapid determination of algal chlorophyll and carotenoid pigments and their breakdown products in natural waters by reverse-phase high-performance liquid chromatography," *Analytica Chimica Acta*, vol. 151, no. 2, pp. 297–314, 1983.

[38] E. Ramsey, Q. Sun, Z. Zhang, C. Zhang, and W. Gou, "Mini-review: green sustainable processes using supercritical fluid carbon dioxide," *Journal of Environmental Sciences*, vol. 21, no. 6, pp. 720–726, 2009.

[39] M. Herrero, J. A. Mendiola, A. Cifuentes, and E. Ibáñez, "Supercritical fluid extraction: recent advances and applications," *Journal of Chromatography A*, vol. 1217, no. 16, pp. 2495–2511, 2010.

[40] F. Sahena, I. S. M. Zaidul, S. Jinap, et al., "Application of supercritical CO_2 in lipid extraction—a review," *Journal of Food Engineering*, vol. 95, no. 2, pp. 240–253, 2009.

[41] G. Brunner, "Supercritical fluids: technology and application to food processing," *Journal of Food Engineering*, vol. 67, no. 1-2, pp. 21–33, 2005.

[42] R. L. Mendes, B. P. Nobre, M. T. Cardoso, A. P. Pereira, and A. F. Palavra, "Supercritical carbon dioxide extraction of compounds with pharmaceutical importance from microalgae," *Inorganica Chimica Acta*, vol. 356, pp. 328–334, 2003.

[43] M. D. Macías-Sánchez, C. Mantell, M. Rodríguez, E. Martínez de La Ossa, L. M. Lubián, and O. Montero, "Supercritical fluid extraction of carotenoids and chlorophyll a from Nannochloropsis gaditana," *Journal of Food Engineering*, vol. 66, no. 2, pp. 245–251, 2005.

[44] R. L. Mendes, A. D. Reis, and A. F. Palavra, "Supercritical CO_2 extraction of γ-linolenic acid and other lipids from arthrospira (Spirulina)maxima: comparison with organic solvent extraction," *Food Chemistry*, vol. 99, no. 1, pp. 57–63, 2006.

[45] M. Herrero, A. Cifuentes, and E. Ibañez, "Sub- and supercritical fluid extraction of functional ingredients from different natural sources: plants, food-by-products, algae and microalgae—a review," *Food Chemistry*, vol. 98, no. 1, pp. 136–148, 2006.

[46] M. D. Macías-Sánchez, C. Mantell, M. Rodríguez, E. Martínez de la Ossa, L. M. Lubián, and O. Montero, "Supercritical fluid extraction of carotenoids and chlorophyll a from Synechococcus sp," *Journal of Supercritical Fluids*, vol. 39, no. 3, pp. 323–329, 2007.

[47] J. K. Abaychi and J. P. Riley, "The determination of phytoplankton pigments by high-performance liquid chromatography," *Analytica Chimica Acta*, vol. 107, pp. 1–11, 1979.

[48] D. P. Sartory, "The determination of algal chlorophyllous pigments by high performance liquid chromatography and spectrophotometry," *Water Research*, vol. 19, no. 5, pp. 605–610, 1985.

[49] S. W. Jeffrey, "Quantitative thin-layer chromatography of chlorophylls and carotenoids from marine algae," *Biochimica et Biophysica Acta*, vol. 162, no. 2, pp. 271–285, 1968.

[50] J. C. Madgwick, "Chromatographic determination of chlorophylls in algal cultures and phytoplankton," *Deep Sea Research and Oceanographic Abstracts*, vol. 13, no. 3, pp. 459–466, 1966.

[51] S. W. Wright and J. D. Shearer, "Rapid extraction and high-performance liquid chromatography of chlorophylls and carotenoids from marine phytoplankton," *Journal of Chromatography A*, vol. 294, pp. 281–295, 1984.

[52] D. Y. C. Lynn Co and S. H. Schanderl, "Separation of chlorophylls and related plant pigments by two-dimensional thin-layer chromatography," *Journal of Chromatography A*, vol. 26, pp. 442–448, 1967.

[53] J. P. Riley and T. R. S. Wilson, "Use of thin-layer chromatography for separation and identification of phytoplankton pigments," *Journal of the Marine Biological Association of the United Kingdom*, vol. 45, no. 3, pp. 583–591, 1965.

[54] S. W. Jeffrey, "Paper-chromatographic separation of chlorophylls and carotenoids from marine algae," *Biochemical journal*, vol. 80, no. 2, pp. 336–342, 1961.

[55] W. T. Shoaf, "Rapid method for the separation of chlorophylls a and b by high-pressure liquid chromatography," *Journal of Chromatography A*, vol. 152, no. 1, pp. 247–249, 1978.

Hindawi Publishing Corporation
International Journal of Chemical Engineering
Volume 2010, Article ID 518070, 9 pages
doi:10.1155/2010/518070

Research Article

Process Optimization for Biodiesel Production from Corn Oil and Its Oxidative Stability

N. El Boulifi, A. Bouaid, M. Martinez, and J. Aracil

Department of Chemical Engineering, Faculty of Chemistry, Complutense University, 28040 Madrid, Spain

Correspondence should be addressed to J. Aracil, jam1@quim.ucm.es

Received 1 December 2009; Revised 3 March 2010; Accepted 4 March 2010

Academic Editor: Michael K. Danquah

Response surface methodology (RSM) based on central composite design (CCD) was used to optimize biodiesel production process from corn oil. The process variables, temperature and catalyst concentration were found to have significant influence on biodiesel yield. The optimum combination derived via RSM for high corn oil methyl ester yield (99.48%) was found to be 1.18% wt catalyst concentration at a reaction temperature of 55.6°C. To determine how long biodiesel can safely be stored, it is desirable to have a measurement for the stability of the biodiesel against such oxidation. Storage time and oxygen availability have been considered as possible factors influencing oxidative instability. Biodiesel from corn oil was stored for a period of 30 months, and the physico-chemical parameters of samples were measured at regular interval of time. Results show that the acid value (AV), peroxide value (PV), and viscosity (ν) increased while the iodine value (IV) decreased. These parameters changed very significantly when the sample was stored under normal oxygen atmosphere. However, the ν, AV, and IV of the biodiesel sample which was stored under argon atmosphere were within the limit by the European specifications (EN 14214).

1. Introduction

In the last few years, the world's energy demand is increasing due to the needs from the global economic development and population growth. However, the most important part of this energy currently used is the fossil energy sources. The problem is fossil fuels are nonrenewable. They are limited in supply and will one day be depleted. There is an increased interest in alternative renewable fuels. As biodiesel is an environmentally friendly fuel, it is the best candidate to replace fossil-diesel, which has lower emissions than that of fossil-diesel, it is biodegradable, nontoxic, and essentially free of sulphur and aromatics [1]. However, only nitrogen oxides increase using biodiesel as fuels [2, 3].

Renewable feedstocks such as vegetable oils and animal fats have been used as raw materials for biodiesel production [4]. The general way to produce biodiesel fuels is transesterification of fat or oil triacylglycerols with short-chain alcohol such as methanol or ethanol in presence of alkaline or acid catalysts [5–7].

Vegetable oils are promising feedstocks for biodiesel production since they are renewable origin and can be produced on a large scale. More than 95% of biodiesel production feedstocks come from edible oils since they are varying considerably with location according to climate and availability. In the United States, soybean oil is the most common biodiesel feedstock, whereas in Europe and in tropical countries, rapeseed oil and palm oil are the most common source for biodiesel, respectively, [8]. However, some of these oil sources are commodities whose prices are strongly influencing biodiesel cost, generally in the proportion of 70–80% [9]. In order to reduce the biodiesel cost, many researchers are interested in waste edible oils [10] and nonedible oils like karanja, mahua and jatropha [7, 11, 12].

Another alternative comes into play when looking to other industries. That is the case of ethanol, whose primary feedstock is corn. Plants ethanol from corn gives the integrated biorefineries a hydrocarbon-based source of renewable carbon for the production of fuels and chemicals. Ethanol is formed when starch is subjected to hydrolysis, followed by glucose fermentation. During this process, also some by-products including corn gluten meal, gluten feed and corn oil are formed. Therefore, corn oil can be extracted

as a by-product by using new technology that will make ethanol production more efficient. This corn oil can be converted into a biofuel, such as biodiesel [13].

Biodiesel is being commercialized as a substitute or blending stock of fossil-diesel. However, biodiesel is less resistant to oxidation than typical fossil fuel and therefore doping of biodiesel in fossil-diesel will affect the stability of fuel significantly [14]. Thus, as the demand and the production of biodiesel grows fast, the development of methods to ensure the quality of the biodiesel industry and standardization becomes an urgent topic for market introduction of biodiesel.

As corn biodiesel chemically is a mixture of long-chain fatty acid methyl esters (FAMEs), it is more susceptible to autoxidation and thus has a higher level of chemical reactivity than fossil-diesel. This oxidation instability is dependant on the number and location of methylene-interrupted double bounds in the FAMEs. Thus carbons that are simultaneously allylic to two olefinic groups will be extremely susceptible to the initiation of peroxidation. An early study [15] measured the relative rate of oxidation for the methyl esters of oleic (18 : 1), linoleic (18 : 2) and linolenic (18 : 3) acids to be 1 : 12 : 25.

A number of reports have appeared on the storage and oxidative stability of biodiesel synthesized from different vegetable and frying oils (including sunflower, soybean and rapeseed oil) [16–18]. However, there is no available information about storage stability of biodiesel from corn oil. These stability studies were carried out under different storage condition, such as elevated temperature and exposure to light, air, water, and other contaminants. In other studies biodiesel was subjected to accelerated methods of oxidation, including EN 14112 (Rancimat method) and pressurized differential scanning calorimetry [19, 20]. The oxidation stability does not only depend on the raw material on the production process, but also on how the oil pressed and refined [21].

In a previous work [16], long-term storage tests on biodiesel from different sources have been conducted under different storage condition. Some chemicals properties have been severely affected by oxidation of the FAMEs, when the biodiesel was exposed to air and daylight. In order to understand whether normal oxygen atmosphere availability can adversely affect these properties, the study of the change in chemical and physical proprieties of biodiesel in absence of oxygen (under argon atmosphere) becomes necessary.

In this paper, the storage stability of biodiesel made from corn oil was investigated over a storage time of 30 months under argon atmosphere conditions, whose properties were compared to a corn biodiesel sample which stored under normal oxygen atmosphere. The focus of the study was on the influence of storage time on the biodiesel properties, such as PV, AV, IV and ν. This work also discusses the results of experiments carried out to evaluate the different variables affecting the alkaline methanolysis of corn oil. The optimum value for the variables affecting the process will be determined by application of factorial design and response surface methodology.

Factorial design of experiments gives more information per experiment than unplanned approaches; it allows to see interactions among experimental variables within the range studied, leading to better knowledge of the process and therefore reducing research time and costs [22].

2. Experimental Section

2.1. Equipment. Reactions were carried out in a batch stirred reactor of 500 cm^3 volume, equipped with a reflux condenser and a mechanical stirrer. The impeller speed was set at 600 rpm to avoid external mass transfer limitation [6].

2.2. Materials. Corn oil was supplied by Koipe Spain. The quality control of the corn oil used in this study is presented in Table 1. The characteristics were determined according to AOCS official method. Methanol of 99.8% purity was supplied by Panreac (Spain). The catalyst used was potassium hydroxide purchased from Merck (Barcelona, Spain).

2.3. Production of Corn Oil FAMEs. The corn oil FAMEs were produced via a transesterification process in which a strong alkali catalyst was used. This latter is frequently used in the transesterification reaction, primarily due to its significant advantages in terms of the smaller quantity of catalyst used and the shorter reaction time required [6].

Corn oil was used as the raw oil to be transesterified with methanol in a reacting tank. The temperature values are below the boiling point of methanol (63°C), to prevent the methanol in the reactant mixture from evaporating. The molar ratio of the methanol and corn oil was set at 6 : 1. The potassium hydroxide was stirred with methanol for 10 minutes using an electric-magnetic stirrer to form potassium methoxide, which was then poured into the reacting tank and mixed with the corn oil. The total reaction time was 60 minutes. Almost total conversion to corn oil FAMEs was achieved quickly after a few minutes from the start of the reaction, depending on the reaction conditions.

2.3.1. Fatty Acid Methyl Esters (FAMEs) Purification. At the end of a run the reaction mixture was allowed to cool down. The upper phase consisted of FAME, and the lower phase was glycerol.

Once the glycerol and FAME phases have been separated, the last one was purified by gentle washing with distilled water to remove residual catalyst, glycerol, and soaps. The pH of washing water was initially very high 10.22 due to the dissolved KOH. After 3 successive rinses with water, the washing water became clear and its pH was 7.9. The washing process was continued (twice more) until a pH of about 7 was achieved. Finally, the methyl ester phase was distilled to remove the residual water.

The final water content of the corn oil FAME was less than 0.01%. Water in the sample can promote microbial growth, lead to tank corrosion, participate in the formation of emulsions, as well as cause hydrolysis or hydrolytic oxidation [23].

Table 1: Composition analysis results of corn oil.

PV	AV	ν	IV	Main fatty acid composition (%)					
(meq/Kg)	(mg KOH/g)	(cst at 40°C)	(mg I_2/g)	Palmitic (C16 : 0)	Stearic (C18 : 0)	Oleic (C18 : 1)	Linoleic (C18 : 2)	Linolenic (C18 : 3)	other
2.26	0.23	39.28	125.4	12	2.4	27.3	55.8	1	1.5

PV: peroxide value; AV: acid value; ν: viscosity; IV: iodine value.

2.4. Analytical Method. Reaction products were monitored by capillary column gas chromatography, using a Hewlett-Packard 5890 series II equipped with a flame ionization detector (FID). The injection system was split-splitless. The carrier gas was helium at a flow rate of 1 mL/minutes. The analytical procedures and operating conditions have been described in detail in a previous work [24]. The internal standard technique was used to quantify the amount of the chemical species.

2.5. Preparation the FAME Samples. Two biodiesel samples, three litres each of were stored at ambient temperature for 30 months at two different storage conditions: the samples were stored in closed glass exposed to daylight, one under normal oxygen conditions and the other under atmosphere argon. During storage, samples were taken out periodically and different quality parameters (PV, AV, IV, and ν) were monitored. The analyses were done according to the following procedures: PV (AOCS Cd 8-53), AV (AOCS-Ca 5a-40), ν (ISO 3104), and IV (AOCS cd 1-25).

3. Results and Discussion

3.1. Statistical Analysis. The synthesis of biodiesel was studied using factorial design of experiments. The experimental design applied to this study was a full two-level factorial design 2^2 (two factors each, at two-levels) and extended to response surface methodology (RSM).

The response selected, Y, was the yield of methyl ester. The factors chosen were reaction temperature, X_T, and initial catalyst concentration, X_C. Initial alcohol/oil molar ratio was fixed at 6 : 1.

Selection of the levels was carried out based on the results obtained in preliminary studies [25]. Temperature levels were selected according to reactants properties, thus the lower value was set at 34.4°C and the higher at 55.6°C. The levels of catalyst concentration were chosen on the basis of preliminary experiments where the amount of catalyst was progressively increased, and the ester yield monitored versus time. The levels chosen were 0.86 and 1.18 wt.%, based on the total mass reaction.

The statistical analysis was thereafter applied. The experimental matrix for the factorial design is shown in Table 2. All the runs were performed at random. Four experiments were carried out at the centre point level, coded as "0", for experimental error estimation.

The use of analysis and factorial design of experiments allowed us to express the amount of ester produced as a polynomial model (if the levels of the factors are equally spaced, then orthogonal polynomials may be used). The response, yield of ester, may be thus expressed as a function of the significant factors.

Table 2: Experimental matrix and experimental results.

Run	X_C	X_T	C (%)	T (°C)	Y(%)
1	−1	−1	34.4	0.86	94.40
2	+1	−1	55.6	0.86	98.25
3	−1	+1	34.4	1.18	96.50
4	+1	+1	55.6	1.18	99.48
5	0	0	45	1.02	98.25
6	0	0	45	1.02	97.85
7	0	0	45	1.02	98.30
8	0	0	45	1.02	98.40
9	$-\alpha$	0	30	1.02	97.50
10	$+\alpha$	0	60	1.02	98.70
11	0	$-\alpha$	45	0.80	96.9
12	0	$+\alpha$	45	1.24	96.4

Note: T: temperature; C: catalyst concentration; X: coded value; Y: biodiesel yield.

3.1.1. Linear Stage. A linear stage was considered in the first step. Table 2 shows the experiments corresponding to the 2^2 factorial design (experiments 1–4) and four experiments in the centre point to evaluate the experimental error (experiments 5–8). A statistical analysis was carried out on these experimental values, and the main effects and interaction effects of the variables were calculated. The analysis of the main effects and its interaction for the chosen response and the test of statistical significance are given in Table 3.

Temperature (X_T), catalyst concentration (X_C), and catalyst concentration-temperature interaction effects (X_{TC}) were fitted by multiple regression analysis to a linear model. The response function for the significant main effects and interactions is

$$Y = 97.16 + 1.7X_C + 0.83X_T - 0.21X_{TC}, \quad r = 0.98. \tag{1}$$

The statistical analysis of experimental results revealed that the most significant factor is the catalyst concentration, while it also shows a significant value for curvature for the chosen responses. These data indicate the nonlinearity of the model and thus justifies planning a more complex design to fit the data to a second-order model.

3.1.2. Nonlinear Stage. To better predict the effect of variables, a quadratic model was investigated. Here, the 2^2

Table 3: 2^2 factorial design: statistical analysis.

Response:	Y(%)
Number of experiments:	4
Degree of freedom:	3
Results of statistical analysis	
Y (average)	97.16
Main effects and interactions	
$X_T = 1.66$, $X_C = 3.41$, $X_{TC} = -0.43$	
Statistical Significance of t-test	
Confidence level: 95%,	Standard deviation, $S = 0.24$
Student's t value, $t = 3.182$,	Confidence interval: ± 0.38
Significant effects and Interactions: $X_T(+)$, $X_C(+)$, $X_{TC}(-)$	
Statistical significance of curvature	
$Y_C = 98.2$, $Y = 97.16$	Curvature: $Y_C - Y- = 1.04$
$S = 0.11$, $t = 3.182$	Confidence curvature interval: ± 0.54
	Curvature: significant
Response equation:	
$Y = 97.16 + 1.7X_C + 0.83X_T - 0.21X_{TC}$	$r = 0.98$

experiment design was expanded to a circumscribed central composite design by the addition of 4 new experiments (run 9–12 in Table 2), called start points and coded $\pm\alpha$. The value of α, which is the distance from the center point to the start point, is $2^{n/4}$, where n is the number of factors (for two factors, $\alpha = 1.414$). The corresponding model is the complete quadratic surface between response and the factors, given by the equation

$$Y = \beta_0 + \sum_{i=1}^{2} \beta_i X_i + \sum_{i=1}^{2} \beta_{ii} X_i^2 + \sum_{i \neq j}^{2} \beta_{ij} X_i X_j, \qquad (2)$$

where Y is the response (methyl ester yield), X_i and X_j are the uncoded independent variables, and β_0, β_i, β_{ii}, and β_{ij} are intercept, linear, quadratic and interaction constant coefficients, respectively.

The coefficients of (2) were determined by multiple regression analysis. This analysis includes all the independent variables and their interactions, regardless of their significance levels. The best-fitting response surfaces found can be written as follows:

$$Y = 98.2 + 1.06X_C + 0.32X_T - 0.21X_T X_C + 0.82X_T^2 - 0.1X_C^2, \quad r = 0.97. \qquad (3)$$

The statistical model was obtained from coded levels. Equation (3) can be represented as dimensional surfaces and contour plots, as shown in Figure 1. These show the ester yield predicted for the experimental range of temperature and initial catalyst concentration. The influence of these variables on the ester yield will now be discussed. The influence of the main factors and interactions will be derived from (1) and (3).

3.1.3. Influence of Temperature. For both linear and nonlinear models, the temperature influence is statistically

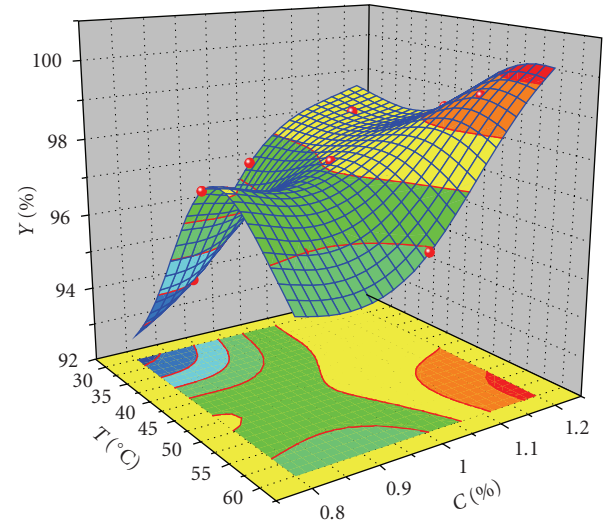

Figure 1: Experimental yield versus temperature and catalyst concentration.

significant in the range studied. This effect has a positive influence on the response. As the temperature increases, the solubility of methanol in the oil increases and so does the speed of reaction. As a matter of fact, at low temperatures, methanol is not soluble at all in the oil; when the stirring is started an emulsion appears. The reaction takes place at the interface of the droplets of alcohol in the oil and then as soon as the first FAMEs are formed, the alcohol solubilizes progressively because the esters are mutual solvents for the alcohol and the oil.

3.1.4. Influence of Catalyst Concentration. From the statistical analysis it can be concluded that, within the experimental range, initial catalyst concentration is the most important

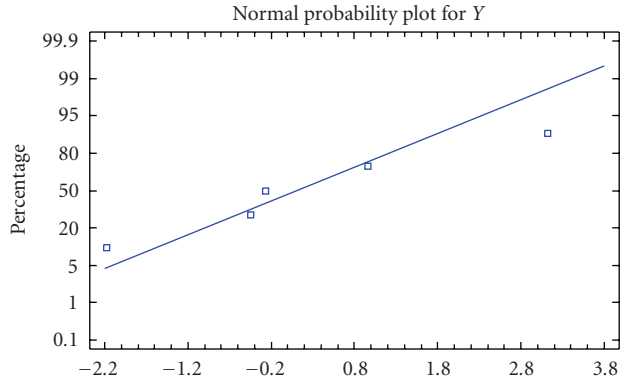

Figure 2: Normal probability plot for the methyl esters yield.

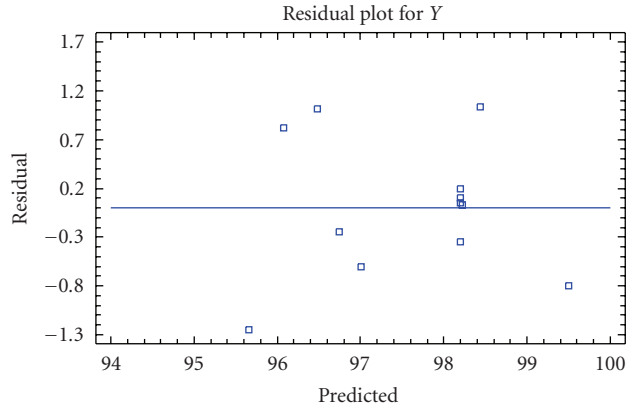

Figure 3: Residual plot of methyl esters yield for the second-order model.

factor on the transesterification process. It has a positive influence on the response; that is, ester yield increases with increasing catalyst concentration.

3.1.5. Influence of Interaction. The nonlinear model (Central Composite Design) gives the binary influences of all the factors used in the design. Interaction of significant main effects temperature and catalyst concentration (T-C) is significant and has a negative influence on the process, this effect may be due to the formation of by-products (soaps).

3.1.6. Analysis of Response: Yield of Ester. The ester yield generally increases with increasing catalyst concentration and temperature, but progressively decreases at higher level of temperature and lower level of catalyst concentration. This finding may be explained by the formation of by-products, possibly due to triglycerides saponification processes, a side reaction which is favoured at high temperatures. This side reaction produces potassium soaps and, thus, decreases the ester yield.

The surface plot and contours of ester yield versus temperature and catalyst concentration obtained when individual experimental data are plotted are shown in Figure 1. A comparison among these plots shows that the maximum ester yield is achieved at the higher level for both temperature and catalyst concentration. Figure 2 present a normal probability plot of methyl ester yield which confirmed the significant influence of catalyst and temperature in the range studied. Figure 3 present a plot of the residual distribution, defined as the difference between calculated and observed values, over the observed values for the response studied FAME. The quality of the fit is good because the residual distribution does not follow a trend with respect to the predicted variables. All the residuals are smaller than 1.7% for FAME yield, which indicate that the model adequately represent the methyl ester yield over the experimental range studied.

Figure 4 presents the plot of experimental values versus predicted ones for biodiesel from Corn oil. From this figure, it can be observed that there are no tendencies in the linear regression fit, so the model explains the experimental range studied adequately.

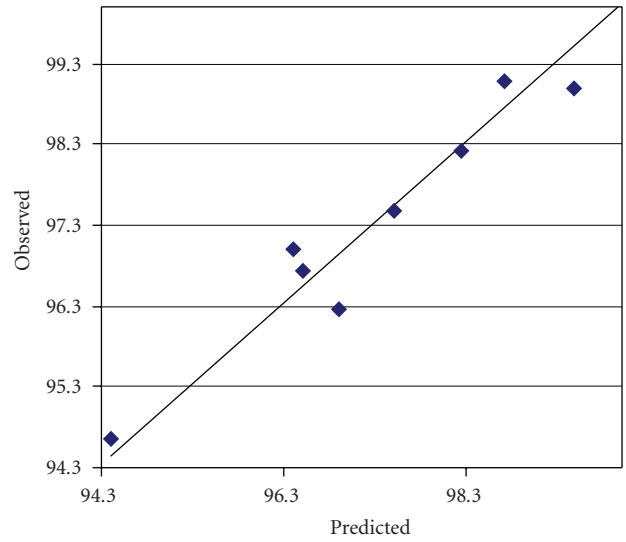

Figure 4: Experimental versus predicted values.

3.2. Long Storage Stability of Biodiesel. The oxidation reactions affect the fuel quality of biodiesel, primarily during extended storage. The oxidation stability study was conducted for a period of 30 months. At regular intervals, samples were taken to measure the following physicochemical quality parameters: PV, AV, IV, and ν.

Some of the most important qualities of biodiesel are shown before and after storage in Table 4. These parameters were compared with some of the biodiesel standards (European Union Standards, EN 14214).

3.2.1. Peroxide Value (PV). Although PV is less suitable for monitoring oxidation [26], and is not specified in the biodiesel fuel standards, this parameter influences cetane number (CN), a parameter that is specified in the fuel standard. An increase in PV involves an increase in CN, and therefore may reduce ignition delay time [27]. The variation of PV of corn oil FAME in two different storage conditions is shown in Figure 5. Sample stored under argon atmosphere showed an increase in PV from 3 to 19.6 meq/kg

Table 4: Quality control of corn oil biodiesel fuels used in this study before and after storage time of 30 months compared to EN 14214

Properties	Unit	Corn biodiesel before storage	Corn biodiesel after storage		Specification EN 14214
			Under argon atmosphere	Under normal oxygen atmosphere	
Viscosity at 40°C	mm^2/s	4.14	4.72	5.82	3.5–5.0
Density at 15°C	g/cm^3	0.865	0.871	0.895	0.86–0.90
Water content	wt%	0.15	0.21	0.29	<0.5
Biodiesel yield	wt%	99.48	98.7	96.23	>96.5
Monoglyceride content	wt%	0.40	0.27	0.3	<0.80
Diglyceride content	wt%	0.11	0.1	0.1	<0.20
Triglyceride content	wt%	0.0	0.0	0.0	<0.20
Free glycerol	wt%	0.01	0.01	0.01	<0.02
Acid value	mg KOH/g	0.047	0.21	0.7	<0.5
Iodine value	mg I_2/g	126.6	98.4	80	<120
Peroxide value	meq/Kg	3.0	14	31.8	—
Cloud point	°C	−5	−4	−3	—
Pour point	°C	−6	−6	−5	—
Cold filter plugging point	°C	−8	−8	−9	<−7

and then a decrease to 14 meq/kg. It can be see that the faster increase rate happens during the first 6 months. The same results were obtained by another author [28]. The reasons why such behaviours exist are not clearly resolved in prior work. However, the increasing of PV during the first 6 months may be due to the presence of the dissolved oxygen remaining in the biodiesel sample that allows the formation of compounds like hydroperoxides. Furthermore, sample stored under normal oxygen atmosphere conditions showed a continuing increase in PV over time. If oxygen is not available in sufficient abundance, the formation of ROOH can slow or even stop while ROOH decomposition continues. This will tend to cause a peak in the ROOH concentration followed by a decrease.

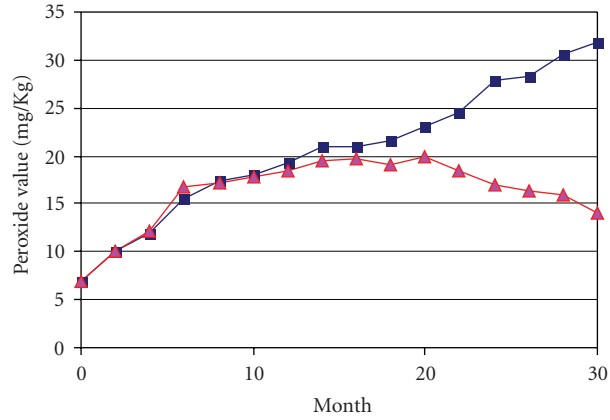

Figure 5: Variation in the peroxide value of corn oil biodiesel stored ■ under normal oxygen atmosphere and ▲ under argon atmosphere.

3.2.2. Acid Value (AV). Once the peroxides have formed, they decompose and interreact to form numerous secondary oxidation products including aldehydes, which further oxidized into acids. Acids can also be formed when traces of water cause hydrolysis of the esters into alcohol and acids. Acid value measured in mg KOH/g is one of the significant indicators of oxidative degradation in lipids. The change in AV during storage for the two corn oil FAME samples is shown in Figure 6. It can be seen that the AV increase continuously in sample stored under normal oxygen atmosphere from 0.047 to 0.7 mg KOH/g. In opposition to it, in the sample stored under argon atmosphere, the AV increased fast during the first 4 months, and then remained almost constant. This behaviour may be due to the presence of the dissolved oxygen remaining in the biodiesel sample that allows the formation of shorter chain fatty acids [18]. In this case, the specification limit of 0.5 mg KOH/g was not exceeded with the corn oil FAME sample stored under argon atmosphere after a storage time of 30 months.

3.2.3. Viscosity (ν). Due to the hydroperoxides decomposition, the oxidative linking of fatty acid methyl ester chains can occur, giving as a result higher molecular weights species. During storage one of the obvious results of polymer formation is an increase in biodiesel viscosity [29]. The formation of higher molecular weight species, with higher viscosity, is a reason why the viscosity specification in biodiesel standards can be used to assess the fuel quality status of stored biodiesel. Figure 7 shows the increase in the kinematic viscosity of the two corn oil FAME samples versus storage time. Corn oil FAME sample which was stored under argon atmosphere, was found to have lower viscosity compared to the sample which was stored under normal oxygen atmosphere. A similar result had been observed previously by other researchers [30]; they noted that the oxidation processes led to the formation of free fatty acids,

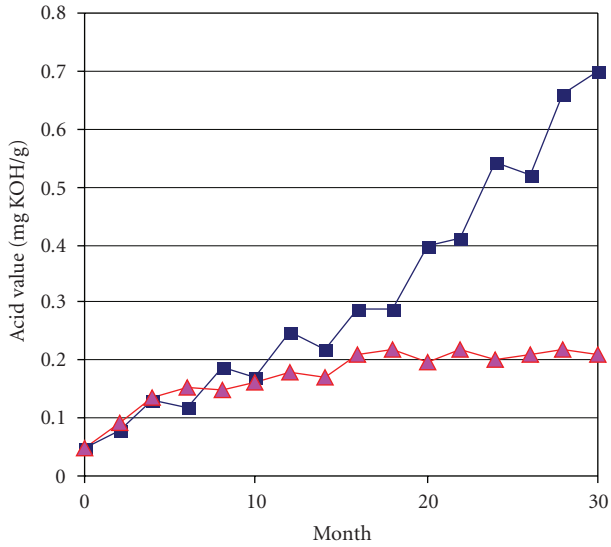

Figure 6: Variation in the acid value of corn oil biodiesel stored ■ under normal oxygen atmosphere and ▲ under argon atmosphere.

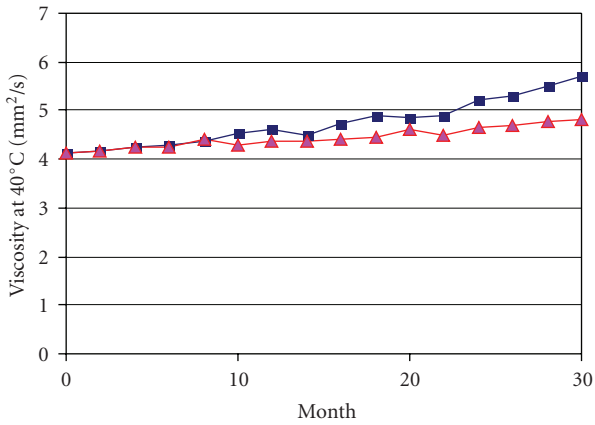

Figure 7: Variation in the iodine value of corn oil biodiesel stored ■ under normal oxygen atmosphere and ▲under argon atmosphere.

double bond isomerization (usually cis to trans), saturation and products of higher molecular weight, and viscosity increases with increasing oxidation. Under conditions where oxygen is available, fatty acid moieties are joined by both C–O–C linkages and C–C linkages [31]. When ROOH decomposition occurs under an inert atmosphere, only C–C linkages in resulting polymers are observed [31].

3.2.4. Iodine Value (IV). One of the oldest and most common methods of determining the level of unsaturation in a fatty oil or ester is the iodine value [32], it purportedly addresses the use of oxidative stability and it is included in the European biodiesel standard. Oxidation, which consists of a complex series of chemical reactions, is characterized by a decrease in the total unsaturated content of biodiesel due to elimination of hydrogen adjacent to a double bond and the formation of free radicals [33]. Our experiment shows that the IV of the two corn oil FAME samples fell along the

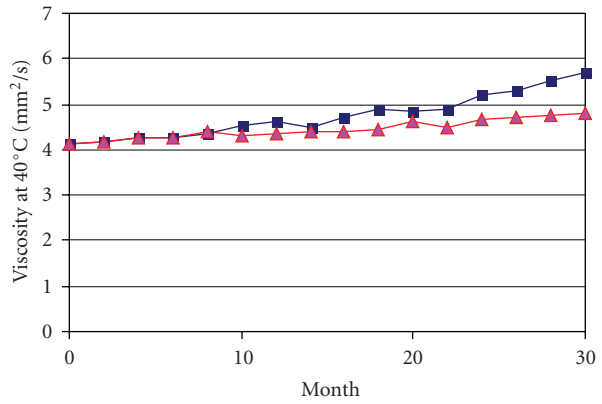

Figure 8: Variation in the kinematic viscosity of corn oil biodiesel stored ■ under normal oxygen atmosphere and ▲ under argon atmosphere.

storage time (Figure 8). The sample which was stored under normal oxygen atmosphere appeared to have the highest rate of reduction in IV, implying that the largest conversion of polyunsaturated fatty acids to hydroperoxides took place. In contrast to this result, the sample which was stored under argon atmosphere was observed to have low rate of decrease in IV. Corn oil FAME samples (IV = 126.6) with a relatively high IV compared to other biodiesel samples [4]; this sample contains low levels of saturated FAME and high levels of mono- and polyunsaturated FAME which make it much susceptible to oxidation.

For biodiesel samples, the peroxide value, acid values, and viscosity tended to increase, and iodine value to decrease over time. The sample stored under argon atmosphere never exceeded the specification limit of the studied parameters along the 30 months of storage. Biodiesel from corn oil stored under argon atmosphere did not demonstrate rapid increase in peroxide value, acid value and viscosity, compared to the one stored under normal oxygen atmosphere.

When storage is done in argon atmosphere condition, at ambient temperature without oxygen availability, PV, AV, and ν increases slowly; while PV peaks and then decreases, AV and ν continue to increase, but at a lower rate. Besides IV decreases during the storage.

Biodiesel kept in an argon atmosphere could increase its stability and also show positive effects retarding oxidative degradation of the biodiesel produced from corn oil.

4. Conclusions

In this work, a fully central composite design has been applied to optimize the synthesis process of FAME from corn oil using potassium hydroxide as catalyst. The study of the factors (temperature and catalyst concentration) affecting the response shows that, within, the experimental range considered, the most important factor is the initial catalyst concentration. For the yield of ester, this factor has a positive influence. The temperature has a positive influence in both responses. The T-C interaction is small and negative, due to the formation of by-products (soaps). According

to this study, and from an economical point of view, the maximum yield of ester (98.75%) can be obtained, working with an initial catalyst concentration (1.1%) and operation temperature (55°C). These models are useful to determine the optimum operating conditions for the industrial process using a minimal number of experiments with the consequent economical benefit.

Biodiesel synthesised, which consists of long-chain FAME, generally suffers from lower oxidation stability. Results from this study suggest that for a remarkably stable biodiesel and in order to avoid oxidation, special precautions must be taken during long storage, such as storage under argon atmosphere. Nevertheless this action delays oxidation but it doesnot prevent it. The results of this work have allowed develop a methodology to overcome the obvious problems of long storage stability of biodiesel. Long-term storage study gives us a better understanding of the effect of the normal oxygen atmosphere on the stability of biodiesel. The use of corn oil as an alternative raw material and renewable feedstock to produce biodiesel which fulfills the specification of EU standards for biodiesel (EN 14214) is of great interest to build an integrated and self-sustained biorefinery.

Acknowledgment

Financial support from the (CICYT), Spanish Project CTQ 2006-10467/PPQ is gratefully acknowledged.

References

[1] F. Staat and E. Vallet, "Vegetable oil methyl ester as a diesel substitute," *Chemistry & Industry*, vol. 21, pp. 856–863, 1994.

[2] M. P. Dorado, E. Ballesteros, J. M. Arnal, J. Gomez, and F. J. L. Gimenez, "Testing waste olive oil methyl ester as a fuel in a diesel engine," *Energy & Fuels*, vol. 17, no. 6, pp. 1560–1565, 2003.

[3] N. Usta, "An experimental study on performance and exhaust emissions of a diesel engine fuelled with tobacco seed oil methyl ester," *Energy Conversion and Management*, vol. 46, no. 15-16, pp. 2373–2386, 2005.

[4] S. P. Singh and D. Singh, "Biodiesel production through the use of different sources and characterization of oils and their esters as the substitute of diesel: a review," *Renewable and Sustainable Energy Reviews*, vol. 14, no. 1, pp. 200–216, 2010.

[5] J. M. Marchetti, V. U. Miguel, and A. F. Errazu, "Possible methods for biodiesel production," *Renewable and Sustainable Energy Reviews*, vol. 11, pp. 1300–1311, 2007.

[6] G. Vicente, M. Martínez, and J. Aracil, "Integrated biodiesel production: a comparison of different homogenous catalysts systems," *Bioresource Technology*, vol. 92, pp. 297–305, 2004.

[7] Y. C. Sharma and B. Singh, "Development of biodiesel from karanja, a tree found in rural India," *Fuel*, vol. 87, no. 8-9, pp. 1740–1742, 2008.

[8] G. Knothe, "Current perspectives on biodiesel," *Information*, vol. 13, no. 12, pp. 900–903, 2002.

[9] H. Shi and Z. Bao, "Direct preparation of biodiesel from rapeseed oil leached by two-phase solvent extraction," *Bioresource Technology*, vol. 99, no. 18, pp. 9025–9028, 2008.

[10] F. Ferella, G. Mazziotti, I. De Michelis, V. Stanisci, and F. Vegliò, "Optimization of the transesterification reaction in biodiesel production," *Fuel*, vol. 89, pp. 36–42, 2010.

[11] S. V. Ghadge and H. Raheman, "Process optimization for biodiesel production from mahua (Madhuca indica) oil using response surface methodology," *Bioresource Technology*, vol. 97, no. 3, pp. 379–384, 2006.

[12] A. K. Tiwaria, A. Kumara, and H. Raheman, "Biodiesel production from jatropha oil (Jatropha curcas) with high free fatty acids: an optimized process," *Biomass and Bioenergy*, vol. 31, no. 8, pp. 569–575, 2007.

[13] *GS AgriFuels to Convert Corn Oil into Biodiesel at Ethanol Facilities*, GS AgriFuels Corporation, New York, NY, USA, 2006.

[14] R. O. Dunn and G. Knothe, "Oxidative stability of biodiesel in blends with jet fuel by analysis of oil stability index," *Journal of the American Oil Chemist's Society*, vol. 80, no. 10, pp. 1047–1048, 2003.

[15] F. D. Gunstone and T. P. Hilditch, "The union of gaseous oxygen with methyl oleate, linoleate, and linolenate," *Journal of the Chemical Society*, pp. 836–841, 1945.

[16] A. Bouaid, M. Martínez, and J. Aracil, "Long storage stability of biodiesel from vegetable and used frying oils," *Fuel*, vol. 86, no. 16, pp. 2596–2602, 2007.

[17] A. Bouaid, M. Martínez, and J. Aracil, "Production of biodiesel from bioethanol and Brassica carinata oil: oxidation stability study," *Bioresource Technology*, vol. 100, no. 7, pp. 2234–2239, 2009.

[18] P. Bondioli, A. Gasparoli, L. D. Bella, and T. Silvia, "Evaluation of biodiesel storage stability using reference methods," *European Journal of Lipid Science and Technology*, vol. 104, no. 12, pp. 777–784, 2002.

[19] B. R. Moser, "Comparative oxidative stability of fatty acid alkyl esters by accelerated methods," *Journal of the American Oil Chemist's Society*, vol. 86, no. 7, pp. 699–706, 2009.

[20] R. O. Dunn, "Effect of oxidation under accelerated conditions on fuel properties of methyl soyate (biodiesel)," *Journal of the American Oil Chemist's Society*, vol. 79, no. 9, pp. 915–920, 2002.

[21] M. H. Chahine and R. F. Macneill, "Effect of stabilization of crude whale oil with tertiary-butylhidroquinone and other antioxidants upon keeping quality of resultant deodorized oil. A feasibility study," *Journal of the American Oil Chemist's Society*, vol. 51, no. 3, pp. 37–41, 1974.

[22] G. Box and J. Hunter, "Response surface methods," in *Statistics for Experiments Part IV: Building Models and Using Them*, chapter 5, John Wiley & Sons, New York, NY, USA, 1978.

[23] G. Knothe, "Analyzing biodiesel: standards and other methods," *Journal of the American Oil Chemist's Society*, vol. 83, no. 10, pp. 823–833, 2006.

[24] T. Garcia, A. Coteron, M. Martínez, and J. Aracil, "Optimization of the enzymatic synthesis of isopropyl palmitate using a central composite design," *Transactions of Chemical Engineers*, vol. 73, pp. 140–144, 1995.

[25] G. Vicente, A. Coteron, M. Martínez, and J. Aracil, "Application of the factorial design of experiments and response surface methodology to optimize biodiesel production," *Industrial Crops and Products*, vol. 8, no. 1, pp. 29–35, 1998.

[26] A. Monyem, M. Canakci, and J. H. Van Gerpen, "Investigation of biodiesel thermal stability under simulated in-use conditions," *Applied Engineering in Agriculture*, vol. 16, pp. 373–378, 2000.

[27] G. Knothe, "Structure indices in FA chemistry. How relevant is the iodine value?" *Journal of the American Oil Chemist's Society*, vol. 79, no. 9, pp. 847–854, 2002.

[28] P. Bondioli, A. Gasparoli, L. D. Bella, S. Tagliabue, and G. Toso, "Biodiesel stability under commercial storage conditions over one year," *European Journal of Lipid Science and Technology*, vol. 105, no. 12, pp. 735–741, 2003.

[29] H. A. Moser, P. C. Cooney, C. D. Evans, and J. C. Cowan, "The stability of soybean oil: effect of time and temperature on deodorization," *Journal of the American Oil Chemist's Society*, vol. 43, no. 11, pp. 632–634, 1966.

[30] G. Knothe and K. R. Steidley, "Kinematic viscosity of biodiesel fuel components and related compounds. Influence of compound structure and comparison to petrodiesel fuel components," *Fuel*, vol. 84, no. 9, pp. 1059–1065, 2005.

[31] M. W. Formo, E. Jungermann, F. Noris, and N. O. V. Sonntag, "Bailey&s Industrial Oil and Fat Products," in *Bailey's Industrial Oil and Fat Products*, D. Swern, Ed., vol. 1, pp. 698–711, John Wiley & Sons, New York, NY, USA, 4th edition, 1979.

[32] G. Knothe and R. O. Dunn, "Dependence of oil stability index of fatty compounds on their structure and concentration and presence of metals," *Journal of the American Oil Chemist's Society*, vol. 80, no. 10, pp. 1021–1026, 2003.

[33] S. Naz, H. Sheikh, R. Siddiqi, and S. A. Sayeed, "Oxidative stability of olive, corn and soybean oil under different conditions," *Food Chemistry*, vol. 88, no. 2, pp. 253–259, 2004.